Influences of skin barrier, a nanoparticle-based vehicle and solvents on cutaneous drug delivery

Inaugural-Dissertation

to obtain the academic degree

Doctor rerum naturalium (Dr. rer. nat.)

submitted to the Department of Biology, Chemistry, and Pharmacy

of Freie Universität Berlin

by

Pin Dong

Berlin

2020

The following PhD dissertation was supervised by Prof. Dr. Monika Schäfer-Korting at the Institute of Pharmacy (Pharmacology and Toxicology) of Freie Universität Berlin, and Prof. Dr. Martina Meinke at the Department of Dermatology and Allergy, Charité-Universitätsmedizin Berlin, corporate member of Freie Universität Berlin, Humboldt-Universität zu Berlin, and Berlin Institute of Health from October 2015 to August 2019 in tight collaboration with the Collaborative Research Center 1112 – Nanocarriers.

1st Reviewer: Prof. Dr. Monika Schäfer-Korting
Institute of Pharmacy (Pharmacology and Toxicology)
Freie Universität Berlin
Königin-Luise-Straße 2+4
14195 Berlin

2nd Reviewer: Prof. Dr. Martina Meinke
Klinik für Dermatologie, Venereologie und Allergologie
Charité - Universitätsmedizin Berlin
Charitéplatz 1
10117 Berlin

Date of defense: 21st February 2020

Hiermit versichere ich, die vorliegende Dissertation selbstständig und ohne unerlaubte Hilfe angefertigt zu haben. Bei der Verfassung der Dissertation wurden keine anderen als die im Text aufgeführten Hilfsmittel verwendet. Ein Promotionsverfahren wurde zu keinem früheren Zeitpunkt an einer anderen Hochschule oder bei einem anderen Fachbereich beantragt.

Berlin, 13 January 2020

Ort, Datum

Pin Dong

Acknowledgment

First and most, I would like to express my sincere gratitude to my supervisors, Prof. Dr. Monika Schäfer-Korting and Prof. Dr. Martina Meinke. I am very grateful for their excellent guidance and adequate support during my study. I have learned a lot from their exceptional expertise and rigorous attitude towards scientific research. I especially thank for their open-mindedness and trust, letting me implement my research ideas. My special thanks go to Prof. Dr. Martina Meinke for inviting me to her family activities, which are unforgettable and wonderful memories.

I want to thank Prof. Dr. Jürgen Lademann for supporting me to conduct experiments in the lab. My special thanks go to him for inviting me to the academic retreats that deepen my understanding of leadership and german culture.

I sincerely thank PD Dr. Alexa Patzelt for being my mentor. She shared her expertise with me in the field of follicular penetration and offered valuable discussions.

I want to express my sincere thanks to all my colleagues at Charité-Universitätsmedizin Berlin for their generous help and sharing many joyful moments. I highly appreciate that Dr. Silke Lohan helped me with operating the EPR spectrometer, as well as academic writing. I also appreciate Dr. Stephanie Albrecht for her help with solving the problems of the EPR spectrometer. I want to thank Dr. Maxim Darvin, Marius Kröger, and Viktor Nikolaev for the efficient cooperation in two-photon microscopy measurements. I very am thankful to Sabine Schanzer and Heike Richter for offering technical support. Special thanks go to Sabine Grenz for proofreading my papers. I want to thank my fellow members, Anja Elpelt, Anna Lena Klein, Yasemin Keziban, and Benchaphorn Limcharoen for their important roles during my time at Charité. We had many exciting conversations about different topics and made unforgettable team activities. I am very thankful for their encouragement. I will miss the time we spend together. I especially thank them for translating the summary of my thesis into german.

Besides, I would like to thank the people that I collaborate in the Collaborative Research Center 1112- Nanocarriers. Prof. Dr. Roland Bodmeier and Dr. Fitsum Feleke Sahle are thanked for providing the pH-sensitive nanoparticles. Prof. Dr. Robert Bittl, Dr. Christian Teutloff, and Dr. Siavash Saeidpour were thanked for their support in analyzing and interpreting EPR results.

I gratefully acknowledge the scholarship from China Scholarship Council.

I deepest gratitude goes to my lovely families. I sincerely thank my parents for supporting my decision to study abroad. In the end, I express my most heartfelt gratitude to my husband Dr. Kezheng Li, for his faithful support and always being by my side.

List of publications and presentations

Publications related to the thesis

P. Dong, F.F. Sahle, S.B. Lohan, S. Saeidpour, S. Albrecht, C. Teutloff, R. Bodmeier, M. Unbehauen, C. Wolff, R. Haag, J. Lademann, A. Patzelt, M. Schäfer-Korting, M.C. Meinke, pH-sensitive Eudragit® L 100 nanoparticles promote cutaneous penetration and drug release on the skin, Journal of Controlled Release, 295 (2019) 214-222.

P. Dong, V. Nikolaev, M. Kröger, C. Zoschke, M.E. Darvin, C. Witzel, J. Lademann, A. Patzelt, M. Schäfer-Korting, M.C. Meinke, Barrier-disrupted skin: Quantitative analysis of tape and cyanoacrylate stripping efficiency by multiphoton tomography, International Journal of Pharmaceutics, (2019). Available online: https://doi.org/10.1016/j.ijpharm.2019.118843.

P. Dong, C. Teutloff, J. Lademann, A. Patzelt, M. Schäfer-Korting, M.C. Meinke, Solvent effects on skin penetration and spatial distribution of the hydrophilic nitroxide spin probe PCA investigated by EPR, Cell Biochemistry and Biophysics, (2019) under revision.

Other publications and patents

S.B. Lohan, S. Saeidpour, A. Solik, S. Schanzer, H. Richter, P. Dong, M.E. Darvin, R. Bodmeier, A. Patzelt, G. Zoubari, M. Unbehauen, R. Haag, J. Lademann, C. Teutloff, R. Bittl, M.C. Meinke, Investigation of the cutaneous penetration behavior of dexamethasone loaded to nano-sized lipid particles by EPR spectroscopy, and confocal Raman and laser scanning microscopy, European Journal of Pharmaceutics and Biopharmaceutics, 116 (2017) 102-110.

P. Dong, J. Stellmacher, L.M. Bouchet, A. Kumar, E. Osorio, G. Nagel, S.B. Lohan, A. Patzelt, M. Schäfer-Korting, M. Calderón, M.C. Meinke, U. Alexiev, Multiplexed Fluorescence lifetime Imaging and EPR-based Quantification: A new versatile tool for target detection and quantification in tissue, Scientific Reports, (2019) submitted. P. Dong, J. Stellmacher, and L.M. Bouchet share the first authorship.

Patent CN201510460617.6A, C. Wu, P. Dong, M. Lu, Solid dispersion of itraconazole and preparation method and application of solid dispersion, China. https://worldwide.espacenet.com/publicationDetails/biblio?CC=CN&NR=105126110A&KC=A&FT=D

Oral presentations

P. Dong, J. Lademann, A. Patzelt, M. Schäfer-Korting, M.C. Meinke, Eudragit pH-sensitive nanoparticle promoted cutaneous penetration and drug release on the skin, Final Colloquium of SFB 1112, at Freie Universität Berlin, Berlin, Germany, 2018.

Directory

Abbreviations

AD	Atopic dermatitis
a_N	Hyperfine coupling constant
CLSM	Confocal laser scanning microscopy
CMS	Dendritic core-multishell
CS	Cyanoacrylate stripping
DxPCA	PCA-labeled dexamethasone
EPR	Electron paramagnetic resonance
FLIM	Fluorescence lifetime imaging microscopy
HF	Hair follicle
Log *P*	Logarithmic octanol/water partition coefficient
NP	Nanoparticle
PBS	Phosphate-buffered saline
PCA	2,2,5,5-Tetramethyl-3-pyrrolidine-1-oxyl-3-carboxylic acid
SC	Stratum corneum
SG	Stratum granulosum
TPM	Two-photon microscopy
TS	Tape stripping
VE	Viable epidermis

1 Introduction

1.1 The skin

The skin is an essential interface between the body and environmental surroundings [1]. The primary role of the skin is to serve as a physical barrier resisting penetration by pathogenic organisms and potential toxins while keeping moisture and nutrients inside the body [2]. This chapter centers on the structure of the skin, the skin penetration pathways, the skin barriers, and the physiochemical characteristics of the skin surface.

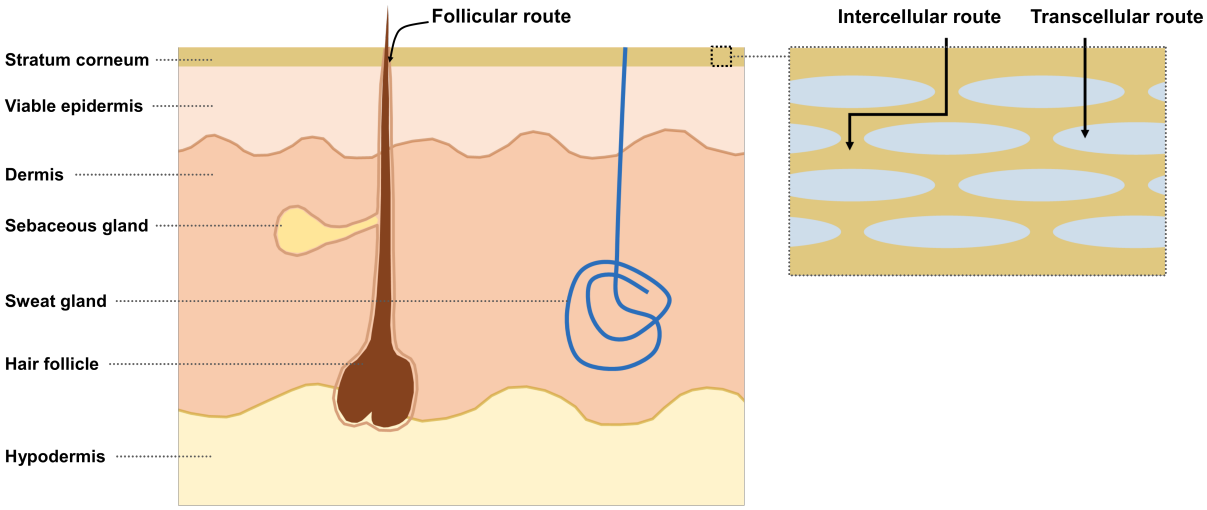

Figure 1 Schematic skin structure and penetration pathways.

1.1.1 Structure of the skin

The skin comprises three major zones: the epidermis, the dermis, and the hypodermis (Figure 1). The epidermis is mainly made up of keratinocytes and divided into the outermost stratum corneum (SC) and the viable epidermis (VE) beneath. Depending on keratinocytes at different stages of differentiation, the VE is divided into the stratum granulosum (SG), the stratum spinosum, and the stratum basale [3]. From the stratum basale, keratinocytes proliferate and are pushed upward by newly formed cells into the SG and eventually become enucleated and flattened cells called corneocytes, which are terminally differentiated cells in the SC [4]. The SC is stacked with 10-20 layers of corneocytes that are embedded in the intercellular lipids. The intercellular lipids are organized into lamellar bilayers which provide an important barrier to exogenous substances diffusing across the SC [5].

Hair follicles (HFs) are one group of skin appendages, which are mainly located in the dermis and hypodermis, ascend through the epidermis and open to the skin surface (Figure 1) [6]. There are two principal types of human HFs: the terminal and the vellus HFs. A. Vogt et al. measured the histological sections of human HFs from the scalp and the retroauricular regions. They found that terminal HFs with an average length of 3864 μm extend into the hypodermis, while vellus HFs have a length of about 646 μm and extend into the dermis. Diameters of the openings of the terminal and vellus HFs are about 172 μm and 86 μm, respectively [7]. The three regions of the HF from the skin surface to the deeper viable skin layers are infundibulum, the isthmus, and the bulb and suprabulb [8].

1.1.2 Definitions related to dermal absorption

Hereunder, definitions concerning dermal absorption are based on the guideline (SCCS/1358/10) published by the Scientific Committee on Consumer Safety. Skin penetration means the entry of a substance into a particular layer or structure of the skin. Skin permeation is the penetration through one layer into another, which is both functionally and structurally different from the first layer [9].

1.1.3 Mechanisms and pathways of skin penetration

The drug partitioning and diffusion through different skin layers are passive and follow a concentration gradient. When the skin is simplified as a homogenous membrane, the mechanism of skin penetration can be described by the Fick´s first law of diffusion (Equation 1), which expresses the steady-state molecule flux (*J*) as a function of the area and the drug concentration gradient:

$$J = \frac{D \times C_v}{h} \times \frac{S_m}{S_v} = \frac{D \times C_v \times P}{h} \qquad \text{(Equation 1)}$$

where *D* is the diffusion coefficient of the drug in the membrane, *h* is the diffusion path length across the membrane, C_v *is the concentration of the drug dissolved in the vehicle,* S_m *and* S_v *are the solubilities of the drug in the membrane and vehicle, respectively*, and *P* is the partition coefficient of the drug between the membrane and vehicle [10]. Therefore, strategies of increasing *D*, *P*, C_v, and S_m could enhance skin penetration of drugs.

Three potential penetration pathways of topically applied substances into the skin are well-accepted (Figure 1): intercellular, transcellular, and HF routes [10,11]. The intercellular route is considered as the predominant pathway for most drugs across the SC, especially lipophilic chemicals [12]. However, it is still debatable whether hydrophilic compounds prefer a transcellular route. Theoretically, a molecule penetrating via the transcellular route must experience multiple hydrophilic and lipophilic domains, namely corneocyte-lipid lamellae-corneocyte, which is unfavorable for most drugs [13]. H.E. Boddé et al. reported that for mercuric chlorite the intercellular route prevails while the transcellular route is also observed in the apical corneocytes after longer exposure time [14]. So far, only a few chemicals have been investigated about their skin penetration pathways because of technological limitations [15,16].

The HF penetration has recently received considerable attention [17-19]. Even though the area of follicular orifices accounts for less than 0.1% of the total skin area, the internal surface area of HFs is greatly higher than 0.1%, which makes HFs a potential reservoir for dermal penetration [20]. Studies nearly a decade ago mostly focused on how the physicochemical properties of drugs influence the HF penetration. E.A. Essa et al. reported that the HF route significantly contributes to the overall skin penetration of mannitol (hydrophilic) in aqueous solution, whereas it is negligible during the penetration of the saturated aqueous estradiol (lipophilic) solution [17]. The study published by T. Ogiso et al. found that the penetration of hydrophilic fluorouracil dissolved in a mixture of propylene glycol and ethanol is positively correlated to the HF density [21]. However, another study shows that the fluorescent substance Bodipy® 564/570 C5 of high lipophilicity was highly accumulated in HFs compared to Oregon Green® 488 of low lipophilicity. Both of the dyes were dissolved in a citric acid buffer containing 30% (V/V) ethanol [22]. Therefore, the hydrophilicity of a drug does not always correlate to the HF penetrate. One reason could be the influence of different media used to dissolve the tested substances. Recently, using particle-based drug delivery systems to deliver drugs into HFs is gaining interest [23-25]. For example, nanoparticles (NPs) have been shown their advantages in the HF penetration over conventional formulations such as gel and cream [24,25].

1.1.4 Skin barriers

The SC is a significant and first-line barrier to cutaneous penetration. In clinical practice, the amount of drugs penetrated skin only takes up 1-5% of the applied dose [26]. Moreover, among the drugs penetrated in the skin, a considerable amount of drugs are localized in the SC, while a low amount of drugs diffuse across the SC and enter the VE [27,28]. Therefore, the SC is often

regarded as a drug reservoir in skin penetration [29,30]. Another skin barrier is the transition zone between the lipophilic SC and the hydrophilic VE. Even though lipophilic molecules can penetrate into the SC more easily, subsequent diffusion of these molecules into the hydrophilic VE is restricted. Therefore, drugs with intermediate logarithmic partition coefficients (log *P*) between 1 and 3 are optimal for skin penetration [31].

Recently, tight junctions have been discovered in the VE. The tight junction seals the intercellular space of keratinocytes and impedes the transdermal diffusion of molecules across the VE [32]. For instance, S. N. Andrews and coworkers found that the permeabilities of human skin without the epidermis to insulin and sulforhodamine are increased 11 and 7 folds, respectively, compared to that of the skin only without the SC [33]. This study shows that the VE is a significant barrier to the transdermal penetration of these two drugs after removing the SC from the skin. The tight junctions in the VE may play a role in preventing the skin permeation of drugs. Another study used AT1002, a peptide that can open tight junctions in the SG, to successfully deliver siRNA into the AD mice skin while the vehicle without AT1002 failed [34]. These studies reveal that the tight junction is a crucial barrier to overcome to realize transdermal drug delivery.

For the HF penetration, substances often accumulate in the infundibulum of the HF, which is the upper segment of the HF from the orifice to the opening of the sebaceous gland [35]. The storage capacity of the infundibulum underscores the importance of HFs in delivering drugs into skin [36]. However, substances inside HFs are still on the outside of the body. The transfollicular penetration of substances into the VE and the dermis must overcome the barrier of the infundibulum. There are two kinds of barriers in the HF. The upper infundibulum is covered by the keratinized epidermis (i.e., the SC), posing a strong barrier; the lower infundibulum only has a thin horny layer that is fragile and imperfect, forming an inconspicuous barrier to the transfollicular penetration [37]. This makes the HF a promising target that offers a shortcut to deliver drugs to the deep part of the viable skin layers and even the systemic circulation [31].

1.1.5 Physiochemical characteristics of the stratum corneum

The main physicochemical parameters of the SC barrier are skin surface pH, transepidermal water loss, skin hydration, and sebum excretion. A multicentre study measured the volar forearm of 330 subjects and reported that the average skin surface pH is 5.1 $\pm$ 0.56 (Table 1) [38]. This acidic nature of the skin surface originates from the lactic acid secreted by eccrine sweat, and free fatty acids generated from the bulk hydrolysis of epidermal lipids [38]. The

electrode-based pH meter is commonly used to measure the skin surface pH. Besides, another approach using a pH sensor foil has been developed to measure the surface pH of skin equivalents [39,40]. The total water loss from the skin includes water passively evaporating through the SC to the external atmosphere (transepidermal water loss, TEWL) and also water loss as a result of sweating [41]. TEWL values are widely used to indicate the skin barrier function when there are no sweat gland activities [42]. The retention of water in the SC is defined as the skin hydration, which depends on the intercellular lipids of the SC to form a barrier to the transepidermal water loss, as well as the natural moisturizing factors to bind and hold water molecules in corneocytes [43]. The water content in the SC accounts for 15-20% of the total mass of the SC and accumulates mostly inside corneocytes. It sharply raises at the boundary between the SC and the SG [44]. Sebum is a highly viscous fluid and a mixture of non-polar lipids. It is produced by sebaceous glands and contributes to moistening the SC [41].

The above four physiochemical parameters are interrelated and often altered due to skin diseases. Atopic dermatitis (AD) is the most common chronic inflammatory skin disease accompanied by an impaired skin barrier and characterized by intense itch [45]. Many studies have found that the skin surface pH of AD patients is elevated, which is in a range of 5.5-6.1 [46-48]. Besides, the AD skin exhibits significantly lower water content of the SC and sebum amount on the skin surface compared with those of healthy skin [49-51]. The TEWL value of AD skin is found to be about 2-fold higher than healthy skin [52]. These changes in the physicochemical characteristics of the SC could affect skin penetration. For example, the concentration of metronidazole in the dermis of the AD skin, sampled by microdialysis, was 2.4-fold higher than that in the uninvolved skin [53]. Children with AD who were frequently exposed to emollients containing low-molecular-weight phthalates had significantly higher urinary levels of the phthalate metabolites when compared to children without AD [54]. Further studies show that compositions and organizations of the intercellular skin lipid in the AD skin are aberrant, which is directly related to the skin barrier function [55-57].

1.2 *Ex* vivo barrier-disrupted skin models

In vivo human skin is the targeted structure to evaluate the *in vivo* performance of dermal or transdermal drug delivery systems. However, it is generally not feasible during the initial development stage of a novel formulation or a new drug candidate. Therefore, excised human skin and isolated animal skin models are frequently used to improve our understanding of the skin penetration process, as well as to shorten and economize the process of drug development and minimize the number of human studies [58,59]. However, these *ex vivo* skin

models are associated with limited tissue durability and do not have an intact physiologic and metabolic system present in *in vivo* models [60]. With the awareness of animal welfare and new regulations in place (76/768/EEC, February 2003), reconstructed human skin equivalents have become an alternative to animal skins for skin absorption testing and toxicity studies [61].

1.2.1 *Ex vivo* skin models

Excised human skin is often obtained from plastic surgery, such as abdominal and breast skin. The *in vivo* human abdominal skin has 12.0 µm thick SC measured by two-photon microscopy [62], and its vellus HF density is about 17 hairs/cm^2 [63,64]. The diameter of the infundibulum opening of vellus HFs in the abdomen has not been investigated yet, but it could be referred to the value of retroauricular skin, which is 86-100 µm [7] (Table 1). A. Patzelt et al. reported that the follicular opening of excised human skin is constricted as the elastic fibers are cut during excision. Consequently, the amount of curcumin in HFs of excised skin after the topical application was reduced by more than 90% in comparison to the *in vivo* results. This study suggests that excised human skin is not a suitable skin model for studying the HF penetration, whereas porcine skin would be an alternative [65].

However, the availability of excised human skin is limited, particularly diseased human skin. Therefore, animal skin models are frequently used, such as primates, porcine, mouse, rat, guinea pig and snake models [59]. The use of primates is highly restricted and limited by cost [60]. Porcine skin is readily available and regarded as a good animal model for human skin because of its physiological and anatomical similarities [66,67]. Flank and ear are commonly used sites and their skin surface pH is in the range of 5.30-7.70, which is higher than the value of human skin [68,69]. M. Dime et al. investigated the HF pH of *ex vivo* porcine ear using a pH-sensitive dendritic polyglycerol nanogel and found that the pH of HFs increases from 6.5 at the skin surface to 7.4 in deeper regions [70]. The SC thickness of the porcine ear is determined to be 18 µm using confocal Raman microscopy based on the water concentration profile along with the skin depth [71]. The HF density of pig ear is about 20 hairs/cm^2, and the orifice of the follicular infundibulum is 173-229 µm in diameter[72]. The lipids of porcine SC are packed predominately in a hexagonal lattice (more disordered), while the lipids of human SC is packed in a denser orthorhombic lattice [73] (Table 1). This may indicate a higher SC barrier function of human skin compared to that of porcine skin [74].

The correlation of skin penetration and permeability of substance between porcine skin and human skin has been reported in several studies. A multicenter study conducted by M.

Schäfer-Korting and coworkers investigated the permeabilities of excised human epidermis and porcine skin to nine substances, covering a wide spectrum of physicochemical properties. The apparent permeation coefficient values obtained from both skin types correlate well [75,76]. Besides the skin permeability, the correlation of skin penetration of drugs between human and porcine skin needs consideration too, especially when only skin is the target. However, thorough investigations including a sufficient number of drugs have not been conducted so far. Only a few publications report the skin penetration of specific drugs into human and porcine skin. For example, the hydrophilic antifungal drug climbazole, dissolved in propylene glycol or Transcutol® P, exhibited significantly higher skin penetration into porcine skin than human skin, whereas the skin permeation through both skin types was similar [77]. For the hydrophilic compound niacinamide dissolved in propylene glycol or Transcutol® P, significantly more drugs permeated across the full-thickness porcine skin compared to the excised human skin, yet the drugs penetrated in porcine skin were much less than that in human skin [78]. The explanation for the inconsistency of the results in these two studies needs further investigations. The difference of SC and HFs between the two skin types might play a role.

Table 1 Comparison of *in vivo* human abdominal skin and *ex vivo* porcine ear

Parameters	Human abdominal skin	Porcine ear
SC thickness (μm)	12 [62]	18 [71]
pH of the SC surface	5.1 ± 0.56 [38]	5.30-7.70 [68,69]
HF density (hairs/cm^2)	17 [63,64]	20 [72]
Infundibulum diameter (μm)	86-100 [7]	173-229 [72]
Dominant lipid packing in SC	Orthorhombic lattice [73]	Hexagonal lattice [73]

Reconstructed human skin equivalents have been developed for the past three decades, and are categorized into epidermal and full-thickness models [61,79]. The Organization for Economic Cooperation and Development has approved the use of reconstructed human epidermis for acute skin irritation and skin corrosion testing [80]. However, the application of reconstructed human equivalents to skin absorption testing needs thorough validation. In a validation study published by M. Schäfer-Korting et al., three commercially-available reconstructed human epidermis models were compared with the *ex vivo* human epidermis [75]. The permeation of the reconstructed human epidermis models to nine substances exceeded that of the human epidermis by 2-30 folds due to a less developed barrier function of the reconstructed human epidermis models [75,81]. However, the ranking of the permeation of these nice substances through the three tested reconstructed skin models reflected the permeation results for the human epidermis. This study suggests that reconstructed human epidermis models could be suitable for the *in vitro* assessment of skin permeation and penetration of substances; however, product-specific overpredictability needs to be taken into account [75,76]. Besides, reconstructed

human epidermis models do not possess HFs or sweat glands. Thus, the only relevant penetration pathways are inter- and transcellular.

1.2.2 *Ex* vivo barrier-disrupted skin models

Diseased skin often exhibits impaired barrier function and altered physicochemical characteristics of the skin surface, which could consequently affect the cutaneous penetration and permeation of drugs. Therefore, topical formulations that are designed for the treatment of skin diseases should be evaluated on diseased skin. However, it is impossible to test any formulation or drug directly on patients at an early pharmaceutical development phase. In recent years, a wide range of animal models of skin diseases have been reported spanning from mice, rats, rabbits, dogs, monkeys, and fishes [82,83]. For example, AD mouse models can be induced by allergens or established by transgenic or gene knockout techniques [82]. However, the drawbacks of animal models are long disease induction phase and limited reproducibility [84]. The reconstructed human skin equivalents emulating AD have a long viability period and good reproducibility, yet it is of high-cost and not easily accessible [85]. In comparison, it would be an efficient strategy to induce an acute barrier disruption in *ex vivo* skin for preclinical assessment of novel dermal/transdermal drug delivery systems.

Acute skin barrier disruption can be induced by physical and chemical approaches. Tape stripping (TS) and cyanoacrylate stripping (CS) are widely used physical methods [86-90]. TS is an established procedure used in dermatopharmacology research for selectively removing the SC [87]. Generally, an adhesive film is pressed onto the test site of the skin, and then is abruptly removed, to which a certain amount of the SC adheres [91]. The amount of SC removed by tapes is influenced by many factors, such as the type of tape, application pressure, and duration of the pressure [92]. Cyanoacrylate is an FDA-approved tissue adhesive for wound closure [93]. Besides, it is also introduced to collect the SC for further analyses of skin lipids and uptaken drugs [87,94]. The liquid cyanoacrylate monomers polymerize into long chains and form a solid film upon the contact with water in the skin, leading to an adhesion of the film to the SC. Then the superficial layer of the SC is removed while removing the cyanoacrylate film with the sampling support such as polyethylene and glass [95].

The skin barrier disruption induced by TS or CS is due to the removal of the SC. Several studies have employed these two methods to develop *ex vivo* barrier-disrupted skin models. A. Vogt et al. used excised human skin whose skin barrier was impaired by one CS for studying transcutaneous immunization [96]. L. Simonsen et al. consecutively performed 25 tape strips on

porcine skin to simulate the AD skin. The increased TEWL value of the barrier-disrupted skin is in the range reported for the skin lesions of AD. Moreover, similar permeabilities of the barrier-disrupted skin model to fusidic acid and betamethasone in two formulations accord with the similar clinical effects of the two formulations on AD [97]. Besides, the skin surface pH of barrier-disrupted skin induced by TS or CS could also simulate the elevated pH of AD skin because the pH value gradually increases with the SC depth [98,99].

However, the correlation of the skin barrier function with the number of applied TS or CS has been scantly investigated [100]. TEWL value is a frequently used indicator for skin barrier function. Yer, TEWL measurement is not sensitive enough. The increase of the TEWL value of *in vivo* human skin can only be detected after applying more than 20 consecutive tape strips [92]. In comparison, the absolute SC thickness remaining on the skin after being subjected to a certain number of TS or CS would directly reflect changes in the skin barrier function.

Besides physical methods, the detergent sodium lauryl sulfate and the organic solvent acetone are typical chemicals used to induce acute skin barrier disruption, which results from the removal of intercellular lipids of the SC and structural changes of keratin in corneocytes [101,102]. As evidenced, epidermal swelling and spongiosis are observed in the excised human skin exposed to 5% sodium lauryl sulfate for 4 h [103]. However, it usually takes hours to reach a significant skin barrier disruption by using sodium lauryl sulfate [104]. In comparison, a few minutes of exposure to acetone can remarkably increase the TEWL of human skin *in vivo*; meanwhile, the skin surface pH is unchanged [105]. Using sodium lauryl sulfate and acetone is relatively hard to control and adjust the extent of skin barrier impairment. By contrast, the physical approaches, TS and CS, can easily realize different degrees of skin barrier disruption by adjusting the number of applied strippings; the induced barrier disruption is relatively reproducible when the TS and CS are performed under an established protocol.

1.3 Topical dermal drug delivery systems

The skin provides a promising site for the administration of substances for local or systemic therapies. Topical dermal formulations are mainly designed to target three sites according to the skin depth. First, the activities of some topical formulations are only limited to the skin surface without the SC penetration, such as sunscreen and repellents. Second, some formulations are aimed to deliver drugs into the viable skin layers while avoiding the systemic effect. For instance, topical corticosteroids are one of the most commonly prescribed medications for AD. Since AD is a chronic disease, long-term use of topical corticosteroids

could increase the risk of corticosteroids being absorbed into the bloodstream, which causes internal side effects such as decreased growth in children and Cushing's syndrome [106]. Therefore, a cutaneous drug delivery system that mainly transports drugs into the viable skin layers and limits the entry of drugs into the systemic circulation can reduce the systemic side effects of corticosteroids. Lastly, the transdermal drug delivery system that delivers drugs through the skin and into the bloodstream not only avoids the hepatic first-pass metabolism and gastrointestinal tract exposure but also provides controlled and sustained administration of drugs [107,108]. Thus, transdermal administration is a promising route to deliver drugs, such as its application in the treatment of Parkinson`s disease and contraception [109,110]. Dermal and transdermal drug delivery systems which are highly required in the clinic need first to overcome the SC barrier. To improve skin penetration of drugs, the uses of chemical penetration enhancers and NP-based drug delivery systems are effective strategies [111,112].

1.3.1 Chemical penetration enhancers

Various kinds of chemical penetration enhancers have been utilized to improve skin penetration of drugs [113]. This chapter only focuses on two simple and low toxic solvents: water and ethanol. Water is a natural and safe penetration enhancer; however, the mechanism by which water improves drugs entering skin is not clear. Under normal conditions, the SC has a water content of 15%-20% of its dry weight, which is supplied by the underlying viable tissue [114]. With skin occlusion, the SC hydration rises to 50% and the skin penetration of many compounds is increased [115]. The exogenous water diffuse into the SC too, which is evidenced by the swelling of corneocytes when the SC hydration is above 70% [116]. Therefore, a possible mechanism that water increases skin penetration of drugs is the SC hydration, which increases the partitioning of drugs from vehicles into the SC [113].

Ethanol is a widely used topical penetration enhancer [117]. The mechanisms of ethanol enhancing cutaneous penetration of drugs are still not clear. One proposed mechanism is: ethanol enters the skin and extracts appreciable amounts of lipid from the SC, which leads to a lowered skin barrier function and thus enhanced skin penetration of drugs [118,119]. Some studies report that ethanol could alter the structures of skin lipids and keratin fibrils [120,121]. Additionally, the permeation of drugs is found closely linked to the permeation of ethanol. Thus, one mechanism for ethanol as a skin penetration enhancer is suggested to be a so-called 'pull' or 'drag' effect [122-124].

The mixture of ethanol and water has been reported to synergistically enhance the skin penetration of several drugs [125-127]. For example, among the ethanol concentrations ranging from 0% to 100 % V/V, the ionic molecule sodium salicylate dissolved in the 63% aqueous ethanol solution showed the highest permeation through the human SC [125]. Using ethanol-water mixtures at ethanol concentrations over 0-90% W/W, a maximum flux of the lipophilic drug estradiol through the human epidermis was observed at ethanol concentrations between 40%-60% [127]. Mechanisms of the synergistic skin penetration enhancement for ethanol-water mixtures have not been elucidated.

1.3.2 Nanoparticles for dermal drug delivery

Apart from the penetration enhancers, NPs are gaining much interest in the research of dermal and transdermal drug delivery. Major types of NPs currently developed for skin drug delivery are lipid-based, polymeric and inorganic NPs [128]. According to the definition of the International Standards Organization, an NP is an object with at least one dimension below 100 nm. However, NPs in many published studies in the pharmaceutics and medicine field are in a size of 100-1000 nm, which should be categorized as sub-microparticles [25,129-135]. Nevertheless, the term NP used in the context below is based on the cited literature.

NPs have shown many advantages over conventional topical formulations such as creams, emulsions, gels, and ointments. i) NPs improve the skin penetration of physically-loaded therapeutics and model drugs [129,132,136]. For instance, the cutaneous uptake of the lipophilic dye Nile red is increased about fourfold by using solid lipid NPs compared to the uptake obtained following the cream [129]. The dendritic core-multishell (CMS) NP more efficiently delivers dexamethasone (Dx) into the epidermis of excised human skin compared to a commercially available Dx cream [132]. ii) NPs can target HFs [24,25,137]. The fluorescein loaded poly(D,L-lactide-co-glycolide) NPs penetrate much deeper into HFs of porcine skin than a fluorescein-containing hydrogel if a massage is applied [25]. iii) NPs control the release of encapsulated drugs. By tuning the physicochemical properties of NPs, the drug release of NPs can be triggered by exogenous/endogenous factors such as temperature, light, pH, and enzyme [134,138]. For example, NPs made of bovine serum albumin are deposited in HFs and the release of the loaded fluorescein isothiocyanate is triggered by protease which is delivered into HFs by $CaCO_3$ NPs at the same time [139]. 4) NPs could promote the cutaneous penetration of hydrophilic macromolecular drugs [140,141]. Etanercept is a protein drug that reduces the inflammatory response; one of its indications is psoriasis. M. Giulbudagian and coworkers designed a polyglycerol nanogel to encapsulate etanercept for topical application to replace

the currently used subcutaneous injection. The nanogel was found to deliver a significant amount of etanercept to the VE, whereas etanercept in PBS failed to penetrate into the VE [140]. 5) NPs improve the chemical stability of drugs [142,143]. The photolytic degradation of aciclovir that is incorporated into chitosan-tripolyphosphate NPs (suspension) is reduced compared to its aqueous solution [142].

Despite decades of research, there are only a few NP-based dermal/transdermal drug delivery systems on the market [144]. Estrasorb®, a nanoemulsion (about 125 nm in size), is designed to deliver estradiol to the blood circulation following topical skin application [145,146]. Pevaryl Lipogel® containing 1% econazole is the first approved liposome for dermal application [147]. However, its clinical efficacy in the treatment of tinea pedis is not superior to an econazole conventional Cream 1% [148]. Many fundamental and mechanistic questions need to be addressed to promote the clinical translation of NP-based cutaneous/transdermal drug delivery systems. First, the mechanisms of enhanced skin delivery by NPs are still ambiguous. The improved skin penetration using solid lipid NPs could be due to the interaction of the NP lipids with the SC lipids, as well as the skin hydration as the lipid NPs form an occlusive film on the skin surface [130,131]. The polymeric CMS NP is suggested to have interactions with the lipids or proteins of the SC, which favor the skin penetration of drugs [133]. The interaction of NPs with the SC is the first step during skin penetration; however, little is known about the NP-skin interaction because the complexity of the structures of both NPs and the SC makes it challenging to unveil this mystery. More advanced techniques are required. J. Dreier et al. employed two cutting-edge techniques, emission depletion microscopy and raster image correlation spectroscopy, and detected that the liposomes fuse with the outer lipid layers of the SC and then burst their cargoes [149].

Second, the ultimate spatial localization of NPs after applied to the skin is still a controversial topic concerning whether NPs penetrate the skin. The fluorescent polystyrene NPs of size 20-200 nm were observed to infiltrate the depth of 2-3 μm on porcine skin after 16 h exposure [150]. The CMS NPs with a size below 20 nm remain exclusively in the SC of the excised human within 6 hours and then penetrate into the viable skin after 24 hours [133]. However, these studies used the Franz diffusion cell approach in which the skin samples were excessively hydrated and their skin permeability could be significantly altered [151]. In an *in vivo* study, both AD and psoriasis mice models were topically applied with CMS NPs (about 14 nm in size) for five consecutive days, and the NPs were exclusively found in the SC and no penetration in the VE [152,153].

Next, the drug release from NPs is a prerequisite to exert therapeutic effects and thus to treat skin diseases. However, only a few studies have examined the role of drug release in the following skin penetration and permeation. The *in vitro* release of the molecular sunscreen oxybenzone from solid lipid NPs was decreased by 50% compared to that of an equally sized o/w emulsion; the *in vivo* skin penetration of oxybenzone using the solid lipid NPs was greatly lower than that using the emulsion [154]. A liquid crystalline system that sustainably released the loaded drug celecoxib *in vitro* was found to significantly enhance the drug penetration into porcine ear skin, compared to a celecoxib propylene glycol solution at the same concentration [155].

Franz diffusion cells and artificial polymeric membranes have been often used to study the drug release of NPs [156,157]. In this case, NPs are surrounded by abundant aqueous medium, which is far different from the limited water content in the skin surface. One study published by M. Schneider and coworkers was conducted on *ex vivo* skin. PLGA NPs of 290 nm in size were covalently labeled with fluorescein and physically loaded with the model drug Texas Red so that the localization of drugs and NPs can be distinguished by multiphoton microscopy. The results demonstrate that the NPs accumulated in the wrinkles of excised human skin and Texas Red was released and then penetrated into the skin [158].

Furthermore, factors that influence the drug release of NPs have not been fully investigated. One factor is the drug-nanocarrier interaction, which may be a double-edged sword for dermal/transdermal drug delivery systems. The drug-nanocarrier interaction can be exploited to control the drug release for meeting clinical needs [159,160]; however, it may also hinder the drug release and the subsequent skin penetration when the drug-nanocarrier interaction is too strong. For example, the positively charged drug tetracaine has a much stronger ionic interaction with a negatively charged carboxyl-modified polystyrene NP than with a silica NP. When the mixture of tetracaine and the negatively charged polystyrene NP was applied to the porcine epidermis, no tetracaine permeated through the epidermis. However, the addition of silica NPs to the tetracaine solution enhanced the skin permeation [161].

Lastly, how NP properties influence their borne substances to enter the skin still needs further studies, such as size and surface properties [137,162-164]. Liposomes of less than 300 nm in size were found to deliver both the hydrophilic dye carboxyfluorescein and lipophilic dye DiI into deeper skin layers to some extent, while liposomes in a size ≥ 600 failed [164]. Studies about the HF penetration of a polymeric PLGA NP and a $CaCO_3$ NP in different sizes were performed on *ex vivo* porcine ear and *in vivo* rat back, respectively. Both results demonstrate a deeper HF penetration for the particles in a size of around 600 nm [137,162]. Surface properties of NPs

influence the skin penetration of loaded drugs too. For example, a polymeric NP whose surface is modified with oleic acid delivers much more ketoprofen into the excised human skin, as compared to the unmodified NP [165]. Some studies report that positively charged nanoemulsions and polymeric Eudragit RS 100® NPs were superior to their corresponding negatively charged particles in delivering substances into the excised human skin [166,167]. To understand the mechansims of the enhanced skin penetration by NPs, the complicated interplay between drug-nanocarrier interaction, NP-skin interaction and drug release of NPs need to be thoroughly invesitigated.

1.4 Label-based techniques used to investigate skin penetration

Various advanced microscopic and spectroscopic techniques have been employed to answer the above challenging questions. These techniques differ in sensitivity, resolution, depth of optical sectioning, requirements of skin sample preparation, etc. Herein, the techniques are categorized into: i) label-free techniques, including transmission electron microscopy, atomic force microscopy, soft X-ray spectromicroscopy, Raman scattering, and Fourier-transform infrared spectroscopy; ii) label-based techniques, including electron paramagnetic resonance (EPR) spectroscopy, confocal laser scanning microscopy (CLSM), two-photon microscopy (TPM) and fluorescence lifetime imaging microscopy (FLIM). They have been applied to investigate spatial localization of NPs and drugs in different skin layers and skin cells [24,168-173], NP-skin interactions [174,175], drug release of NPs on skin [158,176,177], quantification of drugs in skin [136,171], characterization of NP properties, etc. [140] The following chapter focuses on the label-based techniques of EPR, CLSM, and TPM about their principles, advantages, limitations, and applications.

1.4.1 Electron paramagnetic resonance (EPR) spectroscopy

EPR can detect systems containing unpaired electrons. As shown in Figure 2A, the intrinsic angular momentum of the unpaired electron is called spin, which generates a magnetic field due to the electron charge. The unpaired electron can be regarded as a little bar magnet with a magnetic moment. An external magnetic field B_0 splits free unpaired electron spins into two energy levels: the unpaired electron's magnetic moment parallel and antiparallel with the applied external magnetic field are the low and high energy levels, respectively (Figure 2B). This effect is called Zeeman Effect. Since the electron is a spin ½ particle, the parallel state is denoted as m_s = -½ and the antiparallel state is m_s = +½. The energy of each level is the production of the electron's magnetic moment (μ) and B_0 ($E = \mu B_0$), and $\mu = m_s g_e \beta$, where g_e

is the spectroscopic *g*-factor of the free electron that approximately equals to 2.0023, and β is the Bohr magneton (9.274×10^{-24} J/T). Thus, the energies of the low and high levels are $E_{-½} = -½g_e\beta B_0$ and $E_{+½} = +½g_e\beta B_0$, respectively. The energy difference between the two levels is $\Delta E = g_e\beta B_0$. At the same time, $E = h\nu$, where ν is the frequency and h is the Planck's constant. Therefore, the microwave whose frequency matches the energy difference ΔE will be absorbed by the spins in the low energy state. Then the spins will transit to the high energy state, which is called resonance (Figure 2B). Since any physical system prefers to be in a low-energy state, the radiated electron will jump back to the low-energy state again and gives up its excess energy by re-emitting the electromagnetic radiation at the same frequency. The time of this process is called the electron relaxation time [178].

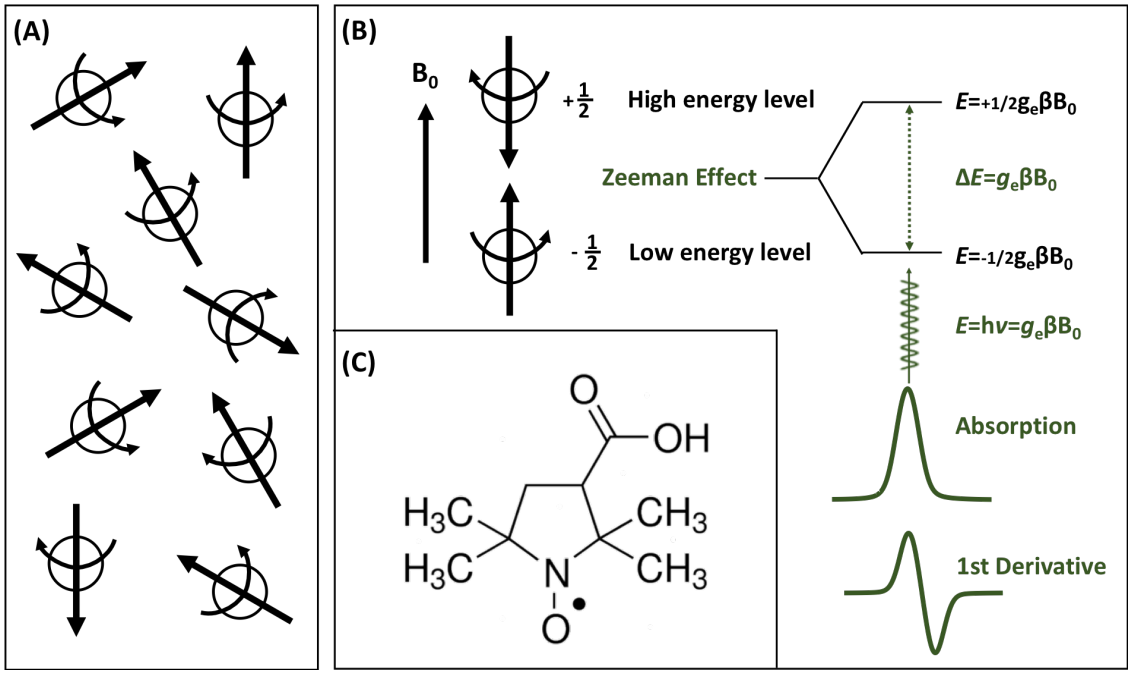

Figure 2 (A) Free unpaired electron spins randomly distributed in the space. (B) Zeeman effect in which an externally applied magnetic field B_0 splits the unpaired spins into the low and high energy levels. Only the electromagnetic radiation of a microwave with a certain frequency that matches the energy difference generated by Zeeman effect, can be absorbed, according to the equation of $\Delta E=h\nu=g_e\beta B_0$, where ΔE is the energy difference between the two levels, *h* is the Planck constant, ν is the frequency of the microwave radiation, g_e is the spectroscopic splitting factor, β is the Bohr magneton, and B_0 is the external applied magnetic field. The absorption curve is often presented as its first derivative curve in commercial EPR spectrometers [178]. (C) Chemical structure of 2,2,5,5-tetramethyl-1-pyrrolidinyloxy-3-carboxylic acid (PCA).

Commercial continuous-wave EPR (cw-EPR) spectrometers hold the frequency of the radiation microwave constant while scanning the magnetic field. The absorption spectrum is

usually recorded in the form of its first derivative (Figure 2B). Therefore, the signal intensity can be calculated by the double integral of the spectrum. The commonly used EPR frequencies in biomedicine are 9 GHz (X-band) and 1 GHz (L-band) [179]. The L-band spectrometer is less sensitive than the X-band, while the penetration depth of the L-band microwave radiation into water-rich samples is about 5-10 mm, which allows *in vivo* measurements such as human arms [180]. The penetration depth of the X-band microwave is limited to 0.5-1 mm in water-containing samples because water and polar lipids of the samples strongly absorbed the microwave energy. Usually, liquid samples and dermatomized skin biopsies can be measured [136].

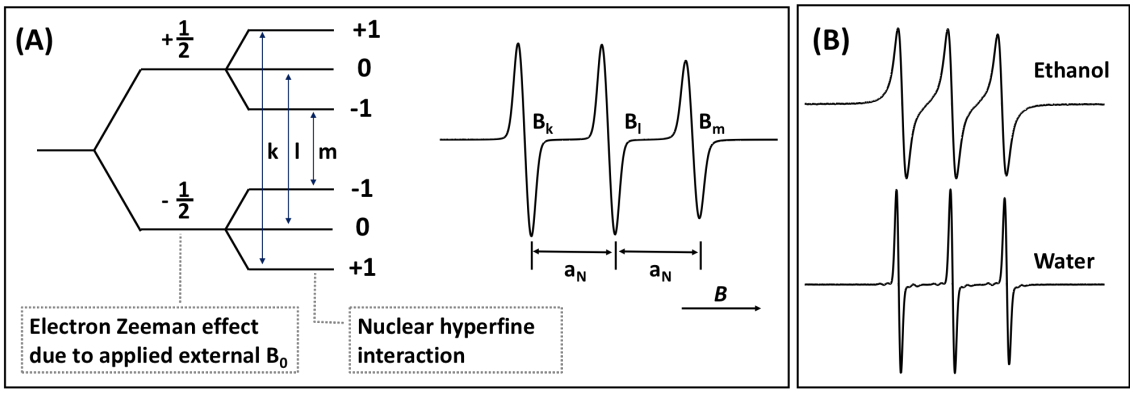

Figure 3 (A) The energy levels of the spin label PCA due to Zeeman effect and nuclear hyperfine interaction. The three different transitions of unpaired electrons between the two corresponding energy states under the microwave radiation are presented as three spectral lines in the EPR spectrum [181]. (B) The EPR spectra of PCA dissolved in ethanol and water.

There are several commercially available chemicals with stable unpaired electrons that are used as spin labels [182,183]. The nitroxide spin label 2,2,5,5-tetramethyl-1-pyrrolidinyloxy-3-carboxylic acid (PCA) is frequently used, which has a molecular weight of 186 g/mol and log *P* of -1.8 (Figure 2C) [184]. Its carboxylic acid group can be labeled with drugs and polymers via an ester or amide bond [183,185]. The unpaired electron of PCA is in the vicinity of the nitrogen nucleus (^{14}N). The nucleus also has a magnetic moment that produces a local magnetic field at the electron. There are three possible orientations of the ^{14}N nuclear magnetic field to the external applied magnetic field B_0 since the nitrogen nucleus ^{14}N has a nuclear spin of 1. Therefore, with the influences of Zeeman effect and nuclear hyperfine interaction, there exist three different transitions of unpaired electrons between the two corresponding energy levels under the microwave radiation, which are presented as three peaks in the EPR spectrum (Figure 3A) [181]. The distance between the first and the second peak is the hyperfine splitting constant a_N, which indicates the strength of the ^{14}N nucleus magnetic influence. The unpaired

electron of PCA is very sensitive to small variations of the charge density caused by surrounding microenvironments. Thus, the microenvironmental changes around PCA-labeled substances can be reflected in the respective EPR spectra. As shown in Figure 3B, PCA molecules, which dissolve in ethanol and water, respectively, exhibit different spectral shapes and broadenings due to different solvent polarities. Spectral interpretations usually require simulations of the EPR spectra. Easyspin, a free toolbox supported by MATLAB, is widely used for simulating cw-EPR spectra [186]. From the simulation, the parameters of a_N, *g*-matrix, and rotational correlation time are obtained. High a_N and low *g*-matrix indicate a hydrophilic microenvironment surrounding spin labels, while low a_N and high *g*-matrix indicate a relatively lipophilic microenvironment. The rotational correlation time represents the mobility of spin labels, which indicates the microenvironmental viscosity [187].

EPR has been widely used in chemistry, biology, pharmaceutics and medicine [188-190]. For example, EPR is used to directly quantify the amount of drugs in the skin, for which the skin sample preparation is simple without homogenization and extraction [136]. EPR has the potential to detect the drug release of formulations [191,192]. In a study, the model drug PCA was dispersed in the egg albumin matrix. The EPR spectra of PCA in the matrix and released into the external medium are different. Thus, the mechanism of drug release from the matrix was elucidated based on the spectra [191]. A hydrophilic spin probe 4 hydroxy-TEMPO was used as the model drug and encapsulated into pellets with different film coatings. The changes of the EPR spectra of 4 hydroxy-TEMPO from immobile to mobile reflected influences of the film coatings on the drug release of pellets [192]. Besides, S.Saeidpour et al. recently employed EPR to investigate the localization of the PCA labeled Dx (DxPCA) in a CMS NP. The simulation results of the magnetic parameters (a_N and *g*-matrix) elucidate that DxPCA is located in the interface between the inner lipophilic shell and the outer hydrophilic shell of the CMS NP [193]. These applications show that EPR not only enables quantitative investigations but also provides information about the microenvironments around spin-labeled drugs. EPR could be a useful technique for the investigation of skin penetration.

1.4.2 Confocal laser scanning microscopy (CLSM)

CLSM is a well-established technique for obtaining high-resolution images (lateral, ~200 nm; axial, ~1 µm) and has been extensively used to study the fates of NPs and the encapsulated drugs in the skin [194,195]. CLSM is usually performed in either reflectance mode or fluorescence mode. The reflectance CLSM has been used for noninvasive diagnosis in the clinic, such as the *in vivo* assessment of melanocytic and non-melanocytic skin tumors [196]. The fluorescence

CLSM provides images with higher contrast and allows investigations on the *ex vivo* and *in vivo* skin [194]. However, fluorescent dyes approved for use in humans are very limited due to safety issues [197]. The following content is focused on the fluorescence CLSM, in which one photon is needed to excite the fluorophore, and the absorbed energy is released as a photon of longer wavelength, referred to as a linear process [196].

The optical sectioning of CLSM reaches the skin depth down to approximately 120 µm [198]. The key element that enables the optical sectioning of CLSM is the pinhole which is an optical filter that only permits light in focus to pass through to the detector. This allows the acquisition of discrete horizontal optical sections of the specimen [199]. Therefore, the spatial localization of fluorescent NPs or encapsulated drugs in different skin layers can be detected by CLSM. If skin layers deeper than 120 µm are of interest such as HFs, then the biopsies need to be prepared into frozen or paraffin sections [24]. For instance, F. Sahle and coworkers covalently labled a nanogel with indodicarbocyanine and physically incorporated coumarin-6 into the nanogel. Different emission wavelengths of indodicarbocyanine and coumarin-6 enable investigating the localization of nanogels and the release of coumarin-6 in porcine HFs [200].

The pinhole is a double-edged sword, which blocks the majority of the out-of-focus fluorescence emission light and increases the resolution of CLSM but also reduces the signal intensity. Therefore, more intense exposure of high-power laser light (excitation light) is required to attain sufficient signal. However, the high-intensity laser illumination of CLSM could be destructive to fluorophores and living tissues, resulting in photobleaching and phototoxicity. Therefore, the stability of fluorophores during CLSM measurements should be considered [196].

1.4.3 Two-photon microscopy (TPM)

TPM is a novel, non-invasive and *in vivo* imaging technique with a high spatial resolution (lateral, ~200 nm; axial, ~1 µm) and holds promise for both basic research and clinical pathology [201]. Different from the single-photon CLSM, in TPM, two near-infrared photons in the spectral range of 800-1200 nm are absorbed simultaneously, and then the combined energy of the two photons is released. In this case, the wavelength of the fluorescence emission light will be shorter than the excitation light whereby the process is nonlinear. To realize this non-linear excitation, it needs a powerful form of femtosecond pulsed infrared light on the order of GW/µm^2 within the excitation volume. So far, the commercial titanium (Ti): sapphire laser can meet this requirement. During the two-photon excitation process, only a very tiny volume of fluorophore in the focal point is excited, and there is no absorption above

or below the focal plane. Therefore, a pinhole is no longer required to realize the optical sectioning for TPM [199]. TPM can image many skin structures based on the intrinsic autofluorescent agents, such as reduced pyridine nucleotides, and oxidized flavin proteins in keratinocytes, and keratin in corneocytes [202]. Besides the two-photon fluorescence excitation, the ultra-short near-infrared laser pulses also produce the non-linear polarization effect of second-harmonic generation from its interaction with non-centrosymmetric biological structures, such as collagen in the dermis. In this process, the combined energy of two photons is not absorbed but generated photons of exactly half the wavelength of the incident photons [203]. Therefore, no dye is required when using TPM to image the morphological skin structure.

TPM has several advantages over one-photon CLSM. i) TPM uses excitation wavelengths in a near-infrared spectral range that penetrate deeper into tissues; therefore, its optical sectioning reaches deeper skin areas than CLSM [204]. ii) The excitation light is restricted to the focal point, and the out-of-plane region of a specimen is not affected. Thus, the photodamage of biological specimens and photobleaching of fluorophores is reduced. iii) TPM has a higher lateral resolution than CLSM when measuring the same skin biopsy [198]. Both CLSM and TPM techniques require a fluorescent dye as a model drug or labeled to NPs when studying skin penetration of drug-loaded NPs.

The aforementioned label-based techniques have both advantages and limitations. A combination of these techniques would draw strength on each technique and enable comprehensive and in-depth investigations on skin penetration. For example, EPR has strength in quantification but lacks spatial resolution. CLSM and TPM can visualize biological specimens at the subcellular level. Therefore, it would be a valuable strategy to combine EPR and CLSM/TPM when quantitatively studying the spatial localization of drugs. In a study published by S. Lohan et al., EPR and CLSM were utilized to quantify the skin penetration of DxPCA following the lipid NP application and visualize the localization of Nile red loaded NPs in HFs [136]. However, only a few studies have employed two complementary techniques in skin penetration studies so far. More combinations of techniques need to be explored.

1.6 Objectives

The SC barrier is the main challenge in dermal drug delivery. Many strategies have been used to enhance the penetration of drugs through this barrier. Among the approaches, NP-based drug delivery systems are superior in controllable and targeted drug release; the penetration enhancer of solvents is easily accessible, low-cost, and flexibly combinable. Besides, the comprised barrier function of diseased skin could also alter the skin penetration of drugs and vehicles. Although considerable progress has been made in enhancing skin penetration of drugs for decades, there are still many unanswered questions (see Chapter 2.2, 3.2 and 3.1). This thesis is aimed to study the roles of skin barrier function, a NP-based drug delivery system, and the solvents of water and ethanol in the cutaneous drug delivery. Three research areas will be investigated in this thesis (Figure 4).

The first research area explores the feasibility of establishing *ex vivo* barrier-disrupted skin models that mimics AD skin to some extent by using the methods of TS and CS. AD is a highly prevalent skin disease across the world. It is of clinical significance to understand how the AD skin barrier influences the skin penetration of drugs and vehicles. The establishment of an *ex vivo* barrier-disrupted skin model would be useful in the early development of formulations and minimize the number of human studies. Specifically, the research objectives in this area are to i) quantitatively evaluate the efficiency of TS and CS for removing the SC, and ii) study the correlation of the SC thickness with the skin permeability.

The second research area comprehensively investigates the influence of skin barrier on the penetration behavior of a DxPCA loaded pH-sensitive NP. AD skin lesions exhibit an elevated skin surface pH in the range of 5.5-6.1 compared to the healthy skin surface pH (5.1). Therefore, a NP whose drug release can be triggered at a pH value above 5.5 would mainly target AD skin lesions while greatly reduce drugs penetrating into healthy skin, thereby reducing the side effects of Dx. Accordingly, a pH-sensitive NP which is made of Eudragit® L100 has been designed by Dr. Fitsum Sahle et al. in the group of Prof. Roland Bodmeier [205,206]. The labeling of PCA to Dx (DxPCA) is for EPR measurements and has been completed by Dr. Karolina Walker et al. in the group of Prof. Rainer Haag [185]. After these preparations by the collaborators, the important goals of this research area involve: i) characterization of the drug release of this pH-sensitive NP on *ex vivo* skin with either intact or disrupted SC barrier, and ii) investigation of the spatial localization of the drug DxPCA and the NP in the skin.

The third research area investigates the role of solvents in the cutaneous penetration of drugs. Water and ethanol have low skin toxicity and are almost omnipresent in dermal formulations,

serving as dissolution media and penetration enhancers. Different concentrations of ethanol aqueous solvents have shown their influences on the permeation of drugs through the epidermis which is separated from the skin by heating [125-127]. However, little is known about the effects of ethanol aqueous solvents on the skin penetration of drugs. This motivates the following objective of this research area: understanding the role of ethanol aqueous solvents at different concentrations in the cutaneous penetration of a hydrophilic model drug PCA, including the macroscopic localization of drugs in different skin layers and the microscopic localization of drugs in the lipids and corneocytes of the SC at the cellular level (Figure 4).

The investigations of the above three research areas will have the following contributions to the current research on cutaneous drug delivery: i) providing fundamental information about the relationship between the extent of skin barrier disruption with the number of applied TS or CS, ii) giving insight into the controlled and targeted drug release of the pH-sensitive NP on the barrier-disrupted skin and evaluating the feasibility of reducing the side effects of Dx in the treatment of AD by using pH-sensitive NPs as drug delivery systems, and iii) deepening the understanding of solvent effects on the skin penetration of drugs.

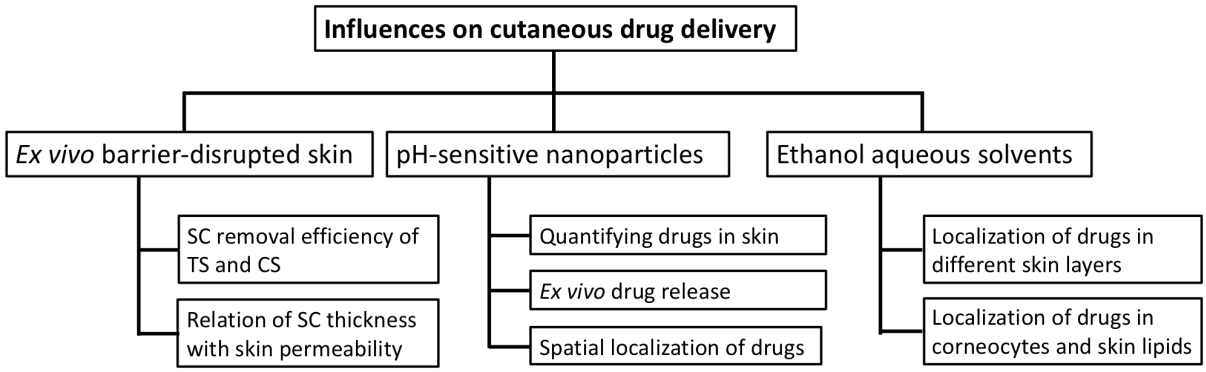

Figure 4 The objectives of the doctoral thesis

2 Publications and Manuscripts

In the following chapters, the published articles and submitted manuscripts are listed, and the contributions of the author are specified.

2.1 Barrier-disrupted skin: Quantitative analysis of tape and cyanoacrylate stripping efficiency by multiphoton tomography

Authors: Pin Dong, Viktor Nikolaev, Marius Kröger, Christian Zoschke, Maxim E. Darvin, Christian Witzel, Jürgen Lademann, Alexa Patzelt, Monika Schäfer-Korting, Martina C. Meinke.

Journal: International Journal of Pharmaceutics, 574 (2020), 118843.

Available online: https://doi.org/10.1016/j.ijpharm.2019.118843

Amount performed by Pin Dong:
Design of experiments: 80%
Practical, experimental part: 75%
Data analysis: 95%
Interpretation of results: 100%
Writing: 95%

2.2 pH-sensitive Eudragit® L 100 nanoparticles promote cutaneous penetration and drug release on the skin

Authors: Pin Dong, Fitsum Feleke Sahle, Silke B. Lohan, Siavash Saeidpour, Stephanie Albrecht, ChristianTeutloff, Roland Bodmeier, Michael Unbehauen, Christopher Wolff, Rainer Haag, Jürgen Lademann, Alexa Patzelt, Monika Schäfer-Korting, Martina C. Meinke.

Journal: Journal of Controlled Release, 295 (2019), 214-222.

Available online: https://doi.org/10.1016/j.jconrel.2018.12.045

Amount performed by Pin Dong:
Design of experiments: 90%
Practical, experimental part: 90%
Data analysis: 90%
Interpretation of results: 90%
Writing: 90%

2.3 Solvent effects on the cutaneous penetration and distribution of the hydrophilic nitroxide spin probe PCA

Authors: Pin Dong, Christian Teutloff, Jürgen Lademann, Alexa Patzelt, Monika Schäfer-Korting, Martina C. Meinke.

Journal: Cell Biochemistry and Biophysics (Submitted)

Amount performed by Pin Dong:
Design of experiments: 100%
Practical, experimental part: 100%
Data analysis: 100%
Interpretation of results: 95%
Writing: 95%

Cell Biochemistry and Biophysics

Solvent effects on skin penetration and spatial distribution of the hydrophilic nitroxide spin probe PCA investigated by EPR

--Manuscript Draft--

Manuscript Number:	CBBI-D-19-00188
Full Title:	Solvent effects on skin penetration and spatial distribution of the hydrophilic nitroxide spin probe PCA investigated by EPR
Article Type:	Original Article
Keywords:	Corneocytes; electron paramagnetic resonance; small hydrophilic molecule; skin lipids; skin pathway.
Corresponding Author:	Martina Meinke, Dr. rer. nat. Charite Universitatsmedizin Klinik fur Dermatologie Venerologie und Allergologie Berlin, GERMANY
Corresponding Author Secondary Information:	
Corresponding Author's Institution:	Charite Universitatsmedizin Klinik fur Dermatologie Venerologie und Allergologie
Corresponding Author's Secondary Institution:	
First Author:	Pin Dong, Master
First Author Secondary Information:	
Order of Authors:	Pin Dong, Master
	Christian Teutloff, Dr. rer. nat.
	Jürgen Lademann, Dr. rer. nat.
	Alexa Patzelt, Dr. med.
	Monika Schäfer-Korting, Dr.
	Martina C. Meinke, Dr. rer. nat.
Order of Authors Secondary Information:	
Funding Information:	
Abstract:	Oxidative stress occurs in extrinsic skin aging processes and diseases when the enhanced production of free radicals exceeds the homeostatic antioxidant capacity of the skin. The spin probe, 3-(carboxy)-2,2,5,5-tetramethylpyrrolidin-1-oxyl (PCA), is frequently used to study the cutaneous radical production by electron paramagnetic resonance (EPR) spectroscopy. This approach requires delivering PCA into the skin, yet solvent effects on the skin penetration and spatial distribution of PCA have not been thoroughly investigated. Three solvents of ethanol, phosphate-buffered saline (PBS) and ethanol-PBS (1:1) were studied. For both human and porcine skin ex vivo , the amount of PCA in the SC was the lowest when using ethanol and very similar for PBS and ethanol-PBS. The highest amount of PCA in the viable skin layers was detected for ethanol-PBS, yet it only took up less than 5% of the total amount. The majority of PCA was localized in the SC, among which PCA with high mobility was predominantly distributed in the hydrophilic microenvironment of corneocytes and PCA with lower mobility was mainly in the less hydrophilic microenvironment of intercellular skin lipids. A higher ethanol concentration in the solvent could improve the distribution of PCA in the hydrophilic microenvironments of the SC. The results suggest that ethanol-PBS (1:1) is best-suited for delivering most PCA deep into the skin. This work enhances the understanding of solvent effects on the skin penetration and distribution of PCA and supports the utilization of PCA in studying cutaneous radical production.
Suggested Reviewers:	Bernard Gallez, Dr. Prof., Universite Catholique de Louvain Faculte des sciences de la motricite bernard.gallez@uclouvain.be

	Prof. Gallez has experience with EPR method.
	Albert W. Girotti, PhD Prof., Medical College of Wisconsin agirotti@mcw.edu Prof. Girotti has experience of using EPR to study oxidative stress.
	Ben-Zhan Zhu, PhD Prof., University of the Chinese Academy of Sciences bzhu@rcees.ac.cn The research field of Prof. Zhu covers radical formation.
	Izabela Sadowska-Bartosz, Dr. Prof., Uniwersytet Rzeszowski isadowska@poczta.fm Prof. Sadowska-Bartosz has experience with EPR method.
	Georg Thomas Wondrak, PhD Prof., University of Arizona wondrak@pharmacy.arizona.edu The research field of Prof. Wondrak covers radicals.
	Michael Rallis, Dr. Prof., National and Kapodistrian University of Athens Faculty of Pharmacy rallis@pharm.uoa.gr The Research field of Prof. Rallis covers skin Penetration.

Solvent effects on skin penetration and spatial distribution of the hydrophilic nitroxide spin probe PCA investigated by EPR

Pin Dong [ab], Christian Teutloff [c], Jürgen Lademann [a], Alexa Patzelt [a], Monika Schäfer-Korting [b], Martina C. Meinke [a].

[a] Charité - Universitätsmedizin Berlin, corporate member of Freie Universität Berlin, Humboldt-Universität zu Berlin, and Berlin Institute of Health, Department of Dermatology, Venereology and Allergology, Berlin, Germany

[b] Freie Universität Berlin, Institute of Pharmacy, Pharmacology and Toxicology, Berlin, Germany

[c] Freie Universität Berlin, Institute of Experimental Physics, Department of Physics, Berlin, Germany

Corresponding author:
Prof. Dr. Martina Meinke
Charité – Universitätsmedizin Berlin
Department of Dermatology, Venereology and Allergology
Center of Experimental and Applied Cutaneous Physiology
Charitéplatz 1
10117 Berlin, Germany
Tel.: +49 (030) 450 518 244
martina.meinke@charite.de

Abstract

Oxidative stress occurs in extrinsic skin aging processes and diseases when the enhanced production of free radicals exceeds the homeostatic antioxidant capacity of the skin. The spin probe, 3-(carboxy)-2,2,5,5-tetramethylpyrrolidin-1-oxyl (PCA), is frequently used to study the cutaneous radical production by electron paramagnetic resonance (EPR) spectroscopy. This approach requires delivering PCA into the skin, yet solvent effects on the skin penetration and spatial distribution of PCA have not been thoroughly investigated. Three solvents of ethanol, phosphate-buffered saline (PBS) and ethanol-PBS (1:1) were studied. For both human and porcine skin *ex vivo*, the amount of PCA in the SC was the lowest when using ethanol and very similar for PBS and ethanol-PBS. The highest amount of PCA in the viable skin layers was detected for ethanol-PBS, yet it only took up less than 5% of the total amount. The majority of PCA was localized in the SC, among which PCA with high mobility was predominantly distributed in the hydrophilic microenvironment of corneocytes and PCA with lower mobility was mainly in the less hydrophilic microenvironment of intercellular skin lipids. A higher ethanol concentration in the solvent could improve the distribution of PCA in the hydrophilic microenvironments of the SC. The results suggest that ethanol-PBS (1:1) is best-suited for delivering most PCA deep into the skin. This work enhances the understanding of solvent effects on the skin penetration and distribution of PCA and supports the utilization of PCA in studying cutaneous radical production.

Keywords

Corneocytes; electron paramagnetic resonance; small hydrophilic molecule; skin lipids; skin pathway.

Introduction

Oxidative stress plays a significant role in extrinsic skin aging processes [1] and diseases [2]. It occurs when the production of oxygen and nitrogen radicals [3] overwhelms the homeostatic antioxidant capacity of the skin [4]. Radicals are molecules with unpaired electrons, which can be detected by electron paramagnetic resonance (EPR) spectroscopy [5, 6]. However, a direct EPR detection of endogenous free radicals in the skin under physiological conditions remains challenging due to their short lifetime [7]. Therefore, alternative approaches are utilizing spin traps and probes to investigate the free radical production in the skin [8].

Spin traps scavenge reactive free radicals effectively and form more stable paramagnetic spin adducts to facilitate EPR measurements. Different radical species can be distinguished from their unique EPR spectra of spin adducts [9]. Spin traps are often influenced by impurity [10] and dissolving media [11]. They are also less sensitive and less reliable for the quantitative determination of radicals [12]. In comparison, spin probes are molecules with stable free radical character and can be reduced to EPR silent hydroxylamine by free radicals generated in the skin [13]. Therefore, the intensity reduction of spin probes correlates well with the production of free radicals. This approach is widely used to study skin oxidative stress [12-14]. The spin probe of 3-(carboxy)-2,2,5,5-tetramethylpyrrolidin-1-oxyl (PCA), with low toxicity and low irritation to the skin [15], is often used in medical and cosmetic studies [16-19], such as photodynamic therapy [20, 21], light-induced radical production and sunscreen development [13, 18, 19, 22, 23]. In these *in vivo* studies, the skin was incubated with PCA solution from the outermost SC, and in some applications, test products were applied subsequently. Then the radical formation under light irradiation was investigated by EPR. Therefore, the prerequisite of this approach is to deliver PCA into the skin.

In vivo application of PCA demands a formulation with simple and non-toxic compositions. Thus, PCA is often dissolved in phosphate-buffered saline (PBS), ethanol, or the mixture of PBS and ethanol [12, 18]. PBS is a non-toxic and well-suited solvent due to the hydrophilicity of PCA [24]. Ethanol is a widely used penetration enhancer [25]. The ethanol-PBS cosolvent system has been found superior to transport drugs into the skin compared to the unary solvents [26-29]. Yet, solvent effects on the skin

penetration amount and depth of PCA, as well as the spatial distribution, have not been thoroughly investigated so far [13, 22]. In this work, the penetration of PCA on human and porcine skin delivered by the three solvents (ethanol, PBS, and ethanol-PBS 1:1) were quantified by EPR. Furthermore, the influences of these solvents on the spatial distribution of PCA in the skin were analyzed.

Materials and methods

PBS (Gibco™) was purchased from ThermoFisher Scientific (Waltham, MA, USA). PCA (98%), ethanol (Uvasol®, for spectroscopy) and Triton X-100 (laboratory grade) were bought from Sigma-Aldrich (Merck, Darmstadt, Germany). Cyclohexane (Rotisolv® HPLC) was bought from Carl Roth GmbH + Co. KG (Karlsruhe, Germany).

Skin samples

Excised human abdominal skin was donated by female volunteers with no medical history of dermatological diseases who underwent plastic surgery after informed written consent. The Ethics Committee of Charité-Universitätsmedizin Berlin approved the study in accordance with the principles expressed in the Declaration of Helsinki. After excision, the subcutaneous fatty tissue was removed from the skin specimen using a scalpel, and subsequently, the remaining skin samples were cleaned with PBS.

Porcine ears were obtained from a local slaughterhouse with the approval of the Commission of Consumer Protection and Agriculture, District Dahme-Spreewald, Germany. The ears were cleaned with cold tap water and gently dried with paper towels. The hairs were carefully cut with scissors without damaging the SC. All human and porcine skin samples were stored at 4 °C and used within 24 h.

PCA application and incubation protocol

For human skin, each skin sample was stretched and fixed with needles on a styrofoam plate and stripped with one tape to remove fatty substances on the skin surface. Six areas of each skin sample (n = 8) and each area in the size of 3 × 7 cm^2 were prepared. Each area was placed two stacked paper discs (Finn Chambers®, Φ 12 mm), leaving safety margins of about 9 mm to the skin border to avoid lateral

penetration. Then 100 µl of 0.4 % PCA solutions dissolved in ethanol, PBS, and ethanol-PBS 1:1 were pipetted onto the paper discs, respectively. Every solution was applied to two areas of each skin sample. After occlusion of the skin areas by Finn Chambers® (Φ 12 mm), the skin samples were incubated for 40 min at 32 ºC. This procedure was done in the same way as published *in vivo* studies [19, 23, 30]. For porcine ear skin, six areas of each pair (n = 6) were treated in the same procedure as for human skin.

Skin sample preparation for EPR measurements

After incubation, the paper discs were removed and subsequently all skin samples were subjected to 3 tape strippings because the high amount of PCA accumulated on the skin surface resulted in the spin-spin effect that depletes the EPR signal in EPR measurements [31]. Among the six areas of each skin sample, half of them exposed to the three PCA solutions, respectively, were removed the entire human stratum corneum (SC) by performing 4 times cyanoacrylate strippings (5 times for porcine skin) as previously described [32]. Afterward, all skin samples were dermatomed to a thickness of 300 µm (Aesculap, Tuttlingen, Germany) and punched into discs of 5 mm in diameter for EPR measurements. PCA in the non-stripped and cyanoacrylate-stripped skin samples represented the amount of PCA penetrated in the whole skin (i.e. the SC plus viable skin layers) and only in the viable skin layers, respectively. The difference between these two values was the amount of PCA in the SC.

Incubation of PCA with skin lipids

To obtain the EPR spectrum of PCA in skin lipids, they were extracted from porcine ear skin by using a mixture of cyclohexane and ethanol (4:1, V/V) [33]. A 15 ml Falcon™ centrifuge tube with an area of 2.27 cm^2 was filled with 1 ml of the solvent mixture and then it was held firmly against the skin while being shaken for 1 min. About 30 skin areas were performed, and each area was extracted twice. The collected solvent was centrifuged at 10000 rpm (Hettich AG, Switzerland) for 10 min to remove a few exfoliated corneocytes (precipitates). After overnight evaporating under a fume hood, the skin lipids were collected. Afterward, the skin lipids and PCA were dissolved in cyclohexane-ethanol (4:1) and evaporated again to obtain samples of PCA in skin lipids at a concentration of 0.001% (W/W).

Incubation of PCA with corneocytes

Corneocytes were prepared by the detergent scrub method [34, 35]. A fresh porcine ear placed in a glass Petri dish was rubbed by a polyester sponge soaked with 0.1% Triton X-100 in PBS. Any skin area was scrubbed 50 times and the washed fluid was sub-packed into 2 ml tubes, which were subsequently centrifuged at 10000 rpm for 10 min. The supernatant was discarded, and the precipitated corneocytes in each tube were resuspended with 2 ml PBS. The procedure of centrifugation-resuspension was repeated 5 times to wash away Triton X-100 [36]. Afterward, the collected corneocytes were incubated with 200 µl of 0.4 % PCA in ethanol-PBS (1:1) for 40 min at 32 ^{o}C. After the incubation, PCA in the external medium was removed with PBS in the same way as removing Triton X-100, and the procedure was repeated ten times. The supernatant after each washing step and the precipitated corneocytes after 10 times washing were measured by EPR.

EPR measurements

All measurements were conducted with an X-band EPR spectrometer (Elexsys E500, Bruker BioSpin, Karlsruhe, Germany) at ambient temperature. An SHQE resonator (E4122011SHQE, Bruker Biospin, Germany) and a TMHS resonator (E2044500TMHS, Bruker BioSpin) were used, which were matched to a sample holder of a capillary (2.0/1.0 mm in o.d./i.d., Hirschmann Laborgeräte, Germany) and a tissue cell (ER 162TC-Q, Bruker Biospin,), respectively. The instrumental settings of microwave power (mW) and field modulation amplitude (mT) are summarized in Table 1. The field modulation frequency was 100 kHz in all measurements.

(Please insert Table 1 here)

The total numbers and concentrations of PCA were quantified by the Bruker device control software Xepr. EPR spectra of PCA in skin samples, skin lipids, and corneocytes were simulated using EasySpin [37], a toolbox package for Matlab (The MathWorks GmbH, Natick, MA, USA). The *chili* function [38] was used for the simulation, and the magnetic parameters of *g*-matrix and 14N hyperfine coupling constant were referred to the published values [39].

Statistical analysis

Data are shown as mean ± standard error of the mean (SEM). Comparisons of the PCA transported into the human or porcine skin by the three solvents were evaluated by the nonparametric 2-related samples Wilcoxon test. The differences of PCA penetrated into human and porcine skin using the same solution were determined through the nonparametric 2-independent samples Mann-Whitney U test. The minimal significance level was set at $p \leq 0.05$.

Results and discussion

Skin penetration of PCA

The amounts of PCA transported into the SC and viable skin layers by ethanol, PBS and ethanol-PBS (1:1), respectively, are shown in Fig. 1a. For human skin, about 2.3 μg/cm^2 PCA was found in the SC using ethanol, which is the lowest among the three solvents. Ethanol is a well-known penetration enhancer, whereas it showed little improvement for the skin penetration of PCA. This could be due to the fast evaporation of ethanol. Many white PCA precipitates were seen on the skin surface after the incubation, which were formed due to the evaporation of ethanol, even though an occlusive chamber was used to reduce the evaporation. The precipitation of PCA could hinder the cutaneous penetration of PCA. Thus, pure ethanol is not recommended to deliver PCA into the skin. In comparison, the amounts of PCA in the human SC were 4.5 times increased in both cases of PBS and ethanol-PBS (1:1). This is different from many published findings, which stated that the PBS-ethanol cosolvent was better than the pure solvents, e.g. ethanol or PBS [26-29]. PCA is a small hydrophilic molecule (186 g/mol) with a natural logarithmic partition coefficient of -1.8 [40]. With the hydration of the SC by PBS [41, 42], possibly the solubility of PCA in the SC was increased, and hence the penetration of PCA into the SC could be enhanced.

In addition, the amount of PCA in the human viable skin layers was also quantified. Fig. 1b shows that the highest amount of PCA was delivered by ethanol-PBS (1:1). PBS facilitated slightly more PCA penetration into the viable skin compared to ethanol, even though there was no statistical significance in human skin due to high inter-donor variances. The results demonstrated the advantage of combining

ethanol with PBS to transport more PCA into the viable skin layers. The addition of PBS not only reduced the ethanol evaporation [43] but also hydrated the SC; while ethanol could extract appreciable amounts of lipids from the SC or influenced the structures of both corneocytes and skin lipid lamellar, and consequently may lower the skin barrier function [44, 45].

(Please insert Fig. 1 here)

For porcine skin, the amounts of PCA delivered into the SC by the three solvents were in the same order as human skin (ethanol-PBS ≈ PBS > ethanol). There was no difference in the amount of PCA in the SC between human and porcine skin subjected to the same PCA solution. This indicates that porcine skin could be a good substitute for human skin to study the skin penetration of PCA (Fig. 1a). The amounts of PCA in the porcine viable skin layers using the three solvents were in a similar order as human skin, i.e. ethanol-PBS > PBS > ethanol. However, the absolute values were lower than those of human skin, although there was no statistical difference between porcine and human skin treated with the same PCA solution. This might be the result of an enhanced transfollicular penetration in human skin since its hair follicles might have been impaired when removing the subcutaneous fat tissue before the penetration studies. By contrast, the penetration studies of porcine skin were performed on intact porcine ears without any skin separation.

The fractions of the amount of PCA in the viable skin layers to the total amount of PCA in the skin are shown in Fig. 1c. For human skin, the fractions were in the range of 1.3% - 4.9% when using the three solvents, and no statistical differences were found within the solvents due to the high inter-donor variation. For porcine skin, the highest fraction was about 1.2% in the case of ethanol-PBS, while it was less than 1% when using ethanol and PBS.

The above results show that PCA in the viable skin constituted less than 5% of the total penetration amount and more than 95% PCA accumulated in the SC. This is important information for studies of skin radical formation under light irradiation. First, PCA needs to be delivered to the depth of viable skin layers, because red light used in the photodynamic therapy and UVA to near-infrared light of the sun spectrum penetrate deep into the viable skin, meaning that free radicals would be induced in both the SC and viable skin layers [21, 46, 47]. If no PCA molecules penetrated into the viable skin layers,

free radicals produced there could not react with PCA. Consequently, the measured amount of free radicals would be lower than the actual amount of free radicals.

This is particularly important for quantitative measurements of free radicals. The free radical threshold value in the human skin is about 3.5×10^{12} radicals/mg, beyond which all the endogenous antioxidants in the skin could be consumed [48]. External stimuli that induce oxidative stress in the skin, such as light irradiation, would generate free radicals above this threshold [12]. This means that more than 3.5×10^{12} of PCA molecules/mg should be delivered into the viable skin layers to ensure that most free radicals are reacted with PCA. By using ethanol, PBS and ethanol-PBS, the amount of PCA in the viable skin layers that normalized to the skin weigh was about 1×10^{12}, 5×10^{12} and 9×10^{12} radicals/mg, respectively, when $1 g/cm^3$ was roughly taken as the density of the skin [49]. Therefore, the amount of PCA in the viable skin delivered by ethanol-PBS (1:1) could be enough to determine the threshold.

Nevertheless, the amount of free radicals produced in the viable skin layers depends on the extent of applied external stimuli, such as the irradiation dose. A linear decay of PCA could be a good indication to assume that the amount of PCA transported into the skin is sufficient to detect all free radicals [23]. Otherwise, a few tape strippings can be used to slightly disturb the SC barrier before applying PCA solutions to human skin *in vivo*, through which the amount of PCA penetrating into the viable skin could be increased. Alternatively, longer incubation time and/or potent penetration enhancers could be possible strategies to enhance the skin penetration of PCA. However, for *in vivo* studies, long incubation time would be poorly compliant, and potent penetration enhancers could have an issue of skin toxicity. In contrast, PBS as a safe solvent and ethanol as an FDA-approved solvent for skin application, they are favored for *in vivo* studies. But it should be mentioned that viable skin cells (e.g. keratinocytes and fibroblasts) and reconstructed human skin models are sensitive to ethanol. The concentration of ethanol above 3% could make half of the cells die [50]. Therefore, when PCA is used for skin cells or reconstructed models, only PBS should be used as the solvent.

Distributions of PCA in skin

Microenvironments of PCA in the whole skin layers

Apart from the influences on the skin penetration amount and depth of PCA, solvent effects on the skin distribution of PCA were analyzed by interpreting the spectral shape with simulations of the EPR spectra. The magnetic and dynamic parameters obtained from the simulations could reveal the microenvironments around the PCA molecules in the skin, such as polarity and viscosity [51]. For both human and porcine skin, PCA in the whole skin (containing the SC and viable skin layers) exhibited different spectral broadening in the EPR spectra when using the three solvents (Fig. 2a and Fig. S1a of the supplementary material). The broadening decreased with the increase of ethanol concentration in the solvent. In contrast, PCA in the viable skin layers of both human and porcine skin showed similar EPR spectra among the cases of three solvents (Fig. 2b and Fig. S1b of the supplementary material). The results indicate that PCA had similar microenvironments in the viable skin layers regardless of the solvents because the SC barrier strongly prevented the solvents from entering the viable skin layers to alter the microenvironments of PCA there.

We assume that the spectral broadening could be due to the partitioning of PCA in two different skin microenvironments. Therefore, the spectra were simulated considering two components to get magnetic and dynamic parameters, i.e. the hyperfine coupling matrix (a_{xx}, a_{yy}, a_{zz}) , the g-matrix (g_{xx}, g_{yy}, g_{zz}), and the rotational correlation time (T_{corr}), among which a_{zz} and g_{xx} are sensitive to the changes of the microenvironmental polarity and T_{corr} reveals the mobility of the spin probe [39]. A higher A_{zz} together with a lower g_{xx} indicates a hydrophilic microenvironment, whereas vice versa a less hydrophilic or lipophilic microenvironment is present. A decrease of T_{corr} suggests higher mobility of the spin probe.

(Please insert Fig. 2 here)

The simulation of the EPR spectrum of PCA in the whole human skin treated with PCA PBS solution was shown as an example owing to the remarkable spectral broadening (Fig. 2c). The simulation revealed that the spectrum comprised two kinds of spectra. As shown in Table 1 and Fig. 2c, the narrow spectrum represents PCA with the T_{corr} of about 0.1 ns, the higher hyperfine coupling constant of (15 15

106) MHz, and the lower *g*-matrix of (2.00805 2.00596 2.00212), which is attributed to PCA with high mobility in a hydrophilic microenvironment (PCA_{mobile}). The broad spectrum represents PCA with the T_{corr} of about 0.7 ns, the lower hyperfine coupling constant of (13 13 102) MHz, and the higher *g*-matrix of (2.00815 2.00596 2.00212), which belongs to PCA with less mobility in a less hydrophilic microenvironment ($PCA_{less\ mobile}$). The estimated T_{corr} of PCA_{mobile} was close to the T_{corr} of PCA in water (0.08 ns) [39]. Therefore, PCA_{mobile} could be localized in the water domains of corneocytes, intercellular regions, cytoplasm, etc [41].

(Please insert Table 2)

Besides, the EPR spectrum of PCA in the viable skin layers was simulated (Fig. 2d), and PCA molecules were found to have the same T_{corr} and magnetic parameters as PCA_{mobile}. It means that PCA in the viable skin layer was of high mobility and in a hydrophilic microenvironment (Table 1). PCA is generally considered as a cell membrane-impermeable probe due to its hydrophilicity, [40]. However, several studies showed that PCA could enter cells, even though the intracellular amount was much lower than the intercellular one [52, 53]. Therefore, PCA in the hydrophilic microenvironment of the viable skin could be mostly distributed in the aqueous regions of the intercellular space and a few might be in the cytoplasm of the viable skin cells. As the above results have shown, PCA in the whole skin (containing the SC plus viable skin layers) comprised PCA_{mobile} and $PCA_{less\ mobile}$, and PCA in the viable skin layers only included PCA_{mobile}. Thus, $PCA_{less\ mobile}$ can be assigned as PCA in the SC.

Additionally, one of eight human skin samples and one of six porcine skin samples exposed to the PCA PBS solution could be simulated with three components, too (see Fig. S3 of the supplementary material). Besides PCA_{mobile} and $PCA_{less\ mobile}$, the third component had the same magnetic parameters as $PCA_{less\ mobile}$, while its T_{corr} was ten times slower than that of $PCA_{less\ mobile}$ (6.3 ns), indicating reduced mobility of PCA ($PCA_{immobile}$). Yet, the fraction of PCA_{mobile} did not change whether the EPR spectrum was simulated with two or three components (see Fig. S3 in the supplementary materials). Considering the same magnetic parameters and similar reduced mobility, the fractions of $PCA_{less\ mobile}$ and $PCA_{immobile}$ of the EPR spectra were summed up as the fraction of $PCA_{less\ mobile}$ in the following calculation. The occurrence of $PCA_{immobile}$ might be explained by the dryness of the skin sample. The SC hydration could

be the most likely mechanism for PBS to deliver PCA into the skin [54]. In the time of sample processing after the incubation, PBS absorbed in the outmost layer of the SC might evaporate, leading to the immobilization of PCA in the upper SC layers.

Quantification of PCA in different skin microenvironments

The simulations of the EPR spectra of PCA in the whole skin provided the total fractions of PCA_{mobile} and $PCA_{less\ mobile}$, respectively. The fraction of PCA_{mobile} in the viable skin layers was calculated by the amount of PCA in the viable skin layers and total PCA amount in the skin. Hence, the fraction of PCA_{mobile} in the SC is the difference between the total fraction of PCA_{mobile} and the fraction of PCA_{mobile} in the viable skin layers. In Fig. 3a, the PCA composition in the whole skin is shown. It consisted of PCA_{mobile} and $PCA_{less\ mobile}$ for both human and porcine skin samples after exposure to the three PCA solutions, respectively. Concerning the skin distribution of PCA_{mobile}, the majority of PCA_{mobile} was distributed in the SC, while only a few of PCA_{mobile} was in the viable layers skin. All $PCA_{less\ mobile}$ were localized in the SC and the fraction of $PCA_{less\ mobile}$ among was increased with the decreased ethanol concentration in the solvent. From the solvent of ethanol to PBS, the fraction of $PCA_{less\ mobile}$ in the human SC increased from 37% to 74%.

(Please insert Fig. 3 here)

The T_{corr} of $PCA_{less\ mobile}$ that indicates the mobility of $PCA_{less\ mobile}$ in the SC is shown in Fig. 3b. For both human and porcine skin, the T_{corr} of $PCA_{less\ mobile}$ when using ethanol as the solvent was significantly higher than the value in the case of ethanol-PBS (1:1), meaning that $PCA_{less\ mobile}$ in the ethanol-treated SC had slower mobility. The evaporation of pure ethanol could cause dehydration of the SC, which could reduce the mobility of $PCA_{less\ mobile}$ in the surrounding microenvironments. For ethanol-PBS (1:1), the addition of PBS not only reduced the evaporation of ethanol but also hydrated the SC, through which the skin penetration of ethanol could be enhanced [55]. Therefore, the lower T_{corr} of $PCA_{less\ mobile}$ in the SC that treated with ethanol-PBS (1:1) could be due to the penetrated ethanol might increase the fluidity of skin lipids, leading to the increased mobility of $PCA_{less\ mobile}$ [44, 56].

Distributions of PCA in the SC

As the above results showed, PCA in the SC took up more than 95% of the total amount of PCA in the whole skin (Fig. 1), including all the $PCA_{less\ mobile}$ and most PCA_{mobile} (Fig. 2c-d and Fig. 3a). Corneocytes and intercellular skin lipids mainly constitute the SC. Thus, the distributions of $PCA_{less\text{-}mobile}$ and PCA_{mobile} in corneocytes and skin lipids were further investigated. First, corneocytes from the porcine SC were obtained using the detergent scrub method [34, 35]. As illustrated in Fig. 4a, most corneocytes were nearly elliptical with the conjugate diameters of 35 μm and 28 μm, which were in agreement with the published corneocyte diameter of 32 μm [57].

After incubation with 0.4% PCA ethanol-PBS (1:1), the corneocytes were washed with PBS ten times using centrifugation to remove the external PCA. In Fig. 4b, the EPR signal of PCA in the supernatant decreased with the number of washing cycles, indicating the removal of the external PCA. The supernatant from the 10^{th} washing exhibited only a noise signal in its EPR spectrum, whereas the precipitated corneocytes after 10 times of washing showed a strong EPR signal of PCA. This indicates that PCA could diffuse into corneocytes. In Fig. 4c and Table 1, the simulation shows that PCA in corneocytes had the same hyperfine coupling constant and *g*-matrix as PCA_{mobile} in the skin. This reveals that PCA could be in the hydrophilic microenvironment of corneocytes. The only difference was the T_{corr} of PCA in corneocytes (0.03 ns), which was smaller than that of PCA_{mobile} in the skin, meaning that the mobility of PCA in corneocytes was faster (Table 1). The reason could be that the separated cornoecytes used in this experiment were more hydrated than those in the intact SC [41]. Additionally, the detergent of Triton X-100 that was used to separate corneocytes might cause the structural changes of corneocytes, leading to an enhanced water diffusion into corneocytes.

(Please insert Fig. 4 here)

The EPR spectrum of PCA in the extracted skin lipids was also investigated to mimic the microenvironments of intercellular skin lipids of the SC [33]. In Fig. 4d, the simulation shows that PCA in the skin lipids could have two kinds of microenvironments. About 91% of PCA in skin lipids had the same hyperfine coupling constant and *g*-matrix as $PCA_{less\ mobile}$ in the SC (Table 1), indicating a less hydrophilic microenvironment. The T_{corr} of this part of PCA in the skin lipids (1.6 ns) was slightly larger

than that of $PCA_{less\ mobile}$ in the SC (Table 1). This could be due to that the lamellar structure of the intercellular skin lipids in the SC could be destroyed for the extracted skin lipids and different lipid packing orders might result in different T_{corr} values. The rest part of PCA in skin lipids (9%) were mobile in a hydrophilic microenvironment owing to the same magnetic parameters and T_{corr} as PCA_{mobile} in the skin. The hydrophilic microenvironments of the extracted skin lipids could be due to the water absorbed by the polar skin lipids, such as ceramide 1-3 and cholesteryl sulfate [58].

With the investigations of PCA in corneocytes and the skin lipids, $PCA_{less\ mobile}$ in the SC could be attributed to PCA distributed in the intercellular skin lipids, and PCA_{mobile} in the SC could be predominately localized in corneocytes, as well as a few of them was in the intercellular skin lipids. Corresponding to the results in Fig. 3a, it could be deduced that with the increase of ethanol concentration in the solvent, the fraction of PCA in the less hydrophilic microenvironment of skin lipids (i.e. $PCA_{less\ mobile}$) decreased, while the fraction of PCA in the hydrophilic microenvironments of corneocytes and skin lipids (i.e. PCA_{mobile}) increased. Ethanol was found to perturb both the keratin structure of corneocytes and skin lipids, which might be the reason that ethanol facilitated the distribution of PCA in the hydrophilic microenvironments of corneocytes and skin lipids [59, 60].

Conclusions

This work enhances the understanding of solvent effects on the skin penetration and spatial distribution of PCA. Poor skin penetration of PCA was observed when only ethanol was used, while it was increased 4.5-fold for PBS or ethanol-PBS (1:1). Among the three solvents, ethanol-PBS (1:1) delivered the most PCA into the viable skin layers, which could be sufficient to detect most part of free radicals produced in the viable skin layers. Nevertheless, more than 95% of the total PCA amount in the whole skin was accumulated in the SC, among which PCA with high mobility was predominantly distributed in the hydrophilic microenvironment of corneocytes and PCA with lower mobility was mainly distributed in the less hydrophilic microenvironment of intercellular skin lipids. A higher ethanol concentration in the solvent could improve the distribution of PCA in the hydrophilic microenvironments of the SC. The

study not only suggests that ethanol-PBS (1:1) could be a suitable solvent to transport PCA into the skin but also provides valuable information for using PCA to study skin radical production.

Acknowledgment

Pin Dong acknowledges a doctoral scholarship by the China Scholarship Council. We thank Dr. Christian Witzel of the Department of Surgery, Charité-Universitätsmedizin Berlin for providing excised human skin.

Declaration of interest

The authors report no conflicts of interest.

References

1. Rinnerthaler, M., Bischof, J., Streubel, M.K., Trost, A., and Richter, K. (2015). Oxidative Stress in Aging Human Skin. Biomolecules, 5, 545-589.
2. Bickers, D.R. and Athar, M. (2006). Oxidative Stress in the Pathogenesis of Skin Disease. Journal of Investigative Dermatology, 126, 2565-2575.
3. Newsholme, P., Rebelato, E., Abdulkader, F., Krause, M., Carpinelli, A., and Curi, R. (2012). Reactive oxygen and nitrogen species generation, antioxidant defenses, and β-cell function: a critical role for amino acids. 214, 11.
4. Gagné, F., *Chapter 6 - Oxidative Stress*, in *Biochemical Ecotoxicology*, F. Gagné, Editor. 2014, Academic Press: Oxford. p. 103-115.
5. Hogg, N. (2010). Detection of nitric oxide by electron paramagnetic resonance spectroscopy. Free Radical Biology and Medicine, 49, 122-129.
6. Babić, N. and Peyrot, F. (2019). Molecular Probes for Evaluation of Oxidative Stress by In Vivo EPR Spectroscopy and Imaging: State-of-the-Art and Limitations. Magnetochemistry, 5, 13.
7. Berliner, L.J., Khramtsov, V., Fujii, H., and Clanton, T.L. (2001). Unique in vivo applications of spin traps. Free Radical Biology and Medicine, 30, 489-499.
8. Khramtsov, V.V. (2018). In Vivo Electron Paramagnetic Resonance: Radical Concepts for Translation to the Clinical Setting. Antioxid Redox Signal, 28, 1341-1344.
9. Dąbrowski, J.M., *Chapter Nine - Reactive Oxygen Species in Photodynamic Therapy: Mechanisms of Their Generation and Potentiation*, in *Advances in Inorganic Chemistry*, R. van Eldik and C.D. Hubbard, Editors. 2017, Academic Press. p. 343-394.
10. Finkelstein, E., Rosen, G.M., and Rauckman, E.J. (1980). Spin trapping of superoxide and hydroxyl radical: Practical aspects. Archives of Biochemistry and Biophysics, 200, 1-16.
11. Cohen, M.S., Britigan, B.E., Hassett, D.J., and Rosen, G.M. (1988). Do humans neutrophils form hydroxyl radical? Evaluation of an unresolved controversy. Free Radical Biology and Medicine, 5, 81-88.
12. Albrecht, S., Elpelt, A., Kasim, C., Reble, C., Mundhenk, L., Pischon, H., et al. (2019). Quantification and characterization of radical production in human, animal and 3D skin models during sun irradiation measured by EPR spectroscopy. Free Radical Biology and Medicine, 131, 299-308.
13. Herrling, T., Fuchs, J., Rehberg, J., and Groth, N. (2003). UV-induced free radicals in the skin detected by ESR spectroscopy and imaging using nitroxides. Free Radical Biology and Medicine, 35, 59-67.

14. Herrling, T., Jung, K., and Fuchs, J. (2006). Measurements of UV-generated free radicals/reactive oxygen species (ROS) in skin. Spectrochimica Acta Part A: Molecular and Biomolecular Spectroscopy, 63, 840-845.
15. Fuchs, J., Groth, N., and Herrling, T. (1998). Cutaneous Tolerance to Nitroxide Free Radicals in Human Skin. Free Radical Biology and Medicine, 24, 643-648.
16. Arndt, S., Haag, S.F., Kleemann, A., Lademann, J., and Meinke, M.C. (2013). Radical protection in the visible and infrared by a hyperforin-rich cream – in vivo versus ex vivo methods. Experimental Dermatology, 22, 354-357.
17. Darvin, M.E., Haag, S.F., Lademann, J., Zastrow, L., Sterry, W., and Meinke, M.C. (2010). Formation of Free Radicals in Human Skin during Irradiation with Infrared Light. Journal of Investigative Dermatology, 130, 629-631.
18. Albrecht, S., Ahlberg, S., Beckers, I., Kockott, D., Lademann, J., Paul, V., et al. (2016). Effects on detection of radical formation in skin due to solar irradiation measured by EPR spectroscopy. Methods, 109, 44-54.
19. Haag, S.F., Tscherch, K., Arndt, S., Kleemann, A., Gersonde, I., Lademann, J., et al. (2014). Enhancement of skin radical scavenging activity and stratum corneum lipids after the application of a hyperforin-rich cream. European Journal of Pharmaceutics and Biopharmaceutics, 86, 227-233.
20. Haag, S.F., Fleige, E., Chen, M., Fahr, A., Teutloff, C., Bittl, R., et al. (2011). Skin penetration enhancement of core–multishell nanotransporters and invasomes measured by electron paramagnetic resonance spectroscopy. International Journal of Pharmaceutics, 416, 223-228.
21. Wen, X., Li, Y., and Hamblin, M.R. (2017). Photodynamic therapy in dermatology beyond non-melanoma cancer: An update. Photodiagnosis and Photodynamic Therapy, 19, 140-152.
22. Meinke, M.C., Haag, S.F., Schanzer, S., Groth, N., Gersonde, I., and Lademann, J. (2011). Radical Protection by Sunscreens in the Infrared Spectral Range. Photochemistry and Photobiology, 87, 452-456.
23. Albrecht, S., Jung, S., Müller, R., Lademann, J., Zuberbier, T., Zastrow, L., et al. (2019). Skin type differences in solar-simulated radiation-induced oxidative stress. British Journal of Dermatology, 180, 597-603.
24. Hyodo, F., Yasukawa, K., Yamada, K.-i., and Utsumi, H. (2006). Spatially resolved time-course studies of free radical reactions with an EPRI/MRI fusion technique. Magnetic Resonance in Medicine, 56, 938-943.
25. Heard, C.M., *Ethanol and Other Alcohols: Old Enhancers, Alternative Perspectives*, in *Percutaneous Penetration Enhancers Chemical Methods in Penetration Enhancement: Modification of the Stratum Corneum*, N. Dragicevic and H.I. Maibach, Editors. 2015, Springer Berlin Heidelberg: Berlin, Heidelberg. p. 151-172.

26. Krishnaiah, Y.S., Satyanarayana, V., and Karthikeyan, R.S. (2002). Effect of the solvent system on the in vitro permeability of nicardipine hydrochloride through excised rat epidermis. J Pharm Pharm Sci, 5, 123-130.
27. Kurihara-Bergstrom, T., Knutson, K., DeNoble, L.J., and Goates, C.Y. (1990). Percutaneous Absorption Enhancement of an Ionic Molecule by Ethanol–Water Systems in Human Skin. Pharm Res, 7, 762-766.
28. Berner, B., Mazzenga, G.C., Otte, J.H., Steffens, R.J., Juang, R.-H., and Ebert, C.D. (1989). Ethanol: Water Mutually Enhanced Transdermal Therapeutic System II: Skin Permeation of Ethanol and Nitroglycerin. Journal of Pharmaceutical Sciences, 78, 402-407.
29. Megrab, N.A., Williams, A.C., and Barry, B.W. (1995). Oestradiol permeation across human skin, silastic and snake skin membranes: The effects of ethanol/water co-solvent systems. International Journal of Pharmaceutics, 116, 101-112.
30. Meinke, M.C., Muller, R., Bechtel, A., Haag, S.F., Darvin, M.E., Lohan, S.B., et al. (2015). Evaluation of carotenoids and reactive oxygen species in human skin after UV irradiation: a critical comparison between in vivo and ex vivo investigations. Exp Dermatol, 24, 194-197.
31. Salikhov, K.M. (2010). Contributions of Exchange and Dipole–Dipole Interactions to the Shape of EPR Spectra of Free Radicals in Diluted Solutions. Applied Magnetic Resonance, 38, 237-256.
32. Dong, P., Nikolaev, V., Kröger, M., Zoschke, C., Darvin, M.E., Witzel, C., et al. (2019). Barrier-disrupted skin: Quantitative analysis of tape and cyanoacrylate stripping efficiency by multiphoton tomography. International Journal of Pharmaceutics, Submitted.
33. Monteiro-Riviere, N.A., Inman, A.O., Mak, V., Wertz, P., and Riviere, J.E. (2001). Effect of selective lipid extraction from different body regions on epidermal barrier function. Pharm Res, 18, 992-998.
34. McGinley, K.J., Marples, R.R., and Plewig, G. (1969). A Method for Visualizing and Quantitating the Desquamating Portion of the Human Stratum Corneum**From the Department of Dermatology, University of Pennsylvania School of Medicine, Philadelphia, Pennsylvania 19104. Journal of Investigative Dermatology, 53, 107-111.
35. Watanabe, M., Tagami, H., Horii, I., Takahashi, M., and Kligman, A.M. (1991). Functional Analyses of the Superficial Stratum Corneum in Atopic Xerosis. JAMA Dermatology, 127, 1689-1692.
36. Boczonadi, V. and Määttä, A., *Chapter Sixteen - Functional Analysis of Periplakin and Envoplakin, Cytoskeletal Linkers, and Cornified Envelope Precursor Proteins*, in *Methods in Enzymology*, K.L. Wilson and A. Sonnenberg, Editors. 2016, Academic Press. p. 309-329.
37. Stoll, S. and Schweiger, A. (2006). EasySpin, a comprehensive software package for spectral simulation and analysis in EPR. Journal of Magnetic Resonance, 178, 42-55.

38. Schneider, D.J. and Freed, J.H., *Calculating Slow Motional Magnetic Resonance Spectra*, in *Spin Labeling: Theory and Applications*, L.J. Berliner and J. Reuben, Editors. 1989, Springer US: Boston, MA. p. 1-76.

39. Saeidpour, S., Lohan, S.B., Solik, A., Paul, V., Bodmeier, R., Zoubari, G., et al. (2017). Drug distribution in nanostructured lipid particles. European Journal of Pharmaceutics and Biopharmaceutics, 110, 19-23.

40. David Jebaraj, D., Utsumi, H., and Milton Franklin Benial, A. (2018). Low-frequency ESR studies on permeable and impermeable deuterated nitroxyl radicals in corn oil solution. Magnetic Resonance in Chemistry, 56, 257-264.

41. Bouwstra, J.A., de Graaff, A., Gooris, G.S., Nijsse, J., Wiechers, J.W., and van Aelst, A.C. (2003). Water Distribution and Related Morphology in Human Stratum Corneum at Different Hydration Levels. Journal of Investigative Dermatology, 120, 750-758.

42. van Hal, D.A., Jeremiasse, E., Junginger, H.E., Spies, F., and Bouwstra, J.A. (1996). Structure of Fully Hydrated Human Stratum Corneum: A Freeze-Fracture Electron Microscopy Study. Journal of Investigative Dermatology, 106, 89-95.

43. O'Hare, K.D., Spedding, P.L., and Grimshaw, J. (1993). Evaporation of the Ethanol and Water Components Comprising a Binary Liquid Mixture. Developments in Chemical Engineering and Mineral Processing, 1, 118-128.

44. Bommannan, D., Potts, R.O., and Guy, R.H. (1991). Examination of the effect of ethanol on human stratum corneum in vivo using infrared spectroscopy. Journal of Controlled Release, 16, 299-304.

45. Horita, D., Hatta, I., Yoshimoto, M., Kitao, Y., Todo, H., and Sugibayashi, K. (2015). Molecular mechanisms of action of different concentrations of ethanol in water on ordered structures of intercellular lipids and soft keratin in the stratum corneum. Biochim Biophys Acta, 1848, 1196-1202.

46. Ruggiero, E., Alonso-de Castro, S., Habtemariam, A., and Salassa, L. (2016). Upconverting nanoparticles for the near infrared photoactivation of transition metal complexes: new opportunities and challenges in medicinal inorganic photochemistry. Dalton Transactions, 45, 13012-13020.

47. Amaro-Ortiz, A., Yan, B., and D'Orazio, J.A. (2014). Ultraviolet radiation, aging and the skin: prevention of damage by topical cAMP manipulation. Molecules, 19, 6202-6219.

48. Zastrow, L., Doucet, O., Ferrero, L., Groth, N., Klein, F., Kockott, D., et al. (2015). Free Radical Threshold Value: A New Universal Body Constant. Skin Pharmacol Physiol, 28, 264-268.

49. Morales, M.F., Rathbun, E.N., Smith, R.E., and Pace, N. (1945). Studies on Body Composition .2. Theoretical Considerations Regarding the Major Body Tissue Components, with Suggestions for Application to Man. Journal of Biological Chemistry, 158, 677-684.

50. Ponec, M., Haverkort, M., Soei, Y.L., Kempenaar, J., and Bodde, H. (1990). Use of Human Keratinocyte and Fibroblast Cultures for Toxicity Studies of Topically Applied Compounds. Journal of Pharmaceutical Sciences, 79, 312-316.
51. Haag, S.F., Fleige, E., Chen, M., Fahr, A., Teutloff, C., Bittl, R., et al. (2011). Skin penetration enhancement of core-multishell nanotransporters and invasomes measured by electron paramagnetic resonance spectroscopy. Int J Pharm, 416, 223-228.
52. Swartz, H.M., Sentjurc, M., and Morse, P.D. (1986). Cellular metabolism of water-soluble nitroxides: Effect on rate of reduction of cell/nitroxide ratio, oxygen concentrations and permeability of nitroxides. Biochimica et Biophysica Acta (BBA) - Molecular Cell Research, 888, 82-90.
53. Hahn, S.M., Wilson, L., Krishna, C.M., Liebmann, J., DeGraff, W., Gamson, J., et al. (1992). Identification of nitroxide radioprotectors. Radiat Res, 132, 87-93.
54. Marjukka Suhonen, T., A. Bouwstra, J., and Urtti, A. (1999). Chemical enhancement of percutaneous absorption in relation to stratum corneum structural alterations. Journal of Controlled Release, 59, 149-161.
55. Haddock, N.F. and Wilkin, J.K. (1982). Cutaneous Reactions to Lower Aliphatic Alcohols Before and During Disulfiram Therapy. JAMA Dermatology, 118, 157-159.
56. Pham, Q.D., Topgaard, D., and Sparr, E. (2017). Tracking solvents in the skin through atomically resolved measurements of molecular mobility in intact stratum corneum. Proceedings of the National Academy of Sciences of the United States of America, 114, E112-E121.
57. van der Merwe, D., Brooks, J.D., Gehring, R., Baynes, R.E., Monteiro-Riviere, N.A., and Riviere, J.E. (2005). A Physiologically Based Pharmacokinetic Model of Organophosphate Dermal Absorption. Toxicological Sciences, 89, 188-204.
58. Long, S.A., Wertz, P.W., Strauss, J.S., and Downing, D.T. (1985). Human stratum corneum polar lipids and desquamation. Archives of Dermatological Research, 277, 284-287.
59. Moghadam, S.H., Saliaj, E., Wettig, S.D., Dong, C., Ivanova, M.V., Huzil, J.T., et al. (2013). Effect of Chemical Permeation Enhancers on Stratum Corneum Barrier Lipid Organizational Structure and Interferon Alpha Permeability. Molecular Pharmaceutics, 10, 2248-2260.
60. Horita, D., Hatta, I., Yoshimoto, M., Kitao, Y., Todo, H., and Sugibayashi, K. (2015). Molecular mechanisms of action of different concentrations of ethanol in water on ordered structures of intercellular lipids and soft keratin in the stratum corneum. Biochimica et Biophysica Acta (BBA) - Biomembranes, 1848, 1196-1202.

Figures

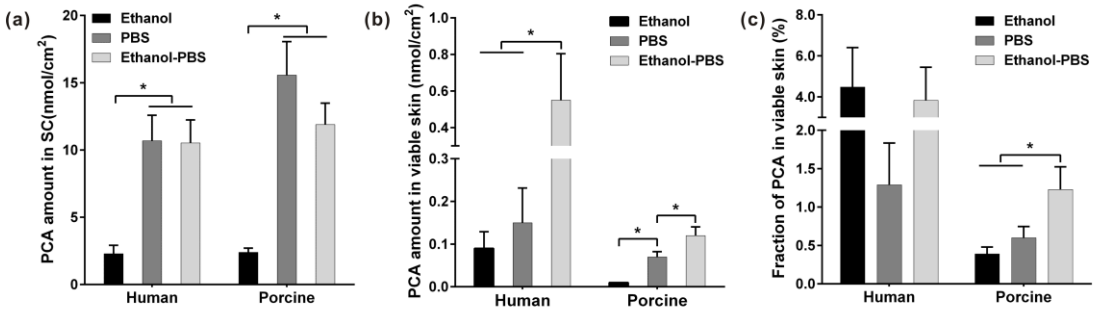

Fig. 1 The amount of PCA in the (a) SC, (b) viable skin layers and (c) the fraction of PCA in the viable skin to the total amount of PCA in the skin after applied 0.4% PCA solution dissolved in ethanol, PBS and ethanol-PBS (1:1, V/V) to human skin (n = 8) and porcine ear skin (n = 6), respectively. The area of every skin biopsy was 0.20 cm^2. The total amount of PCA in the skin is the sum of the amount of PCA in the SC and viable skin layers. Mean ± SEM, * indicates $p < 0.05$. No significant difference was found between human and porcine skin treated with the same PCA solution.

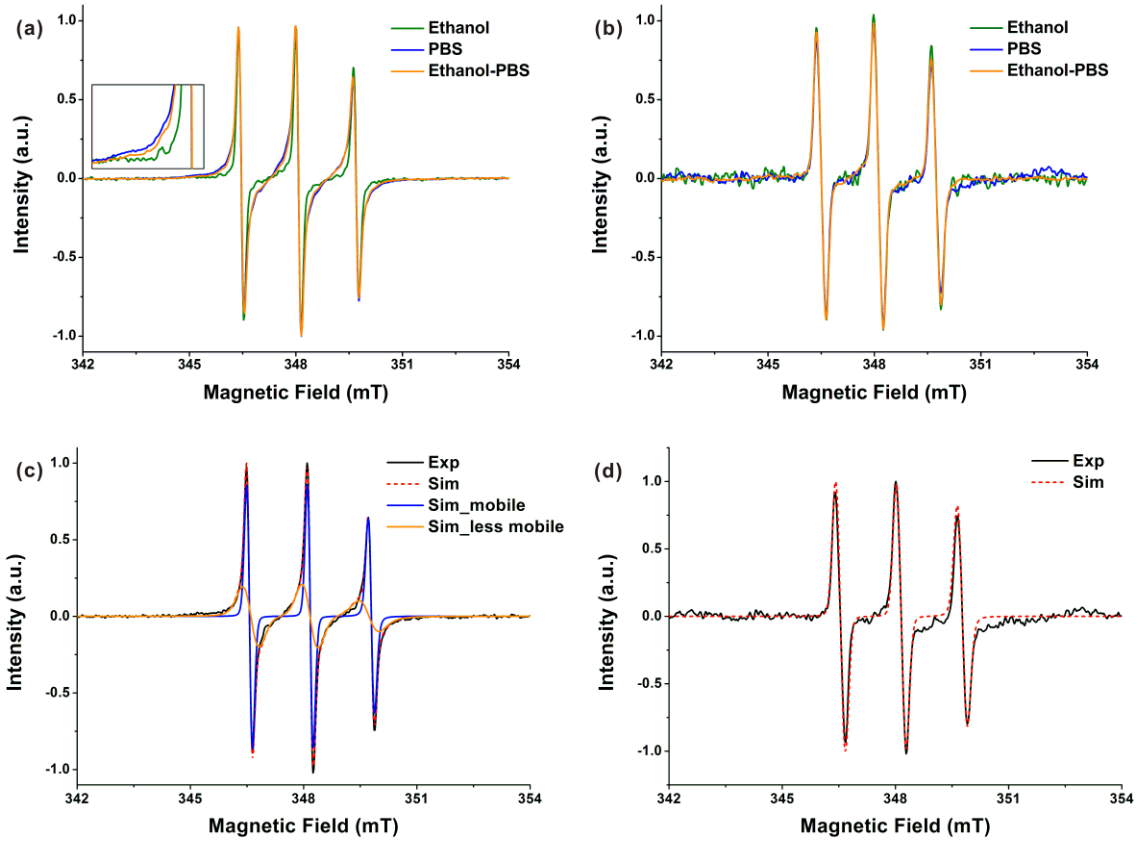

Fig. 2 The averaged EPR spectra (n = 8) of PCA in (a) the whole skin containing the SC plus viable skin layers and (b) only viable skin layers of excised human skin after the treatment with 0.4 % PCA solution dissolved in ethanol, PBS and ethanol-PBS (1:1, V/V), respectively. The inset visualizes the broadening of the spectra in Fig. 2a. The EPR spectra of PCA in porcine skin are presented in Fig. S1 of the supplementary material. Simulation examples of the EPR spectra of PCA in (c) the whole skin consisting of the SC plus viable skin layers and (d) only viable skin layers of excised human skin exposed to 0.4 % PCA PBS solution, from which the fractions of PCA with high mobility in a hydrophilic microenvironment (PCA_{mobile}) and PCA with lower mobility in a less hydrophilic microenvironment ($PCA_{less\ mobile}$) were derived. The hyperfine coupling matrices (a_{xx}, a_{yy}, a_{zz}) of (15 15 106) and (13 13 102) MHz, and the g-matrices (g_{xx}, g_{yy}, g_{zz}) of (2.00805 2.00596 2.00212) and (2.00815 2.00596 2.00212) for PCA_{mobile} and $PCA_{less\ mobile}$, respectively, were used for the simulations. The rotational correlation time T_{corr} of PCA_{mobile} was about 0.1 ns and T_{corr} of $PCA_{less\ mobile}$ was different for the cases of three solvents. The simulations of the EPR spectra of PCA in the skin treated with PCA dissolved in ethanol and ethanol-PBS (1:1, V/V), respectively, are illustrated in Fig. S2 of the supplementary material.

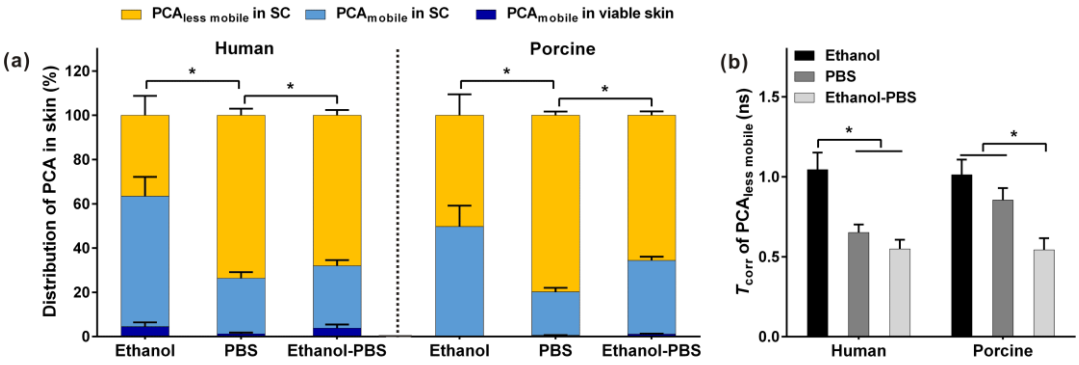

Fig. 3 (a) Distribution of $PCA_{less\ mobile}$ and PCA_{mobile} in the SC and viable skin after the application of 0.4% PCA solution dissolved in ethanol, PBS and ethanol-PBS (1:1, V/V), respectively, to human (n = 8) and porcine ear skin (n = 6), and (b) the rotational correlation time (T_{corr}) of $PCA_{less\ mobile}$ in the SC. Mean ± SEM, * indicates $p < 0.05$. No significant difference was found between human and porcine skin treated with the same PCA solution.

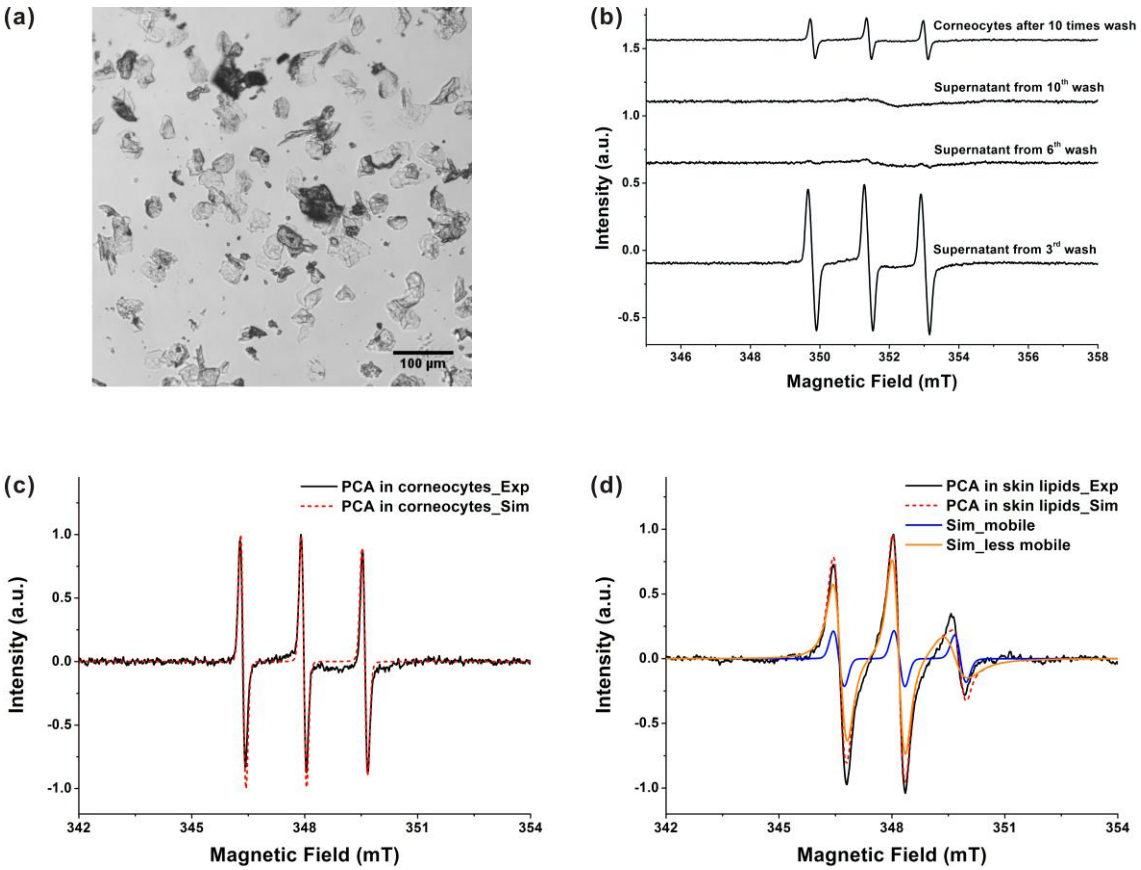

Fig. 4 (a) The microscopic image of the morphology of corneocytes from porcine skin. Scale bar = 100 µm. (b) The EPR spectra of the supernatant of PBS used to wash corneocytes, and the precipitated corneocytes, which were incubated with 0.4% PCA ethanol-PBS (1:1, V/V) for 40 min at 32 °C. The simulation of the EPR spectrum of PCA in (c) corneocytes and (d) skin lipids with the PCA concentration of 0.001% W/W.

Tables

Table 1 EPR experiment settings

Samples	Sample holder	Resonator	EPR settings
Skin containing SC plus viable skin layers	Tissue cell	TMHS	0.1 mT, 0.6 mW
Skin containing only viable skin layers	Tissue cell	TMHS	0.3 mT, 6.3 mW
PCA in skin lipids	Tissue cell	TMHS	0.3 mT, 20 mW
PBS from the washing of corneocytes	Capillary	SHQE	0.3 mT, 20 mW
Corneocytes incubated with PCA	Capillary	SHQE	0.3 mT, 20 mW

Table 2 The EPR magnetic and dynamic parameters of PCA in different biological media obtained from the simulations [a]

PCA in different biological media	PCA_{mobile}			$PCA_{less\ mobile}$		
	Hyperfine coupling constant (a_{xx}, a_{yy}, a_{zz}) MHz	*g*-matrix (g_{xx}, g_{yy}, g_{zz})	Rotational correlation time T_{corr} (ns)	Hyperfine coupling constant (a_{xx}, a_{yy}, a_{zz}) MHz	*g*-matrix (g_{xx}, g_{yy}, g_{zz})	Rotational correlation time T_{corr} (ns)
PCA in whole skin [b]	15 15 106	2.00805 2.00596 2.00212	0.1	13 13 102	2.00815 2.00596 2.00212	1.0-0.5
PCA in viable skin [b]	15 15 106	2.00805 2.00596 2.00212	0.1	No		
PCA in corneocytes	15 15 106	2.00805 2.00596 2.00212	0.03	No		
PCA in skin lipids [c]	15 15 106	2.00805 2.00596 2.00212	0.1	13 13 102	2.00815 2.00596 2.00212	1.6

[a] These are only estimated results from the simulations and used for the relative comparison.

[b] Skin samples were treated with 0.4% PCA solution dissolved in ethanol, PBS, and ethanol-PBS (1:1, V/V), respectively.

[c] The concentration of PCA in skin lipids was 0.001%.

Supplementary material

Solvent effects on skin penetration and distribution of the hydrophilic nitroxide spin probe PCA investigated by EPR

Pin Dong [ab], Christian Teutloff [c], Jürgen Lademann [a], Alexa Patzelt [a], Monika Schäfer-Korting [b], Martina C. Meinke [a].

[a] Charité - Universitätsmedizin Berlin, corporate member of Freie Universität Berlin, Humboldt-Universität zu Berlin, and Berlin Institute of Health, Department of Dermatology, Venereology and Allergology, Berlin, Germany

[b] Freie Universität Berlin, Institute of Pharmacy, Pharmacology and Toxicology, Berlin, Germany

[c] Freie Universität Berlin, Institute of Experimental Physics, Department of Physics, Berlin, Germany

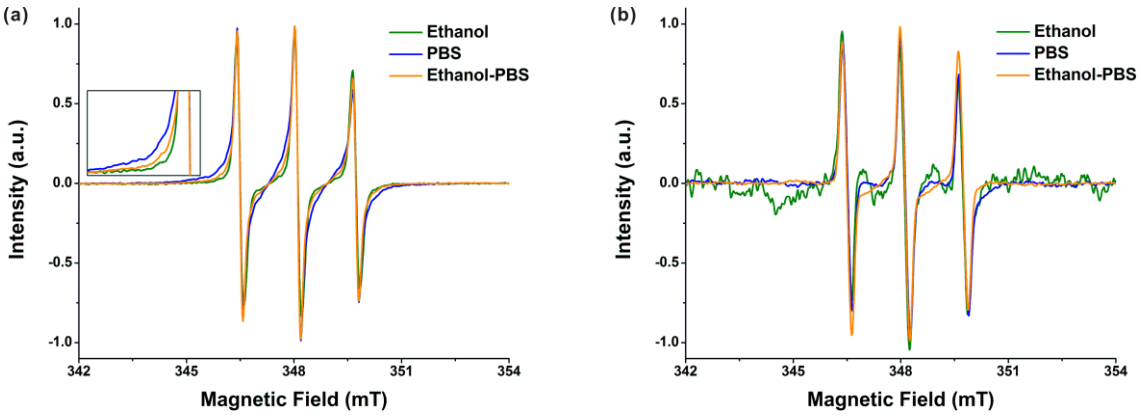

Fig. S1 The averaged EPR spectra (n = 6) of PCA in the (a) skin samples containing the SC plus viable skin and (b) viable skin of porcine ear skin after treated with 0.4 % PCA dissolved in ethanol, PBS and ethanol-PBS (1:1, V/V), respectively. The inset is a magnified spectral part.

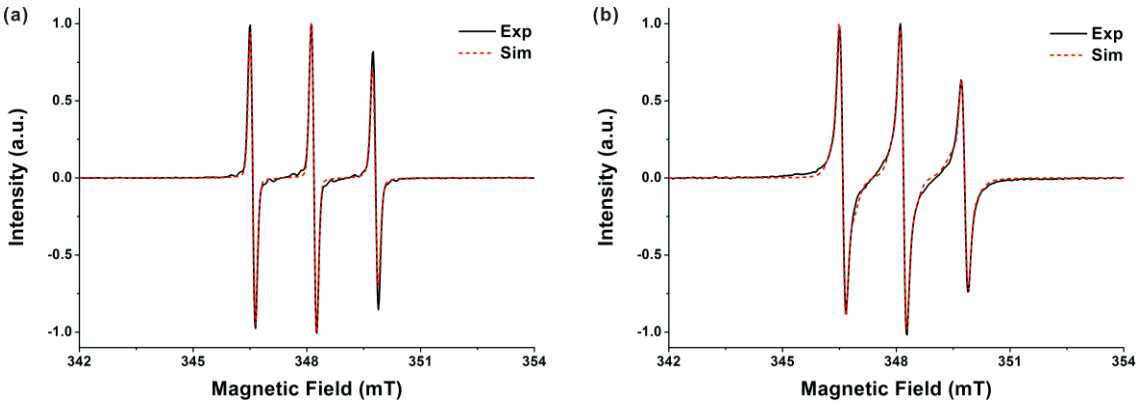

Fig. S2 Simulation examples of the EPR spectra of PCA in the human skin samples containing the SC plus viable skin exposed to 0.4 % PCA dissolved in (a) ethanol and (b) ethanol-PBS (1:1, V/V) respectively, from which the fractions of PCA with high mobility in a hydrophilic microenvironment (PCA_{mobile}) and PCA with less mobility in a less hydrophilic microenvironment ($PCA_{less\ mobile}$) were derived. The hyperfine coupling matrices (a_{xx}, a_{yy}, a_{zz}) of (15 15 106) and (13 13 102) MHz, and the *g*-matrices (g_{xx}, g_{yy}, g_{zz}) of (2.00805 2.00596 2.00212) and (2.00815 2.00596 2.00212) for PCA_{mobile} and $PCA_{less\ mobile}$, respectively, were used for the simulation. The rotational correlation time of PCA_{mobile} was about 0.1 ns.

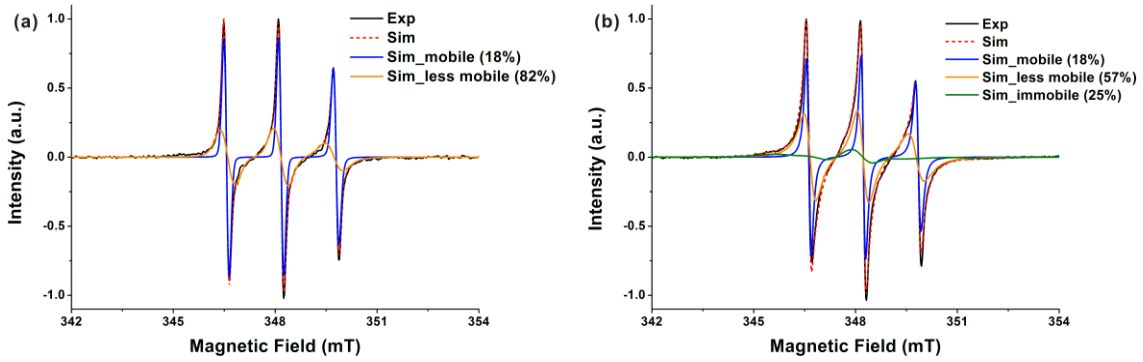

Fig. S3 The EPR spectrum of one human skin sample containing the SC and viable skin exposed to 0.4% PCA PBS was simulated as (a) two components or (b) three components. The values in the brackets represent the fractions of the components. When simulating as two components, the hyperfine coupling matrices (a_{xx}, a_{yy}, a_{zz}) of (15 15 106) and (13 13 102) MHz, the g- matrices (g_{xx}, g_{yy}, g_{zz}) of (2.00805 2.00596 2.00212) and (2.00815 2.00596 2.00212), the correlation time of 0.1 ns and 0.7 ns for PCA_{mobile} and $PCA_{less\ mobile}$, respectively, were used for the simulation. When including the third component, its magnetic parameters were the same as those of $PCA_{less\ mobile}$, and only its rotational correlation time is 6.3 ns. Thus, the third component can be regarded as PCA with slow mobility in the less hydrophilic microenvironment ($PCA_{immobile}$). Here, the summed up fraction of $PCA_{less\ mobile}$ and $PCA_{immobile}$ was equal to the fraction of $PCA_{less\ mobile}$ when simulating the spectrum as two components. Therefore, the fraction of PCA_{mobile} of did not change in both simulation strategies.

3 Discussions

The study of a newly developed skin formulation has many aspects. Among them, the selection of skin models, the ways of topical application, and the evaluation of the applied product will be discussed in this thesis. The last one contains the quantification of drugs in different skin layers, the kinetics of drug release from the vehicles, and the spatial localization of drugs and vehicles in the skin.

3.1 Selection of *ex vivo* barrier-disrupted skin models

3.3.1 *Ex vivo* barrier-disrupted skin model simulating AD skin

In the present thesis, the pH-sensitive Eudragit® L 100 NP is designed to selectively deliver Dx into the AD skin lesions. Therefore, it is the basic step to develop an *ex vivo* barrier-disrupted skin model that simulates AD skin for evaluating the cutaneous drug delivery of the pH-sensitive NP at the initial stage of formulation development. Herein porcine ear skin subjected to 30 consecutive tape strips (Tesa ®) was used as the model. Porcine skin rather than excised human skin was chosen because the shrink of human HFs after excision underestimates the HF penetration of NPs [65]. Besides, porcine skin is easily accessible and has a similar HF density to human skin (Table 1). The comparison between the barrier-disrupted porcine skin model and the *in vivo* human AD skin is illustrated as follows: i) the skin surface pH of the model is about 5.9 (see chapter 2.2), which is close to the pH value of AD patients (5.5-6.1) [46-48]; ii) the TEWL of the model is about 2.6-fold increased compared to the intact porcine skin, while the TEWL of AD skin is found 2-fold higher than that of healthy human skin [52,207]; iii) the skin permeability of the model is significantly increased (see chapter 2.1), which is also evidenced in AD skin [53,54]; iv) the SC thickness of the model is reduced to 5 μm, which resembles the fact that the AD skin has a thinner SC compared to healthy human skin, although the absolute SC thickness of the model is different from that of the AD skin [208-210]. These similarities show that the *ex vivo* barrier-disrupted model could simulate the AD skin to some extent and could be useful for the evaluation of dermal formulations at the early development stage.

Besides, the performance of 3 times CS resulted in a similar SC thickness left on the porcine ear skin. This indicates that the barrier-disrupted skin established by 3 times CS may have a similar skin surface pH and permeability compared to the skin model developed by 30 tape

strips. However, different from TS, CS has been reported to impair the infundibulum of HFs apart from removing the SC [87]. The unpublished data of the present thesis show that the amount of the Rhodamine-labeled compound in the HFs of barrier-disrupted human skin was remarkably higher than that in the HFs of intact skin. Moreover, the transfollicular penetration of the dye was also observed in the HFs of barrier-disrupted skin (Figure 5). These results show that the impairment of HFs by CS could enhance the HF penetration of drugs and the following transfollicular penetration. Thus, CS could generate a comparable *ex vivo* barrier-disrupted skin model as TS when the skin is bare of HFs.

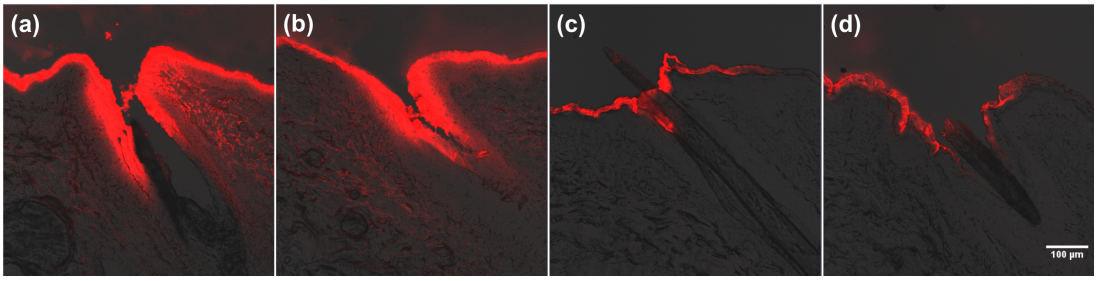

Figure 5 CLSM images of HFs of excised male human abdominal skin whose skin barrier was impared by 4 times CS (a-b) or intact (c-d) after application of a Rhodamine-labeled compound dissolved in PBS-DMSO (95/5, V/V) without massage and incubated for 2 h at 32 °C (unpublished data of the present thesis).

3.3.2 *Ex vivo* skin models with different levels of barrier disruption

Apart from establishing an *ex vivo* skin model to mimic AD skin, the efficiency of TS for removing the SC also provides a reference to inducing different levels of barrier disruption in excised human skin (see Chapter 2.1). The most ordered skin lipids are found at the depth of 20-40% of the human SC, indicating the highest skin barrier function of this region[211]. With the performance of less than 10 tape strips (Tesa®), the SC region of the highest barrier function remains and thus the barrier disruption can be considered as a mild level (Figure 6). When 15 tape strips are applied, the SC region of the highest barrier function is partly removed, resulted in medium skin barrier disruption. After being subjected to more than 20 tape strips, the SC region of the highest barrier function is already removed, leading to a strong barrier disruption. With 50 tape strips, the human skin model without the SC barrier can be attained. The above *ex vivo* skin models with different levels of barrier disruption could meet different experimental requirements. For example, a skin model with mild barrier disruption is suitable for delivering more PCA into the viable skin to study the skin radical formation, meanwhile avoiding the generation of radicals due to invasive treatments [212].

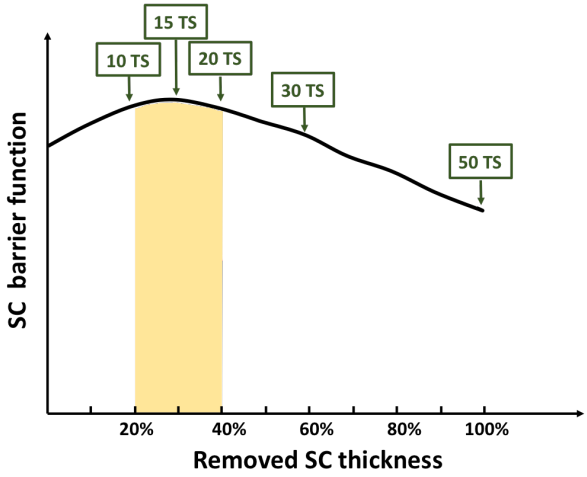

Figure 6 *Ex vivo* human skin with different levels of barrier disruption established by tape stripping (TS). The SC barrier function curve is referred to the publication by M. E. Darvin et al. [211]

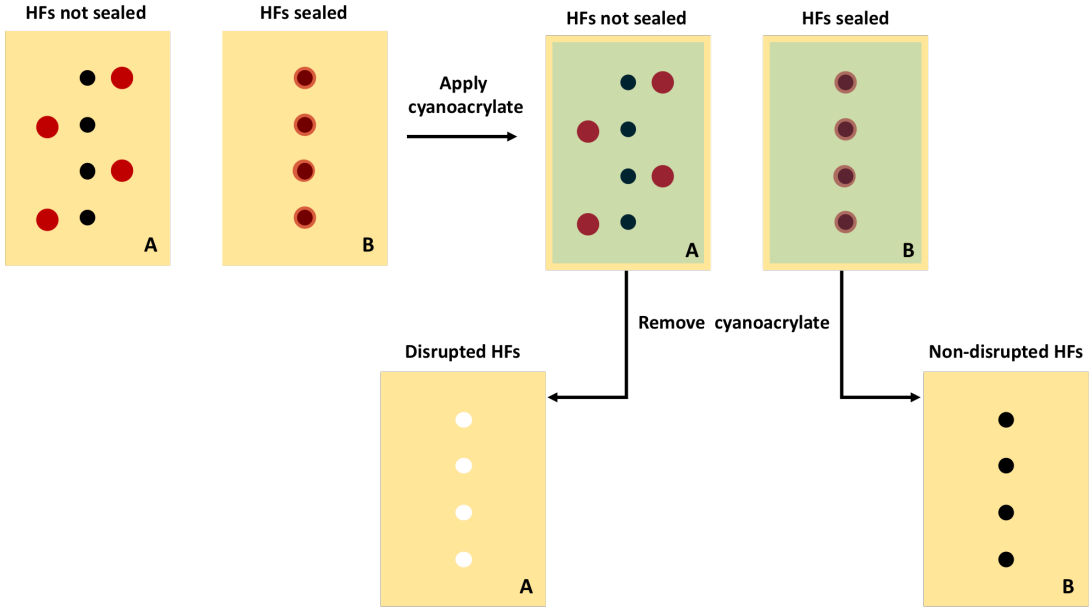

Figure 7 A propsoed skin model with infundibulum disruption of HFs for studying the influence of the HF impairment induecd by CS on skin penetration of drugs. The black, whilte, and red dots represent intact HFs, impaired HFs and sealing material, respectively. The green shadow means cyanoacrylate glue. A and B are two skin areas from the same skin sample with the same HF density.

3.3.3 *Ex vivo* skin model with follicular barrier disruption

The ability of CS to impair HFs provides a strategy for studying the influence of HF disruption on skin penetration of drugs. As illustrated in Figure 7, the skin sample whose hairs are cut

shortly is divided into two parts (A and B), and their HF densities are similar. For part A, the HF sealing material is dropped beside each HF. For part B, all the HFs are sealed [213]. The sealing material is a varnish-wax mixture that rarely affects the SC barrier [18,214]. Subsequently, the cyanoacrylate glue is applied to the skin surface. By removing the solidified cyanoacrylate glue, the HFs of part A are impaired while the HFs of part B remain intact due to the protection of the sealing material. Later on, the difference in the skin penetration of drugs between samples A and B is accounted for the influence of HF disruption. In short, TS and CS have been shown their utilities in establishing different *ex vivo* barrier-disrupted skin models according to various experimental designs.

3.2 Ways of topical application

3.2.1 Occlusion and non-occlusion

The application of formulations to the skin is classified into two ways according to whether an impervious-to-water covering is applied to after the topical administration, i.e., occlusion and non-occlusion. In the investigation of the cutaneous drug delivery of the pH-sensitive NP, the skin samples were incubated in a wet chamber with a humidity of RH 98% (see chapter 2.2). The wet chamber was used to mimic the occlusion condition since the area of the treated skin sites did not fit to the size of the commercial occlusion device, Finn Chamber. Another occlusive material, plastic film, is size-adjustable, yet it leads to overspread of the suspension to the untreated skin area. In the study of the solvent effects on the skin penetration of PCA, the skin samples were occluded by Finn Chamber to enhance the drug skin penetration (see chapter 2.3). However, H. Maibach et al. have reviewed seven original *in vivo* studies about the occlusion effect on the transdermal penetration of compounds and found that occlusion does not uniformly improve the drug flux across the skin, and a correlation between the octanol-water partition coefficient of a compound and its occlusion-induced enhancement has not been determined [115]. Yet, this review neglects the influence of occlusion on vehicles, which also plays an important role in the skin penetration of drugs.

The occlusion effects on vehicles are discussed in three aspects. i) When a formulation contains volatile solvents, the effect of occlusion could be two-edged. If drugs dissolved in a volatile solvent undergo recrystallization due to the evaporation of solvents under non-occlusion, then occlusion could reduce the solvent evaporation and prevent the decrease of the concentration of drugs. This is evidenced in the skin penetration of PCA dissolved in absolute ethanol (see chapter 2.3). Although an aluminum Finn Chamber was used to cover

the treated skin areas, the sealing of the chamber is not effective enough to prevent the evaporation of ethanol, as reported previously [215]. PCA at a concentration of 0.4% in absolute ethanol was observed to aggregate into while powders on the skin after 40 min at 32 °C. Consequently, the skin penetration of PCA was significantly low. If drugs dissolved in a volatile solvent and the solvent evaporation generates a supersaturated solution under non-occlusion, then occlusion could be unfavorable. Several studies have used the combination of volatile and non-volatile solvents to generate a supersaturation solution of drugs through the evaporation of the volatile solvents under the non-occlusive condition to enhance dermal absorption of drugs [216,217]. ii) When a formulation has the occlusive effect by itself such as ointment and lipid-based NPs, an extra occlusion by plastic film might be unnecessary [218]. For example, J. Bouwstra et al. found that the non-occlusive method favored the lipophilic fluorescent dye that incorporated in liposomes penetrating into excised human skin compared with occlusion condition [219]. Another study reported that the penetration of paraben esters into human epidermis following the commercial ointment was significantly decreased by occlusion in comparison to non-occlusion [220]. The reasons might be the generation of the occlusive layer by formulations, changes of drug release kinetics and interactions of skin and formulations under non-occlusion condition [219,220]. iii) When water loss affects the drug release of formulations, then occlusion is indispensable. Especially for some polymeric NPs, external or internal aqueous phases are crucial for the structure and drug release of NPs [221,222]. Dryness due to non-occlusion should be avoided. For example, thermoresponsive nanogels release their incorporated molecules through the expulsion of inner water molecules upon volume phase transition [222]. Therefore, occlusion may prevent the collapse of the nanogel structure. The drug release of NPs triggered by pH or enzymes needs an aqueous medium, otherwise, drugs are restricted inside NPs and hardly penetrate into the skin. Occlusion ascertains an aqueous environment for ion-exchange processes and enzymatic reactions, which is crucial for the drug release of pH- or enzyme-triggered NPs.

3.2.2 Massage

Using massage to apply the suspension of NPs onto the skin has been demonstrated to improve the HF penetration of NPs compared with the application without massage [25]. In the present thesis, a 2 min-massage was used to spread the suspension of the pH-sensitive NP on porcine skin to evaluate the HF penetration of the NPs. The mechanism suggested by R. Netz et al. is that the oscillating radial hair motion generated by massage could transport NPs into HFs [223]. However, this mechanism ignores the influence of the external medium in which NPs are dispersed. Moreover, the mechanism cannot be applied to the cases of liquid and

semi-solid formulations. Whether massage favors the HF penetration of drugs dissolved in liquid vehicles has not been answered. One evidence is the *in vivo* HF penetration of caffeine in ethanol-propylene glycol (3:7, V/V) without massage. In this study, the volunteers were not allowed to cover or touch the test skin areas, therefore the friction between the clothes and skin that might resemble the massage can be ignored [18]. The unpublished data of the present thesis also show that a Rhodamine-labeled compound dissolved in Transcutol® HP freely diffuses into HFs of the excised abdominal human skin without any massage (Figure 8). The shared feature of the Transcutol® HP and the ethanol-propylene glycol is low surface tension (31 mN/m) [224,225]. The surface tension is positively correlated to the contact angle of a drop of a solution on the skin surface [226]. For example, the contact angles of water and ethanol on the skin surface are 88º and 0º, respectively, and their surface tension values are 72 mN/m and 22 mN/m, respectively [227]. Therefore, the contact angle or the surface tension is presumed to play a role in the HF penetration of liquid formulations.

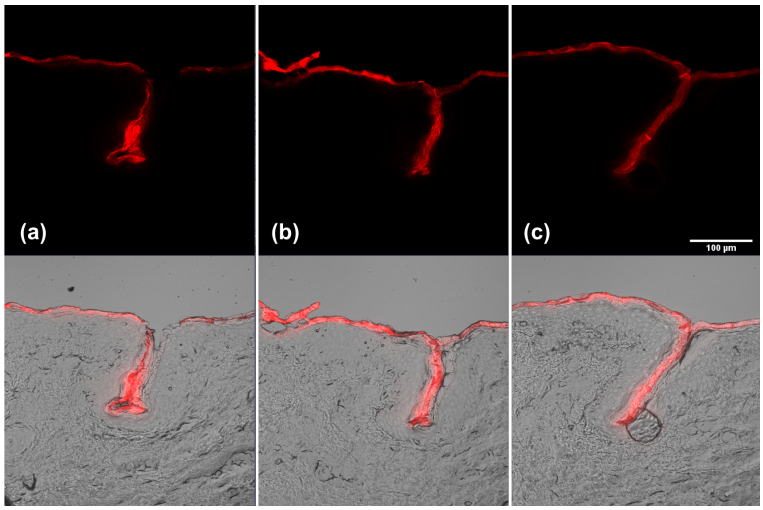

Figure 8 CLSM images of three vellus HFs (a-c) of the excised abdominal human skin whose SC was partially removed by 2 times CS that was applied a Rhodamine-labeled compound dissolved in Transcutol® HP (Gattefossé, France) without massage and incubated for 2 h under 32 °C. The upper row represents images obtained using the fluorescent channel, and the lower row represents the superimposed images obtained by transmittance and fluorescence modes.

HF can be regarded as a capillary with one side closed. The influences of massage on the HF penetration of liquid formulations may be categorized into two cases. i) When a solution has a high contact angle to the skin surface, it hardly goes into HFs. An externally applied lateral vibration has been found to dynamically reduce or increase the contact angle of a water drop on a hydrophobic substrate [228]. Therefore, massage may produce a lateral vibration on the drops of liquid formulations. When the dynamic contact angle of the drops to the skin surface

is reduced, the HF penetration of the drops might be facilitated. ii) When a solution has a very low contact angle to the skin surface, it may enter HFs without massage, as presented in Figure 8. The upper limit of the surface tension of a liquid formulation that does not need the massage to enter HFs needs further studies. A liquid formulation that targets HFs without massage is low-cost and easily applicable in the clinic compared to NPs. The experimental designs in chapter 2.2 and chapter 2.3 provoke thoughts on the necessities of using occlusion and massage to promote the skin drug delivery.

3.2.3 Setups for studying skin penetration and permeation of drugs

Although Franz diffusion cell approach has a drawback of excess skin hydration, it is undoubtedly an important method to study skin penetration and permeability of drugs *in vitro* [75]. In the present thesis, Franz diffusion cell approach was utilized to evaluate the levels of barrier disruption induced by TS by analyzing the skin permeability change (chapter 2.1). For the skin penetration studies of DxPCA loaded pH-sensitive NPs and PCA solutions, intact porcine ear with the whole skin structures and cartilage and full-thickness human skin were used to mimic *in vivo* skin conditions (chapter 2.2 and 2.3).

3.3 Evaluation of dermal drug delivery systems

A comprehensive evaluation of the cutaneous drug delivery of a formulation covers the drug release from vehicles, the quantification of drugs penetrated into the skin, and the spatial localization of drugs and vehicles. Besides, the evaluation cannot be fulfilled without appropriate techniques. The following discussions are centered on these four aspects, based on the investigations in this thesis.

3.3.1 Drug release of formulations on skin

Drug delivery system of pH-sensitive NP

The pH-sensitive NP exhibited a burst drug release *in vitro* when the pH of the external medium is increased to 5.9. However, the drug release of the NPs on the intact porcine skin was hardly detectable by EPR and the release on the barrier-disrupted porcine skin was slow due to the limited water content on the skin surface (chapter 2.2). The difference in the drug release of the NPs between the intact and barrier-disrupted skin could be explained by the SC barrier function. The NP is formed via the precipitation of the carrier Eudragit® L100 when

Eudragit® L100 solution is added to a non-solvent. Re-dissolving or swelling of Eudragit® L100 needs enough external aqueous medium, hydroxyl ions and buffer capacity [206]. The intact porcine skin has a skin surface pH above 5.9, which meets the pH required to dissolve Eudragit® L100; however, the water content on the skin surface is very limited and hardly alters the NP structure. The barrier-disrupted porcine skin whose SC is partly removed permits an increased exchange between the endogenous liquid of the skin (~ pH 7.2) [229] and the external aqueous medium of the NP suspension (pH 4.1) [230]. During the exchange, the pH of the external medium of NPs is gradually elevated, which could slowly change the NP structure to release the drugs. AD skin lesions also have a disrupted SC barrier and an increased skin surface pH (5.5-6.1) [46-48] and would allow the aforementioned medium exchange [46]. Therefore, this pH-sensitive NP may hold promise for targeted drug release on AD skin lesions.

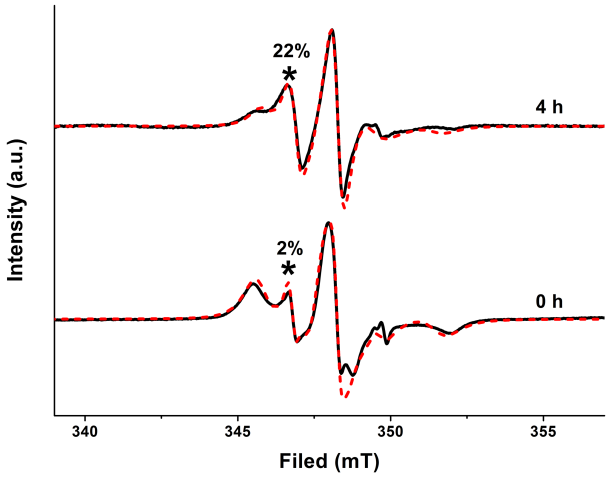

Figure 9 EPR spectra of the pH-sensitive NPs before and after applied onto the surface of the artificial sebum layer for 4 h (unpublished data of the present thesis). The black solid and red dash lines are experimental and simulated spectra, respectively. The peak marked by the asterisk represents DxPCA outside the NPs. The percentage of DxPCA outside the NPs was obtaind from the simulation.

Additionally, the transfollicular penetration of the model drug Nile red following the pH-sensitive NPs indicates the drug release inside porcine HFs. The pH of the porcine HFs is 6.5-7.4, which could theoretically trigger the NPs to release DxPCA [70]. However, HFs are considerably dry but abundant in sebum which is secreted by the associated sebaceous gland. The unpublished data of the present thesis show that sebum could improve the drug release of the pH-sensitive NPs. As shown in Figure 9, the fraction of DxPCA outside the NPs was increased from 2% to 22% after the NPs were applied to the surface of an artificial sebum layer for 4 h. A. Vogt et al., reported a similar finding, showing that the retention of polylactic acid NPs in sebaceous glands was accompanied by the release of the loaded Nile red to the

viable epidermis [231]. These results reflect that many endogenous components of the skin may influence the drug release of the pH-sensitive NPs.

Besides HFs, sebum forms a lipid film with a thickness of 0-4 µm on the skin surface, which mainly comprises triglycerides, wax esters and squalene [232]. In practice, this sebum film would be the first contact for any skin formulation. The influences of this sebum film on the skin penetration of drugs following different vehicles should be considered, such as changing the contact angle of a liquid formulation to the skin surface and the drug release of vehicles [233,234]. Otherwise, the sebum film should be removed before applying a formulation onto the skin to avoid any influences of sebum.

Penetration enhancer strategy by solvents

Different from the pH-sensitive NP, no drug release exists for the PCA ethanol aqueous solutions applied on the skin (see chapter 2.3). Nevertheless, the cutaneous penetration of PCA could be adjusted by changing the compositions of the penetration enhancers of ethanol and water in the solvents [113]. Physiochemical properties of the drug and influences of the penetration enhancers on the skin mainly determine the skin penetration of PCA.

Both penetration enhancers and NPs have their respective advantages. Polymeric nanocarriers with outstanding characteristics endow NPs with tailored drug release and specified targeting. Moreover, NPs are promising vehicles to transport hydrophilic macromolecules into skin [140]. Therefore, NP vehicles would be a superior choice when the aim is sustained or delayed or targeted drug delivery into skin, or improving the skin penetration of macromolecules [134,138,140]. Penetration enhancers are easily accessible, low-cost and flexible to make various combinations to meet different demands [235]. Thus, penetration enhancers could be used when a high drug delivery into the skin is the main purpose and the respective cost is limited.

3.3.2 Quantification of drugs in the skin

Drug delivery system of pH-sensitive NP

The pH-sensitive NP was found to deliver significantly more DxPCA into both intact porcine skin and barrier-disrupted skin compared to the reference cream (chapter 2.2). Possible reasons for the penetration enhancement of DxPCA by the pH-sensitive NP are discussed as follows. The concentration of DxPCA molecularly dispersed in the NPs (C_v) is increased, which

improves the flux of DxPCA into the skin, according to Fick´s first law of diffusion (Equation 1). DxPCA is a poorly water-soluble drug whose solubility in water is about 89 µg/ml. The total concentration of DxPCA in the suspension of NPs is 320 µg/ml, which contains 2.4% of DxPCA in the external medium (equal as 7.68 µg/ml) and 97.6% of DxPCA encapsulated inside the NPs (Figure 10). With knowing the loading capacity of the NP (5.5%) [205] and the density of Eudragit® L100 (0.85 g/cm^3), the concentration of DxPCA in the NPs is calculated as 46.75 mg/ml that is 525-fold higher than its water solubility. Despite the high concentration, DxPCA molecules inside the NPs are found in an amorphous state [205]. This demonstrates that Eudragit® L100 has good compatibility with DxPCA [236]. In contrast, the reference cream with the same concentration only had a few DxPCA dissolved and a majority of DxPCA aggregated (see chapter 2.2). The DxPCA aggregates have to dissolve first before entering into the SC. Similar amounts of DxPCA following the cream in both intact skin and barrier-disrupted skin indicate that the dissolution of DxPCA aggregates is a rate-limiting step for the cutaneous penetration of drugs from the cream. For the NPs, the release of DxPCA is a determinant for the skin penetration of drugs and no dissolution of DxPCA is needed. The controlled drug release of NPs might favor the skin penetration of DxPCA. However, the relationship of the drug release from NPs with the skin penetration of drugs needs further research.

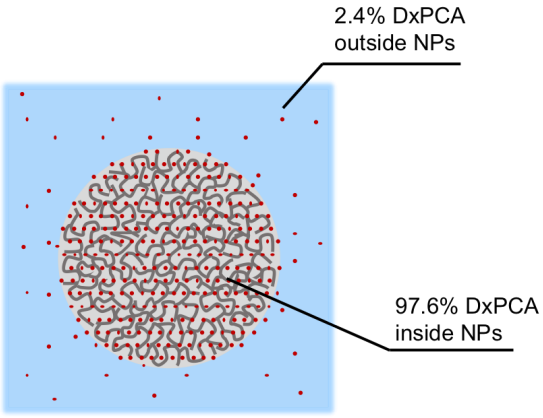

Figure 10 Proposed localization of the drug DxPCA in the suspension oft he pH-sensitive Eudragit® L100 NP. The blue background represents the external aqueous medium.

Using the pH-sensitive NP, the amount of DxPCA delivered into the viable skin layers of the barrier-disrupted skin was doubled compared to that of the intact skin. This could be due to not only the increased skin permeability to DxPCA of the barrier-disrupted skin but also the more and faster drug release of the NPs on the barrier-disrupted skin (see chapter 3.3.1). The viable skin layers are the target for the treatment of AD. The higher amount of drugs delivered to the viable skin layers of the barrier-disrupted skin shows the possibility of using the pH-

sensitive NP to selectively exert efficacy on the lesional skin sites and reduce the side effects of Dx on uninvolved skin of the AD patient.

Now it raises the question about where the DxPCA molecules in the viable skin layers originate considering that the NP suspension contains both free and encapsulated DxPCA molecules. The NP suspension applied onto skin included 0.27 nmol/cm^2 of free DxPCA and 11.20 nmol/cm^2 of encapsulated ones. The amount of DxPCA in the viable skin layers of barrier-disrupted skin is 0.5 nmol/cm^2, which is much higher than the amount of free DxPCA applied onto the skin. Therefore, it can be concluded that DxPCA in the viable skin layers of the barrier-disrupted skin at least partly belongs to the encapsulated DxPCA which is released from the NPs before entering the viable skin layers. For the intact skin, 0.25 nmol/cm^2 of PCA is found in the viable skin layers, which is similar to the applied amount of free DxPCA. Thus, it is difficult to determine the attribution of DxPCA in the viable skin layers of the intact skin only based on the amounts of drugs in the skin. However, the EPR spectrum of DxPCA in the viable skin layers of the intact skin indicates a restricted microenvironment around DxPCA, similar to that of DxPCA in the NPs (see chapter 2.2). Additionally, the CLSM results show that the NP penetrated into the HFs of the intact skin. Altogether, it could be concluded that part of DxPCA in the viable skin layers of the intact skin belongs to DxPCA from the NPs.

Table 2 Comparsion of different NP-based drug delivery systems for delivering Dx into skin

NP types	Loading capacity [a]	*In vitro* drug release in PBS [b] (Sink condition)	Skin penetration enhancement [c] (Skin type)	Ref.
pH-sensitive Eudragit® L100 NP	5.5%	~90% in 4 h (Sink)	~6.6-fold in 4 h (Whole porcine ear)	205
Solid lipid NP	0.75%	~20% in 4 h (Sink)	~2-fold in 4 h (Whole porcine ear)	136,237
CMS NP	2-5%	~80% in 4 h (Non-sink)	~3.9-fold in 6 h (Full-thickness human skin)	132,238, 239
β-cyclodextrin decorated Nanogel	4.1%	~28% in 4 h (unknown)	~4-fold in 4 h (Full-thickness human skin)	240
Nanocrystal	100%	~100% in 4 h (Sink)	~2.7-fold in 6 h (Full-thickness human skin)	241

[a] Loading capacity is the ratio of the mass of loaded drugs to the mass of nanocarriers.
[b] Percentage of drugs released from NPs compared with the applied dose.
[c] The ratio of the total amount Dx delivered by NPs into skin to that of using a cream.

Penetration enhancer strategy by solvents

The cutaneous penetration of hydrophilic drugs is not easy owing to the hydrophobic SC layer [242]. For instance, the hydrophilic caffeine formulated in a hydrogel is found only 1.66% of the applied dose to penetrate into the excised human skin after 24h exposure; whereas the amount lipophilic tocopherol delivered by the same hydrogel into the skin is 10.54% of the same applied dose [243]. In the present thesis, PCA is used as a hydrophilic model drug. The amount of PCA transported into the excised human skin by ethanol-PBS (1:1) was the highest among the three solvents; however, it only accounted for 0.63% of the applied dose after 40 min exposure, which is in line with the published literature [242,243].

Water is the primary penetration enhancer for hydrophilic drugs; ethanol is a widely used penetration enhancer; both have simple molecular structures and are low toxic to the skin [113]. In the present thesis, ethanol did not show its superiority in improving the skin penetration of PCA among the three solvents, ethanol, ethanol-PBS (1:1) and PBS. Evidenced by the white PCA aggregates on the skin surface, one reason could be that the concentration of PCA in ethanol is so high (0.4% W/V) that PCA crystallizes during the ethanol evaporation. Then the concentration of molecular PCA in the vehicle (C_v) is reduced and consequently the flux of PCA into the skin is reduced (Equation 1). Another reason could be that the dehydration of the SC by the absolute ethanol decreases the solubility of hydrophilic PCA in the skin membrane (S_m), which results in the decrease of PCA partitioning into the SC (Equation 1) [126,244]. The results reveal that using absolute ethanol to improve the skin penetration of drugs could be less controllable, namely the formation of supersaturation or crystallization of drugs due to the ethanol evaporation would lead to enhanced or reduced skin penetration of drugs. Therefore, ethanol should be combined with other penetration enhancers.

The mechanisms that ethanol improves the skin penetration of drugs are still debatable concerning whether ethanol affects the SC barrier function by extracting the skin lipids or disordering the intercellular lipid bilayers [118,120]. However, these conclusions strongly influenced by experiment designs, such as the type of skin samples (i.e. *in vivo* skin and the separated SC), duration of the exposure time and the sensitivity of the measurement techniques. Absolute ethanol was found to penetrate into human skin *in vivo* and extract appreciable amounts of lipid from the SC investigated by infrared spectroscopy [118]. In the present study, the excised human skin was exposed to absolute ethanol for 40 min, therefore ethanol probably penetrated into the skin samples and removed a certain amount of skin lipids from the SC. At the molecular level by using synchrotron X-ray diffraction, ethanol is not observed to change the short or long lamellar spacing of the separated human SC after being

treated for 24 h [245], meanwhile, the structure change of the keratin fibrils in mice SC increases with the concentration of ethanol after 2 h exposure [120]. Therefore, the keratin structure of the excised human skin might be altered in 40 min exposure to absolute ethanol.

PBS was as good as ethanol-PBS (1:1) to deliver PCA into the skin, indicating that water could play an important role in promoting the skin penetration of hydrophilic drugs. In this PBS, water takes up more than 99% besides the potassium and sodium salts, therefore the effect of water on the skin is mainly considered, although potassium and sodium ions are reported to penetrate into the skin [246]. With 40 min exposure, the SC hydration of the excised human skin could be increased to about 55% [247]. The SC hydration, as a result of water uptake in corneocytes and the short lamellar lipid structure of the intercellular skin lipids [248], could facilitate hydrophilic PCA dissolving in the SC. Additionally, a drag effect imposed by the penetration of water might simultaneously enhance the skin penetration of PCA [249].

Table 3 Ethanol concentrations of ethanol-water mixtures that better improves the percutaneous penetration of drugs.

Drugs	Skin types	Ethanol concentration [a]	Ref
Ibuprofen	Human epidermis	50-75%	[235]
Melatonin	Full-thicknes rat skin	50-60%	[250]
Naloxone	Full-thicknes rat skin	66%	[251]
Nitroglycerin	Human epidermis	50-70%	[126]
Oestradiol	Human epidermis	40-60%	[127]
Sodium salicylate	Human epidermis	63%	[125]

[a] Among the ethanol concentrations of 0-100% [125,126,235,250,251] or 0-90% [127] in the ethanol-water mixtures, the concentration that better improves the cutaneous penetration of drugs.

Many studies have reported the synergetic effect of ethanol-water mixtures on improving the percutaneous penetration of both lipophilic and hydrophilic drugs (Table 3). Among the ethanol concentrations in the range of 0-100% or 0-90%, the ethanol-water mixtures at an ethanol concentration of 40-75% are generally observed to produce a higher drug flux across the skin [125-127,235,250,251]. The present investigation found that ethanol-PBS (1:1), namely the ethanol-PBS at the ethanol concentration of 50%, delivered more PCA into the viable skin layers of both the human and porcine skin *ex vivo* compared to PBS and absolute ethanol, which is in line with the published studies. The synergetic effect of ethanol-water mixtures on enhancing the skin penetration drugs might be explained as follows. The skin uptake of ethanol increases with increasing the ethanol concentration in the ethanol-water mixtures, whereas up to a certain ethanol concentration the skin uptake of ethanol starts to decrease due to the SC

dehydration [125,126]. Meanwhile, the skin uptake of water decreases with the increase of the ethanol concentration in the ethanol-water mixtures [127]. Both water and ethanol uptaken into the skin could change the structures of lipids and corneocytes of the SC, pose solvent drag effect [249], and modify the partitioning of hydrophilic and lipophilic drugs between the solvent and the SC [120,127]. Therefore, an ethanol-water mixture that maximizes the above effects for a certain drug could result in a synergetic effect on the skin penetration of this drug.

3.3.3 Spatial localization of drugs and vehicles

Drug delivery system of pH-sensitive NP

The spatial localization of drugs and vehicles is of clinical significance: drugs in different skin layers or structures are related to the clinical efficacy; cutaneous penetration of vehicles is concerned about their skin toxicity. For the pH-sensitive NP, the loaded drug DxPCA was delivered into the SC and viable skin layers of both the intact and barrier-disrupted porcine skin. DxPCA in the SC could be localized in the intercellular skin lipids according to the finding by K. Yamamoto et al. using soft X-ray spectromicroscopy [252]. DxPCA in the viable skin layers might be both inside the viable cells and in the intercellular space since Dx has been found to enter the viable keratinocytes and fibroblasts [253]. As for the localization of the NP, the finding that DxPCA in the viable skin layers of the barrier-disrupted skin was outside the NP suggests that: i) the NPs of 303 nm in size do not readily penetrate across the disrupted SC barrier, let alone the intact SC barrier, which is consistent with the published literature [152,254]; ii) the loaded drug DxPCA could be firstly released from the NPs and then penetrated into the viable skin not the other way around. Besides, CLSM observed the accumulation of the Nile red loaded NP in HFs of the intact porcine skin, demonstrating the localization of the NPs in HFs.

Concerning the HF penetration, the NP showed no advantages over the reference cream in the depth of transporting Nile red into HFs; however, the cumulative intensity of Nile red in HFs following the NP was significantly higher than that of using the cream. The HF penetration depth has been often used as the parameter to assess the HF target of different formulations [24,36]. The present study reveals that the total amount of drugs in HFs is another important parameter. Moreover, the transfollicular penetration of Nile red from the NPs indicates that the pH-sensitive NP could serve as a reservoir where the drug Dx could be slowly released and the following transfollicular penetration could provide a shortcut to deliver Dx into deeper viable skin layers, i.e. the skin target to treat AD. Here the HF penetration of the NPs is driven by the oscillating radial hair motion due to the massage [223]. Yet, the mechanism of the HF penetration

of semi-solid cream has not been reported. The relationship of the rheologic change of creams upon massage with the HF penetration would be interesting for future studies [255].

Penetration enhancer strategy by solvents

For the one-component solvents of water and ethanol, their skin penetration amount and depth largely depend on the exposure time. In the present study, excised human and porcine skin were exposed to the solvents for 40 min. Possible localization of the solvents in the skin are discussed as follows. The *in vivo* study from René M. Rossi found that the human SC is hydrated from the depth of 0 μm to 8 μm after 30 min exposure to water [247]. Additionally, Joke A. Bouwstra et al. conclude that no free water is present in the deepest layers of the SC although the SC hydration reaches 300% [116]. Therefore, it can be inferred that in the present study water could penetrate into the SC but may not reach the VE of the skin. An *in vivo* study using microdialysis found the transdermal penetration of absolute ethanol after 30 min. Thus, an appreciatable amount of ethanol could be expected to penetrate into the SC and viable skin layers of the *ex vivo* human and porcine skin. For the solvent of ethanol-PBS (1:1), ethanol could penetrate into the viable skin layers according to the finding that volunteers are measured ethanol in their blood after 10 min exposure to 55% ethanol solution [256]; while the other component water may localize in the SC. Yet, *in vivo* dermal or transdermal penetration of water has not been investigated.

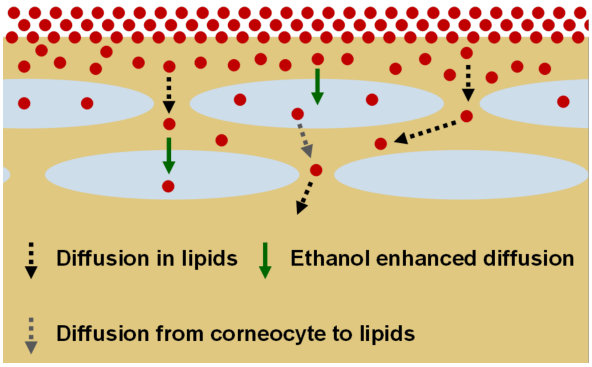

Figure 11 Diffusion of PCA molecules (red dots) in the SC illustrated by i) black dash arrow: in the intercellular lipids (yellow-brown background); ii) green arrow: ethanol enhanced diffusion from the lipids to corneocytes (blue gray elipsoides); iii) grey dash arrow: a low-possibility diffusion from corneocytes to the lipids.

Regarding the localization of drugs, the amount of PCA in the SC by using PBS was higher than that of using ethanol-PBS (1:1), although the total amounts of PCA delivered by these two solvents into the skin were similar. This reflects that solvents could influence the macroscopic localization of drugs. In the microscopic view, PCA in the SC was found to

localize in both the intercellular lipids and corneocytes when using the three solvents. Moreover, the percentage of PCA in the intercellular lipids increased with the decrease of ethanol concentration in the vehicle (see chapter 2.3).

The hypothesis about the solvent effects on the spatial localization of PCA in the SC is described in Figure 11 When the skin is exposed to PCA PBS solution, water molecules penetrate into the skin would first go into the skin lipids and then diffuse into corneocytes since corneocytes are embedded in the skin lipids [248]. The diffusion of water into the intercellular lipids increases the partitioning of PCA from the solvent into the intercellular lipids and has a drag effect on the diffusion of PCA into the lipids [249]. Subsequently, PCA may diffuse into corneocytes when the concentration of PCA in the intercellular lipids is high enough to drive this process. This could explain why a higher percentage of PCA is in the intercellular lipids when the solvent PBS is used. Besides, the natural moisture factors in corneocytes provide a more hydrophilic microenvironment, and the solubility of PCA in corneocytes is theoretically higher than that in the intercellular lipids. Thus, PCA molecules that diffuse into corneocytes may hardly diffuse out of the corneocytes. When the solvent contains ethanol, D. Horita et al. reported that ethanol induces structural changes in the short lamellar and the keratin fibrils with an increase in ethanol concentration [248]. Thus, the diffusion of PCA from the intercellular lipids into corneocytes could be enhanced by ethanol. This could be why a higher ethanol concentration in the solvent results in a lower percentage of PCA in skin lipids. Above all, the intercellular pathway might be dominant for the skin penetration of the hydrophilic chemical PCA; meanwhile, the transcellular pathway might exist too. The coexistence of intercellular and transcellular pathways has been demonstrated by modeling and experiments [257,258]. Additionally, PCA in the viable skin layers could be mostly in the intercellular space of viable skin cells because the cell membrane permeation of the hydrophilic PCA is very low [259].

The skin penetration behaviors of the DxPCA loaded pH-sensitive NP and PCA dissolved in the ethanol-PBS (1:1) solvent are summarized in Table 4. The NP could control the release of DxPCA and exhibited an enhanced drug release on the barrier-disrupted skin, whereas the drug release of PCA was out of the reach of the ethanol-PBS solvent. Both the NP and the solvent transport drugs into the SC and the viable skin layers. However, two drugs have different spatial localization in the SC; DxPCA is demonstrated to be in the intercellular lipids [252], while hydrophilic PCA could be in both the intercellular lipids and corneocytes. Concerning the localization of vehicles, the NP may only stay on the SC, while ethanol in the ethanol-PBS (1:1) probably goes into the SC and the viable skin layers [256]. Besides, the high deposition of the NPs in HFs implies that HFs would be a potential reservoir for the transfollicular

penetration of drugs from NPs. The HF penetration of PCA dissolved in ethanol-PBS (1:1) needs further investigations.

Table 4 Skin penetration behaviors of the DxPCA loaded pH-sensitive NP and PCA dissolved in the ethanol-PBS (1:1) solvent [a].

Formulations	Drug release	Spatial localization of drugs and vehicles							
		SC				Viable skin layers		HFs	
		Intercelluar lipids		Corneocytres					
		Drug	Vehicle	Drug	Vehicle	Drug	Vehicle	Drug	Vehicle
DxPCA loaded pH-sensitive NP	Yes	Yes $_{252}$	No	No	No	Yes	No	Yes	Yes
PCA in ethanol-PBS (1:1)	No	Yes	Yes	Yes	Yes	Yes	Yes	NA	NA

[a] The skin samples were exposed to the DxPCA loaded pH-sensitive NPs and PCA dissolved in the ethanol-PBS (1:1) solvent for 4 h and 40 min, respectively. NA means not available.

3.3.4 Techniques used in the skin penetration studies

Tape stripping (TS) and cyanoacrylate stripping (CS)

The application of TS and CS to establish barrier-disrupted skin models has been discussed in chapter 3.1. The following discussion is focused on the use of TS and CS in quantifying the skin penetration of drugs. TS is commonly used to harvest the whole SC for quantifying drugs in the SC. Yet, the number of TS needed to completely remove the SC is influenced by many factors such as brand, pressure and skin types [92]. Moreover, TS is labor-intensive. For example, in the present study, it takes about 60 min to perform 100 tape stripes to remove the entire SC of porcine skin. In comparison, the CS method is efficient and every CS could remove 2-2.5 μm thick SC. This implies that drugs quantified from the consecutive number of CS could be approximately correlated to the skin depth.

TS and CS methods are also combined to quantify drugs in HFs, namely differential tape stripping which is a direct, non-invasive approach to quantify drugs in HFs [87]. In this approach, 100 consecutive tape strips are applied to remove the SC, and then one CS is used to remove the infundibular part of HFs. The amount of drugs quantified from the second step (one CS) represents the amount of drugs in HFs. However, the present study demonstrates that CS removes not only HFs but also the viable skin layers. Therefore, the prerequisite of differential tape stripping approach is that no drugs penetrate into the viable skin layers, otherwise this

approach would overestimate the amount of drugs in HFs. For example, differential tape stripping can be conducted immediately when skin samples are applied to a test formulation because drugs are impossible to transiently diffuse across the SC and enter the VE. Besides, it is not clear about whether one CS is enough to collect all drugs in HFs. Hence, a new approach for studying the role of HFs in skin penetration of drugs is proposed in Figure 12 based on the present findings that CS removes the SC, viable skin layers and HFs. Two skin areas of A and B from the same skin sample with similar HF densities are selected. The HFs of sample B are sealed by a varnish-wax mixture [18,214], while the sealing material is placed next to the HFs of sample A. After a certain exposure time, the unabsorbed substances on the skin surface are removed. Subsequently, CS is performed to collect drugs in the skin. The number of CS required to collect all drugs in HFs needs further studies. The difference in the amount of drugs penetrated into the skin between sample A and B represents drugs in HFs.

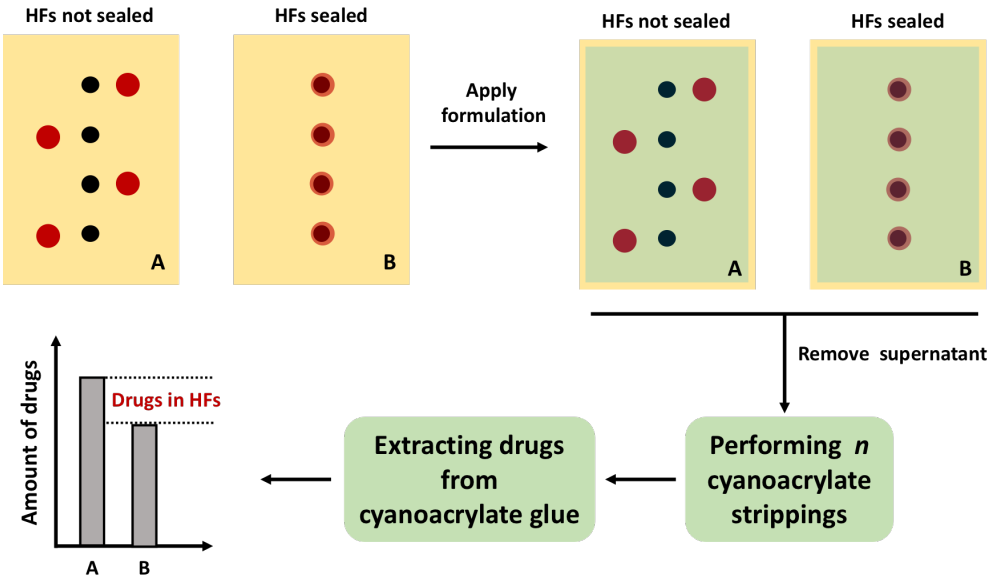

Figure 12 A proposed strategy for studying the role of HFs in the skin penetration of drugs. The black and red dots represent HFs and sealing material, respectively. The green shadow means the applied formulation. A and B are two skin areas from the same skin sample with the same HF density. *n* is the number of cyanoacrylate stripping needed to remove a certain part of the HF.

Two-photon microscopy (TPM)

In the present study, TPM was utilized to measure the thickness of the remaining SC after the skin is subjected to a certain number of TS or CS. The transition zone between the SC and the SG makes it hard to define the endpoint of the SC. TPM makes use of the autofluorescence of endogenous substances in the skin to visualize different skin structures along with the skin

depth. From the tomographic TPM images, the SC can be distinguished from the SG. Among the tomographic images of a skin sample, the image in which the area of corneocytes accounts for less than 50% while viable keratinocytes take up more than 50% of the area is defined as the endpoint of the SC. Based on the setting of 50% for the SC boundary, the SC thickness of the excised abdominal human skin and porcine ear skin were quantified as 12 μm and 16 μm, respectively, which is consistent with the published data [62,71], The present study provides a new non-invasive and high-resolution method to measure the SC thickness method by using TPM.

Currently, *in vivo* imaging techniques of optical coherence tomography, reflectance confocal microscopy, and confocal Raman microscopy are widely used to noninvasively analyze the SC thickness [260]. Conventional optical coherence tomography has a limited spatial resolution to distinguish the SC from the SG with the exception of the palm and plantar region. Even though the high-definition optical coherence tomography has an increased axial resolution, its lateral resolution is still not enough to allow cellular-level imaging [261]. Reflectance confocal microscopy has a high axial and lateral resolution and provides a 3D cellular-level structure of the SC for determining the thickness [260]. Confocal Raman microscopy measures the SC thickness based on the water-, lipid-, and DNA-based concentration profiles, respectively [262]. However, for the barrier-disrupted skin and reconstructed skin models, their increased TEWL leads to difficulty in determining the SC thickness based on the water concentration profile. Lipids in the SC of AD skin differ substantially in compositions from healthy skin, thus lipid-based concentration profiles are not suitable [263]. In comparison, the SC thickness measurement is less affected using confocal Raman microscopy based on the DNA concentration profile. Both reflectance confocal microscopy and TPM have the advantage of high spatial resolution to differ the SC from the SG.

Electron paramagnetic resonance (EPR)

The present study employed EPR to i) quantitatively investigate the localization of drugs inside NPs and in the external suspension medium; ii) directly quantify the amount of spin-labeled drugs in the skin samples without complicated sample preparation; iii) detect the drug release of NPs on the *ex vivo* porcine skin, which can be hardly realized by other techniques because it is challenging to distinguish drugs encapsulated inside NPs and drugs distributed in the skin; iv) study the microscopic localization of PCA in the intercellular skin lipids and corneocytes by analyzing the EPR spectra of PCA in the skin, extracted skin lipids and separated corneocytes. These applications highlight the potential of EPR in skin penetration studies. The label-free technique X-ray spectromicroscopy that has a nanoscopic lateral resolution has also been

used to quantify the drug concentrations in the SC and viable skin. However, this technique cannot directly distinguish drugs in the skin from drugs inside CMS NPs through the oxygen 1s-absorption spectra [264]. Another technique FLIM with high lateral resolution (subcellular level) could detect the drug release of NPs *in situ* because fluorescence lifetime is the characteristic property for a fluorophore and often sensitive to the local environment around the fluorophore [265]. Thus, using a fluorescent dye as the model drug, changes in the fluorescence lifetimes of the model drug in NPs and skin can reveal the drug release. Yet, FLIM can hardly make absolute quantification of drugs in the skin.

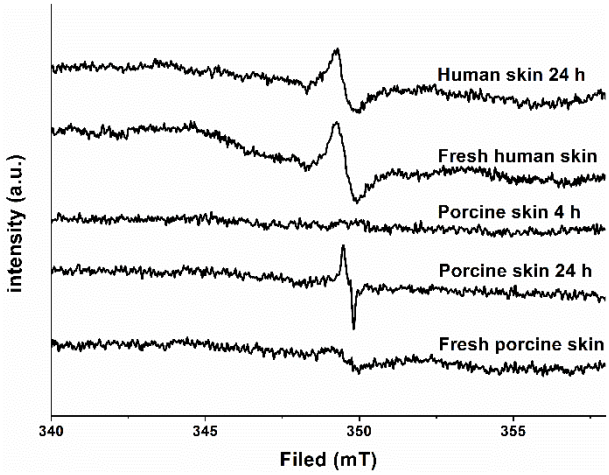

Figure 13 EPR spectra of porcine skin and excised human skin (Fitzpatrick skin type 4) that incubated for 4 or 24 h at 32 °C (unpublished data of the present thesis).

Additionally, the duration of the skin penetration experiment and skin types should be considered when using EPR. As shown in Figure 13, a single narrow biological peak was observed in the EPR spectrum of porcine skin that was incubated for 24 h at 32 °C, while no interference peak appeared after a shorter incubation time of 4 h. The origin of the narrow biological EPR peak needs further investigation. For excised human skin, the EPR spectra of the skin before and after 24 h incubation remained similar. The broad single peak is attributed to melanin in the human skin. The high intensity of the melanin peak is because the skin sample belongs to Fitzpatrick skin type 4, while the procine ear skin used in the present thesis is in white and its melanin content is very low, invisible to human eyes. Both the biological peak and melanin peak overlap the EPR spectrum of PCA or PCA-labeled drugs, which influences the quantification of PCA-labeled drugs in the skin. Therefore, Caucasian skin with low melanin content and 4 h of the incubation time were used in the present studies.

Confocal laser scanning microscopy (CLSM)

In the present study, CLSM was employed to visualize the spatial localization of drugs, especially drugs in HFs by imaging cryo-sectioned skin samples. This technique requires drugs to be fluorescent. Thus, the lipophilic dye Nile red was used as the model drug. The penetration of Nile red into the intact porcine skin following the NPs was at the depth of 160 μm (the dermis), which is in line with the EPR result that the drug DxPCA was transported into the viable skin layers. The physicochemical properties of drugs play a role in skin penetration. Different labelings, i.e. the fluorescent label for CLSM measurements and the spin marker for EPR quantifications, may change the physicochemical properties of the tested drug. This may lead to the inconsistency in the skin penetration results investigated by different techniques. Nile red has the molecular weight of 318 g/mol, the water solubility of <1 μg/ml [266] and log*P* of 5 [267], which can somewhat simulate Dx whose molecular weight is 392 g/mol, water solubility is 89 μg/ml [268] and log*P* is 1.83 [269]. Nevertheless, the correlation between CLSM and EPR results in the skin penetration of drugs needs further studies.

In conclusion, this project established the *ex vivo* barrier-disrupted skin models with different extents of barrier function for various experimental requirements. The pH-sensitive NP was demonstrated to have a controlled drug release, and improved skin penetration of the drug DxPCA on the barrier-disrupted skin, showing that the NP could be promising to reduce the side effects of Dx during the treatment of AD. Besides the NP, solvent effects on the skin penetration of hydrophilic PCA were investigated too. The ethanol aqueous solutions at the ethanol concentrations of 0%, 50%, and 100% were found not only affect the amount and depth of PCA penetrated into the skin, but also the spatial localization of PCA in the intercellular lipids and corneocytes. EPR, as the main technique employed in this project, has shown its high usefulness in the study of cutaneous drug delivery.

4 Outlook

4.1 *Ex* vivo barrier-disrupted skin models

The application of CS to the skin impairs the HFs [87,96], yet no investigations have been conducted regarding the percentages of the HF content are removed by different numbers of CS. Therefore, future studies need to focus on these questions, which is crucial for sampling drugs penetrated in HFs because the follicular infundibulum is the main target of many NPs, and the number of applied CS has to be sufficient to remove the infundibulum part to make sure that most drugs in the HFs are collected (Figure 12). Besides, the difference of the *ex vivo* barrier-disrupted skin models established by TS and CS, and the influences of the HF impairment (Figure 7) on the skin penetration of drugs need further investigations.

4.2 Further investigations about topical formulations

The pH-sensitive NP makes use of the enteric property of Eudragit® L100 to realize the controlled drug release of DxPCA. Apart from Eudragit® L100, NPs made of other enteric polymers such as cellulose acetate phthalate and hydroxypropyl methylcellulose phthalate are worth investigating their cutaneous drug delivery so that an optimal nanocarrier could be screened according to the clinical need. Furthermore, the correlation between the drug release of NPs on the skin *ex vivo* or *in vivo* and the skin penetration of drugs is of great interest. In addition, NPs are initially dispersed in an aqueous medium after the preparation, i.e. NP suspension. However, the dosage forms of cream and gel are favored in the clinic because of their good adhesion and spreadability on the skin. Thus, the combination of NPs with cream or gel, namely NPs dispersed in cream or gel, is a growing trend in the development of topical dermal formulations. Dispersing the pH-sensitive NPs into cream or gel could reduce the dryness of formulations and brings in the occlusion effect. Besides, the combination of two kinds of NPs with fast and delayed drug release could be a feasible strategy to optimize the skin penetration of drugs by adjusting the drug release from NPs, such as nanocrystals with a fast drug release and the pH-sensitive NPs with a delayed drug release. Therefore, in the future, it is worth studying the skin penetration of drugs by using NPs dispersed in cream/gel or the combination of different kinds of NPs, and the corresponding mechanisms and advantages.

Rather than one incubation time, the penetration of the lipophilic drug DxPCA and the hydrophilic model drug PCA in different skin layers over time, namely the dermal pharmacokinetics, need further investigations.

The relationship of the surface tension or the contact angle of a liquid topical formulation on the skin surface with the HF penetration of drugs would be an interesting topic (Figure 5).

The skin lipid film that covers the outmost skin layer SC cannot be ignored when studying the interaction of NPs with the skin surface. Artificial sebum can be used as a substitute for this skin lipid film, and the influences of artificial sebum on the NP structure and its drug release need to be thoroughly studied.

4.3 Techniques for studying skin penetration

The CLSM technique used for studying the HF penetration of NPs requires cryo-sectioning the skin biopsies, which is invasive, time-consuming, and labor-intensive. Moreover, CLSM cannot investigate the same HF at different time points. Thus, the drug release of NPs in HFs over time is difficult to investigate by CLSM. TPM with high resolution and deep optical sectioning could be a better technique to study HF penetration. N. Döge et al. employed wide-field TPM to monitor the HF penetration of NPs *in situ*, in which the skin sample is placed in a lateral position [270]. It seems promising to use wide-field TPM to monitor the drug release of NPs in HFs real-time and *in situ*.

The imaging modality of FLIM that spatially detects fluorescence lifetime can report on the surroundings of a fluorescent molecule at the subcellular level [265]. EPR quantifies the amounts of spin-labeled drugs in different microenvironments but gives no information on spatial localization. Therefore, it would be useful to demonstrate the feasibility of quantifying the spatial localization of drugs in the skin by the combination of FLIM and EPR.

5 Summary

It is challenging to overcome the stratum corneum (SC) barrier to deliver drugs into the skin. Nanoparticle (NP)-based drug delivery systems show the advantages of cutaneous penetration improvement and controllable and targeted drug release. Besides, solvents, as a big group of penetration enhancers, provide another strategy, which is easily accessible, low-cost, and flexibly changeable in components. Apart from the skin penetration enhancement based on formulations, the disrupted barrier of diseased skin could change the skin penetration of drugs too. Thus, the present thesis investigated the influences of the SC barrier function, a pH-sensitive Eudragit® L00 nanoparticle, and the solvents of water and ethanol on cutaneous drug delivery.

To determine the influence of the SC barrier on drug delivery, the SC thickness remaining on the skin after different numbers of tape stripping (TS) or cyanoacrylate stripping (CS) were quantified using two-photon microscopy, and the correlation of the SC reduction with the skin permeability changes was studied. The amount of SC removed by each tape decreased along with the skin depth, while a nearly constant SC thickness was removed by each CS. CS can remove the SC, viable skin layers and the hair follicle (HF), while TS can only remove the SC. Nevertheless, the removal of the entire human SC can be attained by both TS and CS, which were 4 times CS or 50 tape strips. The skin permeability to the model drug PCA linearly increased with the reduction of the SC thickness on the skin. These findings provide useful references to separating different skin layers for the quantification of drugs in the skin and establishing *ex vivo* barrier-disrupted skin models with different extents of barrier disruption. Especially, the barrier-disrupted skin, obtained by performing 30 tape strips on the intact porcine ear skin, could simulate atopic dermatitis (AD) skin to some extent. This *ex vivo* skin model could be used for evaluating dermal formulations in the initial development stage and reduce the number of animal and human studies.

Next, the influences of the SC barrier on the skin penetration behavior of DxPCA-loaded pH-sensitive Eudragit® L100 NPs were investigated by EPR and CLSM using intact and barrier disrupted porcine skin. The pH-sensitive NP exhibited a triggered drug release *in vitro* at a pH above 5.9. When applied to the skin, the drug DxPCA was slowly released from the NPs in the case of the barrier-disrupted skin, whereas this was under the EPR detect limited for the intact skin. The disrupted SC barrier increased the exchange of the endogenous fluid of the skin with the external medium of the NP dispersion. Due to the exchange, the pH of the external medium of the NPs was increased, leading to the change in the NP structure and

thus to the drug release. The improved drug release of the NPs is part of the reason for the higher drug penetration into the viable skin layers of the barrier-disrupted skin compared to the intact skin. These results indicate the feasibility of using this pH-sensitive NP to realize the targeted drug release and enhanced drug delivery into the viable skin layers of the AD skin lesions so that the side effects of the drug Dx could be reduced. Concerning the spatial localization of the NP, the EPR results indicate that the pH-sensitive NPs cannot pass through the disrupted SC of the skin, let alone the intact SC barrier. Besides, the accumulation of Nile red-loaded NPs in HFs and the transfolliclular penetration of Nile red was observed, which indicates that HFs can serve as a reservoir where drugs are sustained released from the NPs and provide a shortcut for drugs to penetrate across the HF into the deep viable skin layers. The drug release of the pH-sensitive NPs inside HFs may be due to the high sebum content and the high HF pH.

Lastly, water and ethanol are omnipresent in topical formulations, serving as dispersion media for NPs, low-toxic dissolution media, and penetration enhancers. The solvent effects of ethanol, PBS and the cosolvent ethanol-PBS (1:1, V/V) on the penetration of the hydrophilic model drug PCA into the excised human skin and porcine ear skin were investigated by EPR. Absolute ethanol showed poor ability to deliver PCA into the skin due to the crystallization of PCA caused by ethanol evaporation. PBS and the cosolvent are superior to ethanol, delivering a similar high amount of PCA into the skin. Despite a similar total amount of PCA in the skin, the cosolvent delivered more drugs into the viable skin compared to PBS. This shows the solvents effects on the macroscopic localization of drugs in the skin. Nevertheless, more than 95% of the penetrated drugs accumulated in the SC regardless of the solvents, showing that the SC is a predominant barrier and the main reservoir for the skin penetration of hydrophilic PCA. Furthermore, the solvents influenced the microscopic localization of PCA in the SC. PCA distributed in both the intercellular skin lipids and corneocytes when using the three solvents. From PBS to ethanol, with more ethanol in the solvent, the fraction of PCA distributed in the intercellular lipids decreased from 74% to 37%. The reason may be that ethanol enhances the diffusion of PCA from the intercellular lipids into the corneocytes, implying the coexistence of intercellular and transcellular skin pathways for PCA.

In conclusion, the studies conducted in this thesis i) provide correlation of the extent of the SC barrier disruption with the number of applied TS or CS and show the feasibility of using TS to establish an *ex vivo* barrier-disrupted skin model that mimics AD skin to some degree; ii) give insights of the influence of the SC barrier on the drug release of NPs on the skin and the following skin penetration of drugs, and show the promising application of the pH-sensitive NP in reducing the side effects of Dx for the treatment of AD; iii) expand the knowledge of solvent

effects on the spatial localization of drugs in the SC and give a hint for the skin pathway of hydrophilic drugs.

Zusammenfassung

Die Barriere des Stratum Corneums (SC) stellt beim Transport von Wirkstoffen in die viable Haut eine große Herausforderung dar. Es wurden viele unterschiedliche Ansätze gemacht, um eine Penetration von Wirkstoffen durch die Hautbarriere zu verbessern. Im Vergleich zu anderen penetrationsverstärkenden Methoden haben nanopartikelbasierte Wirkstofftransportsysteme den Vorteil, dass sie eine kontrollierte und gezielte Wirkstofffreisetzung ermöglichen. Daneben kommen häufig Lösungsmittel zum Einsatz, die als Penetrationsverstärker agieren und die Löslichkeit des Wirkstoffes verbessern. Weiterhin ist diese Strategie kostengünstig, leicht realisierbar sowie flexibel an die jeweiligen Anforderungen anpassbar. Eine penetrationsverstärkende Wirkung kann nicht nur bei einer gezielten Verwendung geeigneter Formulierungen, sondern auch bei einer gestörten Barrierefunktion von erkrankter Haut beobachtet werden. In der vorliegenden Arbeit wurden die Einflüsse der SC-Barrierefunktion, eines pH-sensitiven Eudragit® L00-Nanopartikels sowie der Lösungsmittel Wasser und Ethanol auf die kutane Wirkstoffabgabe untersucht.

Zur Untersuchung der SC-Dicke wurde zunächst das SC mittels unterschiedlicher Anzahl an Tape Stripping (TS) oder Cyanoacrylat Stripping (CS) entfernt und im Anschluss wurde das auf der Haut verbliebene SC mittels der Zwei-Photonen- Mikroskopie quantifiziert und die Korrelation der SC-Reduktion mit den Veränderungen der Hautpermeabilität untersucht. Während das TS mit jeder Anwendung zu einer Abnahme der SC-Dicke führte, blieb die Dicke beim CS nahezu konstant. Weiterhin können mit dem CS das SC, lebensfähige Hautschichten und Haarfollikel (HF) entfernt werden, während das TS nur das SC entfernen kann. Es wurde herausgefunden, dass das Entfernen des gesamten menschlichen SC durch beide Methoden erzielt werden kann. Hierzu werden entweder vier CS oder 50 TS benötigt. Die Hautpermeabilität für das Modellpräparat PCA stieg linear mit der Abnahme der SZ-Dicke auf der Haut. Diese Ergebnisse liefern zur Trennung verschiedener Hautschichten bei der Quantifizierung von Wirkstoffen in der Haut und zur Etablierung von ex vivo Barrierestörungen in Hautmodellen mit unterschiedlichem Ausmaß an Barrierestörungen nützliche Erkenntnisse. Darüber hinaus wurde barriereregestörte Haut als Modell für die atopische Dermatitis (AD) verwendet, indem 30 Klebestreifen-Abrisse (TS) von intakter Schweineohrhaut entfernt wurden. Dieses Ex-vivo-Hautmodell könnte für die Bewertung von dermalen Formulierungen in der ersten Entwicklungsphase verwendet werden und die Anzahl der Tier- und Humanstudien reduzieren.

Anschließend wurden die Einflüsse der SC-Barriere auf das Hautpenetrationsverhalten von DxPCA-beladenen pH-sensitiven Eudragit® L100 NPs mittels EPR und CLSM untersucht. Die pH-sensitiven NPs zeigten in vitro eine gesteigerte Wirkstofffreisetzung bei pH-Werten über 5,9. Bei der ex vivo-Applikation auf Schweinehaut wurde das DxPCA auf der barrieregestörten Haut langsam aus den NPs freigesetzt, während eine Wirkstofffreisetzung bei intakter Haut kaum zu sehen war. Die gestörte SC-Barriere erhöhte den Austausch der körpereigenen Flüssigkeit der Haut mit dem externen Medium der NP-Dispersion. Durch den Austausch wurde der pH-Wert des externen Mediums der NPs erhöht, was zu einer Veränderung der NP-Struktur und damit einer vermehrten Wirkstofffreisetzung sowie einer tieferen Wirkstoffpenetration von DxPCA in die lebensfähigen Hautschichten der barrieregestörten Haut im Vergleich zur intakten Haut führt. Diese Ergebnisse deuten darauf hin, dass mit diesem pH-sensitiven NP eine gezielte Wirkstofffreisetzung und verbesserte Wirkstoffabgabe in die lebensfähigen Hautschichten der AD-Hautläsionen möglich ist. Dadurch könnten die Nebenwirkungen von Dexamethason verringert werden. Hinsichtlich der räumlichen Lokalisation der NP deuten die EPR-Ergebnisse darauf hin, dass die pH-sensitiven NPs die gestörte SC der Haut gestörte und intakte Barriere der Haut nicht passieren können. Außerdem wurde die Anhäufung von Nilrot-beladenen NPs in den HFs und die transfollikuläre Penetration von Nilrot beobachtet, was darauf hinweist, dass die HFs als Reservoir dienen können. Dadurch können die Wirkstoffe aus den NPs nachhaltig freigesetzt und eine Reduktion für das Eindringen von Wirkstoffen über die HF in die tiefen lebensfähigen Hautschichten erzielt werden. Die Wirkstofffreisetzung der pH-empfindlichen NP innerhalb der HFs kann auf den hohen Talggehalt und den hohen HF-pH-Wert zurückgeführt werden.

Schließlich wurde der Einfluss der Lösungsmittel PBS, Ethanol und deren Mischung (1:1, V/V) auf die Hautpenetration des hydrophilen Modellwirkstoffs PCA in die exzidierte menschliche Haut und in die Schweineohrhaut mittels EPR untersucht. Diese Lösungsmittel dienen als Dispersionsmedien für NPs, besitzen penetrationsverstärkenden Eigenschaften sowie geringen Toxizität. Ethanol transportierte nur geringe Mengen an PCA in die Haut, da die Verdampfung des Ethanols zu der Kristallisation der PCA führte. Obwohl bei der Verwendung von PBS und der PBS-Ethanol-Mischung ähnliche Gesamtmengen an PCA in der Haut gefunden wurden, war der Anteil der PCA in der viablen Epidermis und Dermis bei der PBS-Ethanol-Mischung höher. Dennoch sammelten sich mehr als 95% der penetrierten Wirkstoffe unabhängig von den Lösungsmitteln im SC an, was zeigt, dass das SC eine vorherrschende Barriere und das Hauptreservoir für die Hautpenetration hydrophiler PCA bildet. Darüber hinaus beeinflussten die Lösungsmittel die räumliche Verteilung der eingedrungenen PCA im SC. Bei der Verwendung der drei Lösungsmittel verteilte sich die PCA sowohl in den interzellulären Hautlipiden als auch in den Korneozyten. Eine erhöhte Ethanolkonzentration

im Lösungsmittel führte zu einer Abnahme des PCA-Anteils in den interzellulären Lipiden von 74 % auf 37 %, während in den Korneozyten eine Steigerung festgestellt wurde. Der Grund für diese Abnahme könnte eine Verstärkung der Diffusion der PCA von den interzellulären Lipiden in die Korneozyten durch das Ethanol sein, was auf die Koexistenz von interzellulären und transzellulären Hautwegen für die PCA hindeutet.

Zusammenfassend wurden in diesem Projekt ex vivo Hautmodelle mit unterschiedlich starker Barrierestörung etabliert, um verschiedene experimentelle Anforderungen zu untersuchen. Es hat sich zeigt, dass die in dieser Arbeit durchgeführten Studien: i) eine Korrelation des Ausmaßes der Störung der SC-Barriere mit der Anzahl der angewandten TS oder CS liefern sowie die Etablierung eines ex-vivo-Barriere-gestörtes Hautmodell mittels TS ermöglichen, das die AD-Haut bis zu einem gewissen Grad nachahmt; ii) Einblicke bezüglich des Einflusses der SC-Barriere auf die Wirkstofffreisetzung von NPs auf der Haut und die anschließende Hautpenetration von Wirkstoffen geben und die vielversprechende Anwendung der pH-sensitiven NP bei der Reduzierung der Nebenwirkungen von Dx zur Behandlung von AD zeigen; iii) das Wissen über die Lösungsmittelwirkungen auf die räumliche Verteilung von Wirkstoffen im SC erweitern und einen Hinweis auf den Hautpfad von hydrophilen Wirkstoffen geben.

References

1 Dragicevic, N. & Maibach, H. I. *Percutaneous penetration enhancers chemical methods in penetration enhancement*. (Springer, 2016).

2 Grice, E. A. & Segre, J. A. The skin microbiome. *Nat Rev Microbiol* **9**, 244-253, doi:10.1038/nrmicro2537 (2011).

3 Khavkin, J. & Ellis, D. A. Aging skin: histology, physiology, and pathology. *Facial Plast Surg Clin North Am* **19**, 229-234, doi:10.1016/j.fsc.2011.04.003 (2011).

4 Hwa, C., Bauer, E. A. & Cohen, D. E. Skin biology. *Dermatologic therapy* **24**, 464-470 (2011).

5 Elias, P. M. Structure and function of the stratum corneum extracellular matrix. *J Invest Dermatol* **132**, 2131-2133, doi:10.1038/jid.2012.246 (2012).

6 Losquadro, W. D. Anatomy of the skin and the pathogenesis of nonmelanoma skin cancer. *Facial Plast Surg Clin North Am* **25**, 283-289 (2017).

7 Vogt, A. *et al.* Morphometry of human terminal and vellus hair follicles. *Exp Dermatol* **16**, 946-950, doi:10.1111/j.1600-0625.2007.00602.x (2007).

8 Park, A. M., Khan, S. & Rawnsley, J. Hair Biology: Growth and Pigmentation. *Facial Plast Surg Clin North Am* **26**, 415-424 (2018).

9 Safety, S. C. o. C. Basic criteria for the in vitro assessment of dermal absorption of cosmetic ingredients. *Eur. Comm*, 1-14 (2010).

10 Lane, M. E. Skin penetration enhancers. *Int J Pharm* **447**, 12-21, doi:10.1016/j.ijpharm.2013.02.040 (2013).

11 Patzelt, A., Antoniou, C., Sterry, W. & Lademann, J. Skin penetration from the inside to the outside: A review. *Drug Discov Today Dis Mech* **5**, e229-e235, doi:https://doi.org/10.1016/j.ddmec.2008.05.002 (2008).

12 Nemanic, M. K. & Elias, P. M. In situ Precipitation: A novel cyotchemical technique for visualization of permeability pathways in mammalian stratum corneum. *J Histochem Cytochem* **28**, 573-578, doi:Doi 10.1177/28.6.7190175 (1980).

13 Benson, H. A. Transdermal drug delivery: penetration enhancement techniques. *Curr Drug Deliv* **2**, 23-33 (2005).

14 Boddé, H. E., van den Brink, I., Koerten, H. K. & de Haan, F. H. N. Visualization of in vitro percutaneous penetration of mercuric chloride; transport through intercellular space versus cellular uptake through desmosomes. *J Control Release* **15**, 227-236, doi:https://doi.org/10.1016/0168-3659(91)90114-S (1991).

15 Saar, B. G., Contreras-Rojas, L. R., Xie, X. S. & Guy, R. H. Imaging drug delivery to skin with stimulated Raman scattering microscopy. *Mol Pharm* **8**, 969-975, doi:10.1021/mp200122w (2011).

16 Morrow, D. I. *et al.* Influence of penetration enhancers on topical delivery of 5-aminolevulinic acid from bioadhesive patches. *J Pharm Pharmacol* **62**, 685-695, doi:10.1211/jpp.62.06.0004 (2010).

17 Essa, E. A., Bonner, M. C. & Barry, B. W. Human skin sandwich for assessing shunt route penetration during passive and iontophoretic drug and liposome delivery. *J Pharm Pharmacol* **54**, 1481-1490, doi:10.1211/002235702135 (2002).

18 Otberg, N. *et al.* The role of hair follicles in the percutaneous absorption of caffeine. *Br J Clin Pharmacol* **65**, 488-492, doi:10.1111/j.1365-2125.2007.03065.x (2008).

19 Hueber, F., Schaefer, H. & Wepierre, J. Role of transepidermal and transfollicular routes in percutaneous absorption of steroids: in vitro studies on human skin. *Skin Pharmacol* **7**, 237-244 (1994).

20 Otberg, N. *et al.* Variations of hair follicle size and distribution in different body sites. *J Invest Dermatol* **122**, 14-19, doi:10.1046/j.0022-202X.2003.22110.x (2004).

21 Ogiso, T. *et al.* Transfollicular drug delivery: Penetration of drugs through human scalp skin and comparison of penetration between scalp and abdominal skins in vitro. *J Drug Target* **10**, 369-378, doi:10.1080/1061186021000001814 (2002).

22 Grams, Y. Y. & Bouwstra, J. A. Penetration and distribution of three lipophilic probes in vitro in human skin focusing on the hair follicle. *J Control Release* **83**, 253-262 (2002).

23 Toll, R. *et al.* Penetration profile of microspheres in follicular targeting of terminal hair follicles. *J Invest Dermatol* **123**, 168-176, doi:https://doi.org/10.1111/j.0022-202X.2004.22717.x (2004).

24 Limcharoen, B. *et al.* Increasing the percutaneous absorption and follicular penetration of retinal by topical application of proretinal nanoparticles. *Eur J Pharm Biopharm* **139**, 93-100, doi:10.1016/j.ejpb.2019.03.014 (2019).

25 Lademann, J. *et al.* Nanoparticles--an efficient carrier for drug delivery into the hair follicles. *Eur J Pharm Biopharm* **66**, 159-164, doi:10.1016/j.ejpb.2006.10.019 (2007).

26 Surber, C. & Davis, A. F. *Bioavailability and Bioequivalence of Dermatological Formulations*. Vol. 119 (2002).

27 Choe, C., Lademann, J. & Darvin, M. E. Analysis of human and porcine skin in vivo/ex vivo for penetration of selected oils by confocal Raman microscopy. *Skin Pharmacol Physiol* **28**, 318-330, doi:10.1159/000439407 (2015).

28 Teichmann, A. *et al.* Comparison of stratum corneum penetration and localization of a lipophilic model drug applied in an o/w microemulsion and an amphiphilic cream. *Eur J Pharm Biopharm* **67**, 699-706, doi:10.1016/j.ejpb.2007.04.006 (2007).

29 Jacobi, U., Taube, H., Schafer, U. F., Sterry, W. & Lademann, J. Comparison of four different in vitro systems to study the reservoir capacity of the stratum corneum. *J Control Release* **103**, 61-71, doi:10.1016/j.jconrel.2004.11.013 (2005).

30 Hafeez, F. *et al.* Stratum corneum reservoir as a predictive method for in vitro percutaneous absorption. *J Appl Toxicol* **36**, 1003-1010, doi:10.1002/jat.3262 (2016).

31 Schneider, M., Stracke, F., Hansen, S. & Schaefer, U. F. Nanoparticles and their interactions with the dermal barrier. *Dermatoendocrinol* **1**, 197-206, doi:10.4161/derm.1.4.9501 (2009).

32 Kirschner, N., Houdek, P., Fromm, M., Moll, I. & Brandner, J. M. Tight junctions form a barrier in human epidermis. *Eur J Cell Biol* **89**, 839-842, doi:10.1016/j.ejcb.2010.07.010 (2010).

33 Andrews, S. N., Jeong, E. & Prausnitz, M. R. Transdermal delivery of molecules is limited by full epidermis, not just stratum corneum. *Pharm Res* **30**, 1099-1109, doi:10.1007/s11095-012-0946-7 (2013).

34 Uchida, T., Kanazawa, T., Kawai, M., Takashima, Y. & Okada, H. Therapeutic effects on atopic dermatitis by anti-RelA Short Interfering RNA combined with functional peptides Tat and AT1002. *J Pharmacol Exp Ther* **338**, 443-450, doi:10.1124/jpet.111.180042 (2011).

35 Blume-Peytavi, U. & Vogt, A. Human hair follicle: reservoir function and selective targeting. *Br J Dermatol* **165 Suppl 2**, 13-17, doi:10.1111/j.1365-2133.2011.10572.x (2011).

36 Lademann, J. *et al.* Hair follicles - a long-term reservoir for drug delivery. *Skin Pharmacol Physiol* **19**, 232-236, doi:10.1159/000093119 (2006).

37 Plewig, G. & Kligman, A. M. in *Acne: Morphogenesis and Treatment* 3-17 (Springer Berlin Heidelberg, 1975).

38 Lambers, H., Piessens, S., Bloem, A., Pronk, H. & Finkel, P. Natural skin surface pH is on average below 5, which is beneficial for its resident flora. *Int J Cosmet Sci* **28**, 359-370, doi:10.1111/j.1467-2494.2006.00344.x (2006).

39 Vávrová, K. *et al.* Filaggrin deficiency leads to impaired lipid profile and altered acidification pathways in a 3D skin construct. *J Invest Dermatol* **134**, 746-753, doi:https://doi.org/10.1038/jid.2013.402 (2014).

40 Zoschke, C. *et al.* The barrier function of organotypic non-melanoma skin cancer models. *J Control Release* **233**, 10-18, doi:https://doi.org/10.1016/j.jconrel.2016.04.037 (2016).

41 Honari, G. & Maibach, H. Skin Structure and Function. *Applied Dermatotoxicology: Clinical Aspects*, 1-10, doi:10.1016/B978-0-12-420130-9.00001-3 (2014).

42 Wesley, N. O. & Maibach, H. I. Racial (ethnic) differences in skin properties: the objective data. *Am J Clin Dermatol* **4**, 843-860, doi:10.2165/00128071-200304120-00004 (2003).

43 Verdier-Sevrain, S. & Bonte, F. Skin hydration: a review on its molecular mechanisms. *J Cosmet Dermatol* **6**, 75-82, doi:10.1111/j.1473-2165.2007.00300.x (2007).

44 Boer, M., Duchnik, E., Maleszka, R. & Marchlewicz, M. Structural and biophysical characteristics of human skin in maintaining proper epidermal barrier function. *Postepy Dermatol Alergol* **33**, 1-5, doi:10.5114/pdia.2015.48037 (2016).

45 Weidinger, S., Beck, L. A., Bieber, T., Kabashima, K. & Irvine, A. D. Atopic dermatitis. *Nat Rev Dis Primers* **4**, 1, doi:10.1038/s41572-018-0001-z (2018).

46 Jungersted, J. M. *et al.* Stratum corneum lipids, skin barrier function and filaggrin mutations in patients with atopic eczema. *Allergy* **65**, 911-918, doi:10.1111/j.1398-9995.2010.02326.x (2010).

47 Seidenari, S. & Giusti, G. Objective assessment of the skin of children affected by atopic dermatitis: a study of pH, capacitance and TEWL in eczematous and clinically uninvolved skin. *Acta Derm Venereol* **75**, 429-433, doi:10.2340/0001555575429433 (1995).

48 Sparavigna, A., Setaro, M. & Gualandri, V. Cutaneous pH in children affected by atopic dermatitis and in healthy children: a multicenter study. *Skin Res Technol* **5**, 221-227, doi:10.1111/j.1600-0846.1999.tb00134.x (1999).

49 Sator, P. G., Schmidt, J. B. & Honigsmann, H. Comparison of epidermal hydration and skin surface lipids in healthy individuals and in patients with atopic dermatitis. *J Am Acad Dermatol* **48**, 352-358, doi:10.1067/mjd.2003.105 (2003).

50 Firooz, A. *et al.* Comparison of hydration, sebum and pH values in clinically normal skin of patients with atopic dermatitis and healthy controls. *Clin Exp Dermatol* **32**, 321-322, doi:10.1111/j.1365-2230.2007.02364.x (2007).

51 Takigawa, H., Nakagawa, H., Kuzukawa, M., Mori, H. & Imokawa, G. Deficient production of hexadecenoic acid in the skin is associated in part with the vulnerability of atopic dermatitis patients to colonization by Staphylococcus aureus. *Dermatology* **211**, 240-248, doi:10.1159/000087018 (2005).

52 Holm, E. A., Wulf, H. C., Thomassen, L. & Jemec, G. B. Instrumental assessment of atopic eczema: validation of transepidermal water loss, stratum corneum hydration, erythema, scaling, and edema. *J Am Acad Dermatol* **55**, 772-780, doi:10.1016/j.jaad.2006.03.036 (2006).

53 Garcia Ortiz, P., Hansen, S. H., Shah, V. P., Menne, T. & Benfeldt, E. Impact of adult atopic dermatitis on topical drug penetration: assessment by cutaneous microdialysis and tape stripping. *Acta Derm Venereol* **89**, 33-38, doi:10.2340/00015555-0562 (2009).

54 Overgaard, L. E. K. *et al.* Children with atopic dermatitis and frequent emollient use have increased urinary levels of low-molecular-weight phthalate metabolites and parabens. *Allergy* **72**, 1768-1777, doi:10.1111/all.13157 (2017).

55 Janssens, M. *et al.* Increase in short-chain ceramides correlates with an altered lipid organization and decreased barrier function in atopic eczema patients. *J Lipid Res* **53**, 2755-2766, doi:10.1194/jlr.P030338 (2012).

56 van Smeden, J. & Bouwstra, J. A. Stratum corneum lipids: Their role for the skin barrier function in healthy subjects and atopic dermatitis patients. *Curr Probl Dermatol* **49**, 8-26, doi:10.1159/000441540 (2016).

57 Macheleidt, O., Sandhoff, K. & Kaiser, H. W. Deficiency of Epidermal Protein-Bound ω-Hydroxyceramides in Atopic Dermatitis. *J Invest Dermatol* **119**, 166-173, doi:https://doi.org/10.1046/j.1523-1747.2002.01833.x (2002).

58 Abd, E. *et al.* Skin models for the testing of transdermal drugs. *Clin Pharmacol* **8**, 163-176, doi:10.2147/CPAA.S64788 (2016).

59 Godin, B. & Touitou, E. Transdermal skin delivery: predictions for humans from in vivo, ex vivo and animal models. *Adv Drug Deliv Rev* **59**, 1152-1161, doi:10.1016/j.addr.2007.07.004 (2007).

60 Jung, E. C. & Maibach, H. I. Animal models for percutaneous absorption. *J Appl Toxicol* **35**, 1-10, doi:10.1002/jat.3004 (2015).

61 Van Gele, M., Geusens, B., Brochez, L., Speeckaert, R. & Lambert, J. Three-dimensional skin models as tools for transdermal drug delivery: challenges and limitations. *Expert Opin Drug Deliv* **8**, 705-720, doi:10.1517/17425247.2011.568937 (2011).

62 Czekalla, C., Schonborn, K. H., Lademann, J. & Meinke, M. C. Noninvasive determination of epidermal and stratum corneum thickness in vivo using two-photon microscopy and optical coherence tomography: Impact of body area, age, and gender. *Skin Pharmacol Physiol* **32**, 142-150, doi:10.1159/000497475 (2019).

63 Otberg, N. *et al.* Variations of hair follicle size and distribution in different body sites. *J Invest Dermatol* **122**, 14-19, doi:10.1046/j.0022-202X.2003.22110.x (2004).

64 Jönsson, E. H. *et al.* The relation between human hair follicle density and touch perception. *Sci Rep-Uk* **7**, 2499, doi:10.1038/s41598-017-02308-9 (2017).

65 Patzelt, A. *et al.* Differential stripping demonstrates a significant reduction of the hair follicle reservoir in vitro compared to in vivo. *Eur J Pharm Biopharm* **70**, 234-238, doi:10.1016/j.ejpb.2008.02.024 (2008).

66 Simon, G. A. & Maibach, H. I. The pig as an experimental animal model of percutaneous permeation in man: Qualitative and quantitative observations - An overview. *Skin Pharmacol Appl* **13**, 229-234, doi:Doi 10.1159/000029928 (2000).

67 OECD. Guidance document for the conduct of skin absoption studies. Series on testing assessment No. 28. OECD. (2003).

68 Meyer, W. & Neurand, K. Comparison of skin pH in domesticated and laboratory mammals. *Arch Dermatol Res* **283**, 16-18 (1991).

69 Matousek, J. L. & Campbell, K. L. A comparative review of cutaneous pH. *Vet Dermatol* **13**, 293-300 (2002).

70 Dimde, M. *et al.* Synthesis and validation of functional nanogels as pH-sensors in the hair follicle. *Macromol Biosci* **17**, doi:10.1002/mabi.201600505 (2017).

71 Choe, C., Schleusener, J., Lademann, J. & Darvin, M. E. Human skin in vivo has a higher skin barrier function than porcine skin ex vivo—comprehensive Raman microscopic study of the stratum corneum. *J Biophotonics* **11**, e201700355, doi:10.1002/jbio.201700355 (2018).

72 Jacobi, U. *et al.* Porcine ear skin: an in vitro model for human skin. *Skin Res Technol* **13**, 19-24, doi:10.1111/j.1600-0846.2006.00179.x (2007).

73 Caussin, J., Gooris, G. S., Janssens, M. & Bouwstra, J. A. Lipid organization in human and porcine stratum corneum differs widely, while lipid mixtures with porcine ceramides model human stratum corneum lipid organization very closely. *Biochim Biophys Acta* **1778**, 1472-1482, doi:10.1016/j.bbamem.2008.03.003 (2008).

74 Choe, C., Schleusener, J., Lademann, J. & Darvin, M. E. Human skin in vivo has a higher skin barrier function than porcine skin ex vivo-comprehensive Raman microscopic study of the stratum corneum. *J Biophotonics* **11**, doi:10.1002/jbio.201700355 (2018).

75 Schafer-Korting, M. *et al.* The use of reconstructed human epidermis for skin absorption testing: Results of the validation study. *Altern Lab Anim* **36**, 161-187, doi:10.1177/026119290803600207 (2008).

76 Schafer-Korting, M. *et al.* Reconstructed human epidermis for skin absorption testing: results of the German prevalidation study. *Altern Lab Anim* **34**, 283-294, doi:10.1177/026119290603400312 (2006).

77 Paz-Alvarez, M., Pudney, P. D. A., Hadgraft, J. & Lane, M. E. Topical delivery of climbazole to mammalian skin. *Int J Pharm* **549**, 317-324, doi:10.1016/j.ijpharm.2018.07.058 (2018).

78 Zhang, Y. *et al.* A comparison of the in vitro permeation of niacinamide in mammalian skin and in the Parallel Artificial Membrane Permeation Assay (PAMPA) model. *Int J Pharm* **556**, 142-149, doi:10.1016/j.ijpharm.2018.11.065 (2019).

79 Schafer-Korting, M. *et al.* Reconstructed epidermis and full-thickness skin for absorption testing: influence of the vehicles used on steroid permeation. *Altern Lab Anim* **36**, 441-452, doi:10.1177/026119290803600405 (2008).

80 OECD. *Test No. 431: In Vitro Skin Corrosion: Human Skin Model Test*. (2004).

81 Ponec, M., Boelsma, E., Gibbs, S. & Mommaas, M. Characterization of reconstructed skin models. *Skin Pharmacol Appl Skin Physiol* **15 Suppl 1**, 4-17, doi:10.1159/000066682 (2002).

82 Avci, P. *et al.* Animal models of skin disease for drug discovery. *Expert Opin Drug Deliv* **8**, 331-355, doi:10.1517/17460441.2013.761202 (2013).

83 Zhang, J. Y. in *Animal Models for the Study of Human Disease (Second Edition)* (ed P. Michael Conn) 357-375 (Academic Press, 2017).

84 Shiohara, T., Hayakawa, J. & Mizukawa, Y. Animal models for atopic dermatitis: are they relevant to human disease? *J Dermatol Sci* **36**, 1-9, doi:https://doi.org/10.1016/j.jdermsci.2004.02.013 (2004).

85 Löwa, A., Jevtić, M., Gorreja, F. & Hedtrich, S. Alternatives to animal testing in basic and preclinical research of atopic dermatitis. *Exp Dermatol* **27**, 476-483 (2018).

86 Lademann, J., Jacobi, U., Surber, C., Weigmann, H. J. & Fluhr, J. W. The tape stripping procedure--evaluation of some critical parameters. *Eur J Pharm Biopharm* **72**, 317-323, doi:10.1016/j.ejpb.2008.08.008 (2009).

87 Teichmann, A. *et al.* Differential stripping: determination of the amount of topically applied substances penetrated into the hair follicles. *J Invest Dermatol* **125**, 264-269, doi:10.1111/j.0022-202X.2005.23779.x (2005).

88 Vogt, A. *et al.* Hair follicle targeting, penetration enhancement and Langerhans cell activation make cyanoacrylate skin surface stripping a promising delivery technique for transcutaneous immunization with large molecules and particle-based vaccines. *Exp Dermatol* **24**, 73-75, doi:10.1111/exd.12589 (2015).

89 Ostrowski, A. *et al.* Skin barrier disruptions in tape stripped and allergic dermatitis models have no effect on dermal penetration and systemic distribution of AHAPS-functionalized silica nanoparticles. *Nanomedicine* **10**, 1571-1581, doi:10.1016/j.nano.2014.04.004 (2014).

90 Danso, M. O., Berkers, T., Mieremet, A., Hausil, F. & Bouwstra, J. A. An ex vivo human skin model for studying skin barrier repair. *Exp Dermatol* **24**, 48-54, doi:10.1111/exd.12579 (2015).

91 Breternitz, M., Flach, M., Präßler, J., Elsner, P. & Fluhr, J. W. Acute barrier disruption by adhesive tapes is influenced by pressure, time and anatomical location: integrity and cohesion assessed by sequential tape stripping; a randomized, controlled study. *British Journal of Dermatology* **156**, 231-240, doi:doi:10.1111/j.1365-2133.2006.07632.x (2007).

92 Breternitz, M., Flach, M., Prassler, J., Elsner, P. & Fluhr, J. W. Acute barrier disruption by adhesive tapes is influenced by pressure, time and anatomical location: integrity

and cohesion assessed by sequential tape stripping; a randomized, controlled study. *Br J Dermatol* **156**, 231-240, doi:10.1111/j.1365-2133.2006.07632.x (2007).

93 Singer, A. J., Quinn, J. V. & Hollander, J. E. The cyanoacrylate topical skin adhesives. *Am J Emerg Med* **26**, 490-496, doi:https://doi.org/10.1016/j.ajem.2007.05.015 (2008).

94 Imokawa, G. *et al.* Decreased level of ceramides in stratum corneum of atopic dermatitis: An etiologic factor in Atopic dry skin? *J Invest Dermatol* **96**, 523-526, doi:https://doi.org/10.1111/1523-1747.ep12470233 (1991).

95 Piérard, G. E. & Piérard-Franchimont, C. in *Agache's Measuring the Skin: Non-invasive Investigations, Physiology, Normal Constants* (eds Philippe Humbert, Ferial Fanian, Howard I. Maibach, & Pierre Agache) 363-367 (Springer International Publishing, 2017).

96 Vogt, A. *et al.* Hair follicle targeting, penetration enhancement and Langerhans cell activation make cyanoacrylate skin surface stripping a promising delivery technique for transcutaneous immunization with large molecules and particle-based vaccines. *Exp Dermatol* **24**, 73-75, doi:10.1111/exd.12589 (2015).

97 Simonsen, L. & Fullerton, A. Development of an in vitro skin permeation model simulating atopic dermatitis skin for the evaluation of dermatological products. *Skin Pharmacol Physiol* **20**, 230-236, doi:10.1159/000104421 (2007).

98 Ohman, H. & Vahlquist, A. The pH gradient over the stratum corneum differs in X-linked recessive and autosomal dominant ichthyosis: a clue to the molecular origin of the "acid skin mantle"? *J Invest Dermatol* **111**, 674-677, doi:10.1046/j.1523-1747.1998.00356.x (1998).

99 Ohman, H. & Vahlquist, A. In vivo studies concerning a pH gradient in human stratum corneum and upper epidermis. *Acta Derm Venereol* **74**, 375-379, doi:10.2340/0001555574375379 (1994).

100 Jacobi, U., Weigmann, H. J., Ulrich, J., Sterry, W. & Lademann, J. Estimation of the relative stratum corneum amount removed by tape stripping. *Skin Res Technol* **11**, 91-96, doi:10.1111/j.1600-0846.2005.00094.x (2005).

101 Froebe, C. L., Simion, F. A., Rhein, L. D., Cagan, R. H. & Kligman, A. Stratum corneum lipid removal by surfactants: relation to in vivo irritation. *Dermatologica* **181**, 277-283 (1990).

102 Barba, C., Alonso, C., Marti, M., Manich, A. & Coderch, L. Skin barrier modification with organic solvents. *Biochim Biophys Acta* **1858**, 1935-1943, doi:10.1016/j.bbamem.2016.05.009 (2016).

103 Doge, N. *et al.* Assessment of skin barrier function and biochemical changes of ex vivo human skin in response to physical and chemical barrier disruption. *Eur J Pharm Biopharm* **116**, 138-148, doi:10.1016/j.ejpb.2016.12.012 (2017).

104 Tupker, R. A. *et al.* Guidelines on sodium lauryl sulfate (SLS) exposure tests. A report from the Standardization Group of the European Society of Contact Dermatitis. *Contact Dermatitis* **37**, 53-69 (1997).

105 Fluhr, J. W. *et al.* Impact of anatomical location on barrier recovery, surface pH and stratum corneum hydration after acute barrier disruption. *Br J Dermatol* **146**, 770-776, doi:10.1046/j.1365-2133.2002.04695.x (2002).

106 Wood Heickman, L. K., Davallow Ghajar, L., Conaway, M. & Rogol, A. D. Evaluation of hypothalamic-pituitary-adrenal axis suppression following cutaneous use of topical corticosteroids in children: A Meta-Analysis. *Horm Res Paediatr* **89**, 389-396, doi:10.1159/000489125 (2018).

107 Chang, R. K., Raw, A., Lionberger, R. & Yu, L. Generic development of topical dermatologic products: formulation development, process development, and testing of topical dermatologic products. *AAPS J* **15**, 41-52, doi:10.1208/s12248-012-9411-0 (2013).

108 Paudel, K. S. *et al.* Challenges and opportunities in dermal/transdermal delivery. *Ther Deliv* **1**, 109-131, doi:10.4155/tde.10.16 (2010).

109 Burkman, R. T. Transdermal hormonal contraception: benefits and risks. *Am J Obstet Gynecol* **197**, 134.e131-134.e136, doi:https://doi.org/10.1016/j.ajog.2007.04.027 (2007).

110 Pfeiffer, R. F. Potential of transdermal drug delivery in Parkinson's disease. *Drugs & Aging* **19**, 561-570, doi:10.2165/00002512-200219080-00002 (2002).

111 Marwah, H., Garg, T., Goyal, A. K. & Rath, G. Permeation enhancer strategies in transdermal drug delivery. *Drug Deliv* **23**, 564-578, doi:10.3109/10717544.2014.935532 (2016).

112 in *Novel Delivery Systems for Transdermal and Intradermal Drug Delivery* 125-146.

113 Williams, A. C. & Barry, B. W. Penetration enhancers. *Adv Drug Deliv Rev* **56**, 603-618, doi:10.1016/j.addr.2003.10.025 (2004).

114 Spencer, T. S., Linamen, C. E., Akers, W. A. & Jones, H. E. Temperature dependence of water content of stratum corneum. *Br J Dermatol* **93**, 159-164, doi:10.1111/j.1365-2133.1975.tb06735.x (1975).

115 Hafeez, F. & Maibach, H. Occlusion effect on in vivo percutaneous penetration of chemicals in man and monkey: partition coefficient effects. *Skin Pharmacol Physiol* **26**, 85-91, doi:10.1159/000346273 (2013).

116 Bouwstra, J. A. *et al.* Water distribution and related morphology in human stratum corneum at different hydration levels. *J Invest Dermatol* **120**, 750-758, doi:10.1046/j.1523-1747.2003.12128.x (2003).

117 Heard, C. M. in *Percutaneous Penetration Enhancers Chemical Methods in Penetration Enhancement: Modification of the Stratum Corneum* (eds Nina Dragicevic & Howard I. Maibach) 151-172 (Springer Berlin Heidelberg, 2015).

118 Bommannan, D., Potts, R. O. & Guy, R. H. Examination of the effect of ethanol on human stratum corneum in vivo using infrared spectroscopy. *J Control Release* **16**, 299-304, doi:https://doi.org/10.1016/0168-3659(91)90006-Y (1991).

119 Van der Merwe, D. & Riviere, J. E. Comparative studies on the effects of water, ethanol and water/ethanol mixtures on chemical partitioning into porcine stratum corneum and silastic membrane. *Toxicol in Vitro* **19**, 69-77, doi:https://doi.org/10.1016/j.tiv.2004.06.002 (2005).

120 Horita, D. *et al.* Molecular mechanisms of action of different concentrations of ethanol in water on ordered structures of intercellular lipids and soft keratin in the stratum corneum. *Biochim Biophys Acta* **1848**, 1196-1202, doi:10.1016/j.bbamem.2015.02.008 (2015).

121 Goates, C. Y. & Knutson, K. Enhanced permeation of polar compounds through human epidermis. I. Permeability and membrane structural changes in the presence of short chain alcohols. *Biochim Biophys Acta Biomembr* **1195**, 169-179, doi:https://doi.org/10.1016/0005-2736(94)90024-8 (1994).

122 Heard, C. M., Kung, D. & Thomas, C. P. Skin penetration enhancement of mefenamic acid by ethanol and 1,8-cineole can be explained by the 'pull' effect. *Int J Pharm* **321**, 167-170, doi:https://doi.org/10.1016/j.ijpharm.2006.05.018 (2006).

123 Lachenmeier, D. W. Safety evaluation of topical applications of ethanol on the skin and inside the oral cavity. *J Occup Med Toxicol* **3**, 26-26, doi:10.1186/1745-6673-3-26 (2008).

124 Okabe, H., Suzuki, E., Saitoh, T., Takayama, K. & Nagai, T. Development of novel transdermal system containing d-limonene and ethanol as absorption enhancers. *J Control Release* **32**, 243-247, doi:https://doi.org/10.1016/0168-3659(94)90234-8 (1994).

125 Kurihara-Bergstrom, T., Knutson, K., DeNoble, L. J. & Goates, C. Y. Percutaneous absorption enhancement of an ionic molecule by ethanol-water systems in human skin. *Pharm Res* **7**, 762-766 (1990).

126 Berner, B. *et al.* Ethanol: water mutually enhanced transdermal therapeutic system II: Skin permeation of ethanol and nitroglycerin. *J Pharm Sci* **78**, 402-407, doi:https://doi.org/10.1002/jps.2600780512 (1989).

127 Megrab, N. A., Williams, A. C. & Barry, B. W. Oestradiol permeation across human skin, silastic and snake skin membranes: The effects of ethanol/water co-solvent

systems. *Int J Pharm* **116**, 101-112, doi:https://doi.org/10.1016/0378-5173(94)00321-U (1995).

128 Lane, M. E. Nanoparticles and the skin – applications and limitations. *J Microencapsul* **28**, 709-716, doi:10.3109/02652048.2011.599440 (2011).

129 Lombardi Borgia, S. *et al.* Lipid nanoparticles for skin penetration enhancement-correlation to drug localization within the particle matrix as determined by fluorescence and parelectric spectroscopy. *J Control Release* **110**, 151-163, doi:10.1016/j.jconrel.2005.09.045 (2005).

130 Wissing, S. A. & Muller, R. H. A novel sunscreen system based on tocopherol acetate incorporated into solid lipid nanoparticles. *Int J Cosmet Sci* **23**, 233-243, doi:10.1046/j.1467-2494.2001.00087.x (2001).

131 Kuchler, S. *et al.* Nanoparticles for skin penetration enhancement--a comparison of a dendritic core-multishell-nanotransporter and solid lipid nanoparticles. *Eur J Pharm Biopharm* **71**, 243-250, doi:10.1016/j.ejpb.2008.08.019 (2009).

132 Honzke, S. *et al.* Tailored dendritic core-multishell nanocarriers for efficient dermal drug delivery: A systematic top-down approach from synthesis to preclinical testing. *J Control Release* **242**, 50-63, doi:10.1016/j.jconrel.2016.06.030 (2016).

133 Alnasif, N. *et al.* Penetration of normal, damaged and diseased skin--an in vitro study on dendritic core-multishell nanotransporters. *J Control Release* **185**, 45-50, doi:10.1016/j.jconrel.2014.04.006 (2014).

134 Lademann, J. *et al.* Triggered release of model drug from AuNP-doped BSA nanocarriers in hair follicles using IRA radiation. *Acta Biomater* **30**, 388-396, doi:10.1016/j.actbio.2015.11.052 (2016).

135 Safwat, M. A., Soliman, G. M., Sayed, D. & Attia, M. A. Fluorouracil-loaded gold nanoparticles for the treatment of skin cancer: Development, in vitro characterization, and in vivo evaluation in a mouse skin cancer xenograft model. *Mol Pharm* **15**, 2194-2205, doi:10.1021/acs.molpharmaceut.8b00047 (2018).

136 Lohan, S. B. *et al.* Investigation of the cutaneous penetration behavior of dexamethasone loaded to nano-sized lipid particles by EPR spectroscopy, and confocal Raman and laser scanning microscopy. *Eur J Pharm Biopharm* **116**, 102-110, doi:10.1016/j.ejpb.2016.12.018 (2017).

137 Patzelt, A. *et al.* Selective follicular targeting by modification of the particle sizes. *J Control Release* **150**, 45-48, doi:10.1016/j.jconrel.2010.11.015 (2011).

138 Mura, S., Nicolas, J. & Couvreur, P. Stimuli-responsive nanocarriers for drug delivery. *Nat Mater* **12**, 991, doi:10.1038/nmat3776 (2013).

139 Mak, W. C. *et al.* Triggering of drug release of particles in hair follicles. *J Control Release* **160**, 509-514, doi:https://doi.org/10.1016/j.jconrel.2012.04.007 (2012).

140 Giulbudagian, M. *et al.* Breaking the barrier-potent anti-inflammatory activity following efficient topical delivery of etanercept using thermoresponsive nanogels. *Theranostics* **8**, 450-463, doi:10.7150/thno.21668 (2018).

141 Desmet, E. *et al.* An elastic liposomal formulation for RNAi-based topical treatment of skin disorders: Proof-of-concept in the treatment of psoriasis. *Int J Pharm* **500**, 268-274, doi:https://doi.org/10.1016/j.ijpharm.2016.01.042 (2016).

142 Hasanovic, A., Zehl, M., Reznicek, G. & Valenta, C. Chitosan-tripolyphosphate nanoparticles as a possible skin drug delivery system for aciclovir with enhanced stability. *J Pharm Pharmacol* **61**, 1609-1616, doi:10.1211/jpp.61.12.0004 (2009).

143 Jee, J.-P., Lim, S.-J., Park, J.-S. & Kim, C.-K. Stabilization of all-trans retinol by loading lipophilic antioxidants in solid lipid nanoparticles. *Eur J Pharm Biopharm* **63**, 134-139, doi:https://doi.org/10.1016/j.ejpb.2005.12.007 (2006).

144 Singhal, M., Lapteva, M. & Kalia, Y. N. Formulation challenges for 21st century topical and transdermal delivery systems. *Expert Opin Drug Deliv* **14**, 705-708, doi:10.1080/17425247.2017.1311320 (2017).

145 Lee, R. W., Shenoy, D. B. & Sheel, R. in *Handbook of Non-Invasive Drug Delivery Systems* (ed Vitthal S. Kulkarni) 37-58 (William Andrew Publishing, 2010).

146 Hua, S. Lipid-based nano-delivery systems for skin delivery of drugs and bioactives. *Front Pharmacol* **6**, 219, doi:10.3389/fphar.2015.00219 (2015).

147 Naeff, R. Feasibility of topical liposome drugs produced on an industrial scale. *Adv Drug Deliv Rev* **18**, 343-347, doi:https://doi.org/10.1016/0169-409X(95)00080-Q (1996).

148 Korting, H. C., Klövekorn, W., Klövekorn, G. & Group, E. C. S. Comparative efficacy and tolerability of econazole liposomal gel 1%, branded econazole conventional cream 1% and generic clotrimazole cream 1% in tinea pedis. *Clin Drug Investig* **14**, 286-293, doi:10.2165/00044011-199714040-00006 (1997).

149 Dreier, J., Sørensen, J. A. & Brewer, J. R. Superresolution and fluorescence dynamics evidence reveal that intact liposomes do not cross the human skin barrier. *PLoS One* **11**, e0146514, doi:10.1371/journal.pone.0146514 (2016).

150 Campbell, C. S., Contreras-Rojas, L. R., Delgado-Charro, M. B. & Guy, R. H. Objective assessment of nanoparticle disposition in mammalian skin after topical exposure. *J Control Release* **162**, 201-207, doi:10.1016/j.jconrel.2012.06.024 (2012).

151 Levintova, Y., Plakogiannis, F. M. & Bellantone, R. A. An improved in vitro method for measuring skin permeability that controls excess hydration of skin using modified Franz diffusion cells. *Int J Pharm* **419**, 96-106, doi:10.1016/j.ijpharm.2011.07.025 (2011).

152 Radbruch, M. *et al.* Dendritic Core-Multishell Nanocarriers in Murine Models of Healthy and Atopic Skin. *Nanoscale Res Lett* **12**, 64, doi:10.1186/s11671-017-1835-0 (2017).

153 Pischon, H. *et al.* Stratum corneum targeting by dendritic core-multishell-nanocarriers in a mouse model of psoriasis. *Nanomedicine* **13**, 317-327, doi:10.1016/j.nano.2016.09.004 (2017).

154 Wissing, S. A. & Müller, R. H. Solid lipid nanoparticles as carrier for sunscreens: in vitro release and in vivo skin penetration. *J Control Release* **81**, 225-233, doi:https://doi.org/10.1016/S0168-3659(02)00056-1 (2002).

155 Estracanholli, É. A., Praça, F. S. G., Cintra, A. B., Pierre, M. B. R. & Lara, M. G. Liquid crystalline systems for transdermal delivery of celecoxib: In vitro drug release and skin permeation studies. *AAPS PharmSciTech* **15**, 1468-1475, doi:10.1208/s12249-014-0171-2 (2014).

156 Fontana, M. C., Rezer, J. F., Coradini, K., Leal, D. B. & Beck, R. C. Improved efficacy in the treatment of contact dermatitis in rats by a dermatological nanomedicine containing clobetasol propionate. *Eur J Pharm Biopharm* **79**, 241-249, doi:10.1016/j.ejpb.2011.05.002 (2011).

157 Balzus, B. *et al.* Formulation and ex vivo evaluation of polymeric nanoparticles for controlled delivery of corticosteroids to the skin and the corneal epithelium. *Eur J Pharm Biopharm* **115**, 122-130, doi:10.1016/j.ejpb.2017.02.001 (2017).

158 Stracke, F. *et al.* Multiphoton microscopy for the investigation of dermal penetration of nanoparticle-borne drugs. *J Invest Dermatol* **126**, 2224-2233, doi:10.1038/sj.jid.5700374 (2006).

159 Li, Y., Wong, H. L., Shuhendler, A. J., Rauth, A. M. & Wu, X. Y. Molecular interactions, internal structure and drug release kinetics of rationally developed polymer–lipid hybrid nanoparticles. *J Control Release* **128**, 60-70, doi:https://doi.org/10.1016/j.jconrel.2008.02.014 (2008).

160 De Robertis, S. *et al.* Advances in oral controlled drug delivery: the role of drug–polymer and interpolymer non-covalent interactions. *Expert Opinion on Drug Delivery* **12**, 441-453, doi:10.1517/17425247.2015.966685 (2015).

161 Cai, X. J., Woods, A., Mesquida, P. & Jones, S. A. Assessing the potential for drug-nanoparticle surface interactions to improve drug penetration into the skin. *Mol Pharm* **13**, 1375-1384, doi:10.1021/acs.molpharmaceut.6b00032 (2016).

162 Svenskaya, Y. I. *et al.* A simple non-invasive approach toward efficient transdermal drug delivery based on biodegradable particulate system. *ACS Appl Mater Interfaces* **11**, 17270-17282, doi:10.1021/acsami.9b04305 (2019).

163 Kahraman, E., Güngör, S. & Özsoy, Y. Potential enhancement and targeting strategies of polymeric and lipid-based nanocarriers in dermal drug delivery. *Ther Deliv* **8**, 967-985, doi:10.4155/tde-2017-0075 (2017).

164 Verma, D. D., Verma, S., Blume, G. & Fahr, A. Particle size of liposomes influences dermal delivery of substances into skin. *Int J Pharm* **258**, 141-151, doi:https://doi.org/10.1016/S0378-5173(03)00183-2 (2003).

165 P. Shah, P., R. Desai, P. & Singh, M. Effect of oleic acid modified polymeric bilayered nanoparticles on percutaneous delivery of spantide II and ketoprofen. *J Control Release* **158**, 336-345, doi:https://doi.org/10.1016/j.jconrel.2011.11.016 (2012).

166 Baspinar, Y. & Borchert, H.-H. Penetration and release studies of positively and negatively charged nanoemulsions—Is there a benefit of the positive charge? *Int J Pharm* **430**, 247-252, doi:https://doi.org/10.1016/j.ijpharm.2012.03.040 (2012).

167 Contri, R. V. *et al.* Skin penetration and dermal tolerability of acrylic nanocapsules: Influence of the surface charge and a chitosan gel used as vehicle. *Int J Pharm* **507**, 12-20, doi:https://doi.org/10.1016/j.ijpharm.2016.03.046 (2016).

168 Larese, F. F. *et al.* Human skin penetration of silver nanoparticles through intact and damaged skin. *Toxicology* **255**, 33-37, doi:10.1016/j.tox.2008.09.025 (2009).

169 Zhu, Y. J. *et al.* Penetration of silver nanoparticles into porcine skin ex vivo using fluorescence lifetime imaging microscopy, Raman microscopy, and surface-enhanced Raman scattering microscopy. *J Biomed Opt* **20**, doi:10.1117/1.JBO.20.5.051006 (2015).

170 Mohammed, Y. H. *et al.* Support for the safe use of zinc oxide nanoparticle sunscreens: Lack of skin penetration or cellular Toxicity after repeated application in volunteers. *J Invest Dermatol* **139**, 308-315, doi:10.1016/j.jid.2018.08.024 (2019).

171 Yamamoto, K. *et al.* Influence of the skin barrier on the penetration of topically-applied dexamethasone probed by soft X-ray spectromicroscopy. *Eur J Pharm Biopharm* **118**, 30-37, doi:10.1016/j.ejpb.2016.12.005 (2017).

172 Alex, A. *et al.* In situ biodistribution and residency of a topical anti-inflammatory using fluorescence lifetime imaging microscopy. *Br J Dermatol* **179**, 1342-1350, doi:10.1111/bjd.16992 (2018).

173 Zhang, G., Moore, D. J., Sloan, K. B., Flach, C. R. & Mendelsohn, R. Imaging the prodrug-to-drug transformation of a 5-fluorouracil derivative in skin by confocal Raman microscopy. *J Invest Dermatol* **127**, 1205-1209, doi:10.1038/sj.jid.5700690 (2007).

174 Witting, M. *et al.* Interactions of hyaluronic Acid with the skin and implications for the dermal delivery of biomacromolecules. *Mol Pharm* **12**, 1391-1401, doi:10.1021/mp500676e (2015).

175 Mahmoud, N. N., Al-Qaoud, K. M., Al-Bakri, A. G., Alkilany, A. M. & Khalil, E. A. Colloidal stability of gold nanorod solution upon exposure to excised human skin: Effect of surface chemistry and protein adsorption. *Int J Biochem Cell B* **75**, 223-231, doi:10.1016/j.biocel.2016.02.020 (2016).

176 Boreham, A., Pfaff, M., Fleige, E., Haag, R. & Alexiev, U. Nanodynamics of dendritic core-multishell nanocarriers. *Langmuir* **30**, 1686-1695, doi:10.1021/la4043155 (2014).

177 Dong, P. *et al.* pH-sensitive Eudragit(R) L 100 nanoparticles promote cutaneous penetration and drug release on the skin. *J Control Release* **295**, 214-222, doi:10.1016/j.jconrel.2018.12.045 (2019).

178 Eaton, G. R., Eaton, S. S., Barr, D. P. & Weber, R. T. in *Quantitative EPR: A Practitioners Guide* 1-14 (Springer Vienna, 2010).

179 Kempe, S., Metz, H. & Mader, K. Application of electron paramagnetic resonance (EPR) spectroscopy and imaging in drug delivery research - chances and challenges. *Eur J Pharm Biopharm* **74**, 55-66, doi:10.1016/j.ejpb.2009.08.007 (2010).

180 Albrecht, S. *et al.* Skin type differences in solar-simulated radiation-induced oxidative stress. *Br J Dermatol* **180**, 597-603, doi:10.1111/bjd.17129 (2019).

181 in *Electron Paramagnetic Resonance* 36-57.

182 Azarkh, M., Okle, O., Eyring, P., Dietrich, D. R. & Drescher, M. Evaluation of spin labels for in-cell EPR by analysis of nitroxide reduction in cell extract of Xenopus laevis oocytes. *J Magn Reson* **212**, 450-454, doi:10.1016/j.jmr.2011.07.014 (2011).

183 Melanson, M., Sood, A., Torok, F. & Torok, M. Introduction to spin label electron paramagnetic resonance spectroscopy of proteins. *Biochem Mol Biol Educ* **41**, 156-162, doi:10.1002/bmb.20677 (2013).

184 Hyodo, F., Yasukawa, K., Yamada, K. I. & Utsumi, H. Spatially resolved time-course studies of free radical reactions with an EPRI/MRI fusion technique. *Magn Reson Med* **56**, 938-943, doi:10.1002/mrm.21019 (2006).

185 Walker, K. A. *et al.* Spin-labeling of dexamethasone: radical stability vs. temporal resolution of EPR-spectroscopy on biological samples. *Z Phys Chem* **232**, 883-891, doi:10.1515/zpch-2017-1076 (2018).

186 Stoll, S. & Schweiger, A. EasySpin, a comprehensive software package for spectral simulation and analysis in EPR. *J Magn Reson* **178**, 42-55, doi:10.1016/j.jmr.2005.08.013 (2006).

187 Saeidpour, S. *et al.* Drug distribution in nanostructured lipid particles. *Eur J Pharm Biopharm* **110**, 19-23, doi:10.1016/j.ejpb.2016.10.008 (2017).

188 Plonka, P. M. Electron paramagnetic resonance as a unique tool for skin and hair research. *Exp Dermatol* **18**, 472-484, doi:10.1111/j.1600-0625.2009.00883.x (2009).

189 Spasojevic, I. Electron paramagnetic resonance - a powerful tool of medical biochemistry in discovering mechanisms of disease and treatment prospects. *J Med Biochem* **29**, 175-188, doi:10.2478/v10011-010-0020-0 (2010).

190 Lurie, D. J. & Mader, K. Monitoring drug delivery processes by EPR and related techniques--principles and applications. *Adv Drug Deliv Rev* **57**, 1171-1190, doi:10.1016/j.addr.2005.01.023 (2005).

191 Katzhendler, I., Mader, K. & Friedman, M. Correlation between drug release kinetics from proteineous matrix and matrix structure: EPR and NMR study. *J Pharm Sci* **89**, 365-381 (2000).

192 Ensslin, S., Moll, K. P., Metz, H., Otz, M. & Mäder, K. Modulating pH-independent release from coated pellets: Effect of coating composition on solubilization processes and drug release. *Eur J Pharm Biopharm* **72**, 111-118, doi:https://doi.org/10.1016/j.ejpb.2008.11.005 (2009).

193 Saeidpour, S. *et al.* Localization of dexamethasone within dendritic core-multishell (CMS) nanoparticles and skin penetration properties studied by multi-frequency electron paramagnetic resonance (EPR) spectroscopy. *Eur J Pharm Biopharm* **116**, 94-101, doi:10.1016/j.ejpb.2016.10.001 (2017).

194 Alvarez-Roman, R., Naik, A., Kalia, Y. N., Fessi, H. & Guy, R. H. Visualization of skin penetration using confocal laser scanning microscopy. *Eur J Pharm Biopharm* **58**, 301-316, doi:10.1016/j.ejpb.2004.03.027 (2004).

195 Zhang, L. W. & Monteiro-Riviere, N. A. Use of confocal microscopy for nanoparticle drug delivery through skin. *J Biomed Opt* **18**, 061214, doi:10.1117/1.JBO.18.6.061214 (2013).

196 Ilie, M. A. *et al.* Current and future applications of confocal laser scanning microscopy imaging in skin oncology. *Oncol Lett* **17**, 4102-4111, doi:10.3892/ol.2019.10066 (2019).

197 Skvara, H., Plut, U., Schmid, J. A. & Jonak, C. Combining in vivo reflectance with fluorescence confocal microscopy provides additive information on skin morphology. *Dermatol Pract Concept* **2**, 3-12, doi:10.5826/dpc.0201a02. (2012).

198 Ulrich, M. *et al.* In vivo detection of basal cell carcinoma: comparison of a reflectance confocal microscope and a multiphoton tomograph. *J Biomed Opt* **18**, 1-8, 8 (2013).

199 Cornea, A. & Conn, P. M. *Fluorescence Microscopy: Super-Resolution and other Novel Techniques*. (Elsevier, 2014).

200 Sahle, F. F., Giulbudagian, M., Bergueiro, J., Lademann, J. & Calderon, M. Dendritic polyglycerol and N-isopropylacrylamide based thermoresponsive nanogels as smart carriers for controlled delivery of drugs through the hair follicle. *Nanoscale* **9**, 172-182, doi:10.1039/c6nr06435c (2017).

201 De Giorgi, V. *et al.* Combined non-linear laser imaging (two-photon excitation fluorescence microscopy, fluorescence lifetime imaging microscopy, multispectral multiphoton microscopy) in cutaneous tumours: first experiences. *J Eur Acad Dermatol Venereol* **23**, 314-316, doi:10.1111/j.1468-3083.2008.03045.x (2009).

202 Schenke-Layland, K., Riemann, I., Damour, O., Stock, U. A. & Konig, K. Two-photon microscopes and in vivo multiphoton tomographs--powerful diagnostic tools for tissue engineering and drug delivery. *Adv Drug Deliv Rev* **58**, 878-896, doi:10.1016/j.addr.2006.07.004 (2006).

203 Tsai, T. H., Jee, S. H., Dong, C. Y. & Lin, S. J. Multiphoton microscopy in dermatological imaging. *J Dermatol Sci* **56**, 1-8, doi:10.1016/j.jdermsci.2009.06.008 (2009).

204 Oheim, M., Michael, D. J., Geisbauer, M., Madsen, D. & Chow, R. H. Principles of two-photon excitation fluorescence microscopy and other nonlinear imaging approaches. *Adv Drug Deliv Rev* **58**, 788-808, doi:10.1016/j.addr.2006.07.005 (2006).

205 Sahle, F. F., Balzus, B., Gerecke, C., Kleuser, B. & Bodmeier, R. Formulation and in vitro evaluation of polymeric enteric nanoparticles as dermal carriers with pH-dependent targeting potential. *Eur J Pharm Sci* **92**, 98-109, doi:10.1016/j.ejps.2016.07.004 (2016).

206 Sahle, F. F., Gerecke, C., Kleuser, B. & Bodmeier, R. Formulation and comparative in vitro evaluation of various dexamethasone-loaded pH-sensitive polymeric nanoparticles intended for dermal applications. *Int J Pharm* **516**, 21-31, doi:10.1016/j.ijpharm.2016.11.029 (2017).

207 Holm, E. A., Wulf, H. C., Thomassen, L. & Jemec, G. B. E. Instrumental assessment of atopic eczema: Validation of transepidermal water loss, stratum corneum hydration, erythema, scaling, and edema. *J Am Acad Dermatol* **55**, 772-780, doi:https://doi.org/10.1016/j.jaad.2006.03.036 (2006).

208 WHITE, M. I., JENKINSON, D. M. & LLOYD, D. H. The effect of washing on the thickness of the stratum corneum in normal and atopic individuals. *Brit J Dermatol* **116**, 525-530, doi:10.1111/j.1365-2133.1987.tb05873.x (1987).

209 AL-JABERI, H. & MARKS, R. Studies of the clinically uninvolved skin in patients with dermatitis. *Brit J Dermatol* **111**, 437-443, doi:10.1111/j.1365-2133.1984.tb06606.x (1984).

210 Voegeli, R. *et al.* Increased stratum corneum serine protease activity in acute eczematous atopic skin. *Brit J Dermatol* **161**, 70-77, doi:10.1111/j.1365-2133.2009.09142.x (2009).

211 Choe, C., Lademann, J. & Darvin, M. E. A depth-dependent profile of the lipid conformation and lateral packing order of the stratum corneum in vivo measured using Raman microscopy. *Analyst* **141**, 1981-1987, doi:10.1039/c5an02373d (2016).

212 Lohan, S. B. *et al.* Free radicals induced by sunlight in different spectral regions - in vivo versus ex vivo study. *Exp Dermatol* **25**, 380-385, doi:10.1111/exd.12987 (2016).

213 Klein, A. L. *et al.* Solvent-containing closure material can be used to prevent follicular penetration of caffeine and fluorescein sodium salt on porcine ear skin. *Skin Pharmacol Phys*, doi: 10.1159/000505839 (2020).

214 Liu, X. *et al.* Hair follicles contribute significantly to penetration through human skin only at times soon after application as a solvent deposited solid in man. *Br J Clin Pharmacol* **72**, 768-774, doi:10.1111/j.1365-2125.2011.04022.x (2011).

215 Isaksson, M., Gruvberger, B., Frick-Engfeldt, M. & Bruze, M. Which test chambers should be used for acetone, ethanol, and water solutions when patch testing? *Contact Dermatitis* **57**, 134-136, doi:10.1111/j.1600-0536.2007.01094.x (2007).

216 Oliveira, G., Hadgraft, J. & Lane, M. E. The influence of volatile solvents on transport across model membranes and human skin. *Int J Pharm* **435**, 38-49, doi:https://doi.org/10.1016/j.ijpharm.2012.05.037 (2012).

217 Coldman, M. F., Poulsen, B. J. & Higuchi, T. Enhancement of percutaneous absorption by the use of volatile: Nonvolatile systems as vehicles. *J Pharm Sci* **58**, 1098-1102, doi:https://doi.org/10.1002/jps.2600580912 (1969).

218 Hamishehkar, H. *et al.* A comparative histological study on the skin occlusion performance of a cream made of solid lipid nanoparticles and Vaseline. *Res Pharm Sci* **10**, 378-387 (2015).

219 van Kuijk-Meuwissen, M. E. M. J., Junginger, H. E. & Bouwstra, J. A. Interactions between liposomes and human skin in vitro, a confocal laser scanning microscopy study. *Biochim Biophys Acta Biomembr* **1371**, 31-39, doi:https://doi.org/10.1016/S0005-2736(97)00273-3 (1998).

220 Cross, S. E. & Roberts, M. S. The effect of occlusion on epidermal penetration of parabens from a commercial allergy test ointment, acetone and ethanol vehicles. *J Invest Dermatol* **115**, 914-918, doi:https://doi.org/10.1046/j.1523-1747.2000.00151.x (2000).

221 Shah, P. P., Desai, P. R., Patel, A. R. & Singh, M. S. Skin permeating nanogel for the cutaneous co-delivery of two anti-inflammatory drugs. *Biomaterials* **33**, 1607-1617, doi:https://doi.org/10.1016/j.biomaterials.2011.11.011 (2012).

222 Theune, L. E. *et al.* Critical parameters for the controlled synthesis of nanogels suitable for temperature-triggered protein delivery. *Mater Sci Eng C Mater Biol Appl* **100**, 141-151, doi:https://doi.org/10.1016/j.msec.2019.02.089 (2019).

223 Radtke, M., Patzelt, A., Knorr, F., Lademann, J. & Netz, R. R. Ratchet effect for nanoparticle transport in hair follicles. *Eur J Pharm Biopharm* **116**, 125-130, doi:https://doi.org/10.1016/j.ejpb.2016.10.005 (2017).

224 Osborne, D. W. & Musakhanian, J. Skin Penetration and Permeation Properties of Transcutol®—Neat or Diluted Mixtures. *AAPS PharmSciTech* **19**, 3512-3533, doi:10.1208/s12249-018-1196-8 (2018).

225 Romero, C. M. & Paéz, M. S. Surface tension of aqueous solutions of alcohol and polyols at 298.15 K. *Phys Chem Liquids* **44**, 61-65, doi:10.1080/01421590500315360 (2006).

226 Cwikel, D., Zhao, Q., Liu, C., Su, X. & Marmur, A. Comparing contact angle measurements and surface tension assessments of solid surfaces. *Langmuir* **26**, 15289-15294, doi:10.1021/la1020252 (2010).

227 Schott, H. Contact Angles and Wettability of Human Skin. *J Pharm Sci-Us* **60**, 1893-1895, doi:https://doi.org/10.1002/jps.2600601233 (1971).

228 Dong, L., Chaudhury, A. & Chaudhury, M. K. Lateral vibration of a water drop and its motion on a vibrating surface. *Eur Phys J E Soft Matter* **21**, 231-242, doi:10.1140/epje/i2006-10063-7 (2006).

229 Llopis, J., McCaffery, J. M., Miyawaki, A., Farquhar, M. G. & Tsien, R. Y. Measurement of cytosolic, mitochondrial, and Golgi pH in single living cells with green fluorescent proteins. *Proc Natl Acad Sci U S A* **95**, 6803-6808, doi:10.1073/pnas.95.12.6803 (1998).

230 Davies, D. J., Ward, R. J. & Heylings, J. R. Multi-species assessment of electrical resistance as a skin integrity marker for in vitro percutaneous absorption studies. *Toxicol in Vitro* **18**, 351-358, doi:10.1016/j.tiv.2003.10.004 (2004).

231 Rancan, F. *et al.* Investigation of polylactic acid (PLA) nanoparticles as drug delivery systems for local dermatotherapy. *Pharm Res* **26**, 2027-2036, doi:10.1007/s11095-009-9919-x (2009).

232 Sheu, H. M., Chao, S. C., Wong, T. W., Yu-Yun Lee, J. & Tsai, J. C. Human skin surface lipid film: an ultrastructural study and interaction with corneocytes and intercellular lipid lamellae of the stratum corneum. *Br J Dermatol* **140**, 385-391, doi:10.1046/j.1365-2133.1999.02697.x (1999).

233 Mavon, A. *et al.* Sebum and stratum corneum lipids increase human skin surface free energy as determined from contact angle measurements: A study on two anatomical sites. *Colloids Surf B Biointerfaces* **8**, 147-155, doi:Doi 10.1016/S0927-7765(96)01317-3 (1997).

234 Pailler-Mattei, C., Guerret-Piecourt, C., Zahouani, H. & Nicoli, S. Interpretation of the human skin biotribological behaviour after tape stripping. *J R Soc Interface* **8**, 934-941, doi:10.1098/rsif.2010.0672 (2011).

235 Watkinson, R. M. *et al.* Influence of ethanol on the solubility, ionization and permeation characteristics of ibuprofen in silicone and human skin. *Skin Pharmacol Physiol* **22**, 15-21, doi:10.1159/000183922 (2009).

236 Liu, J., Xiao, Y. & Allen, C. Polymer–drug compatibility: A guide to the development of delivery systems for the anticancer agent, ellipticine. *J Pharm Sci* **93**, 132-143, doi:10.1002/jps.10533 (2004).

237 Zoubari, G., Staufenbiel, S., Volz, P., Alexiev, U. & Bodmeier, R. Effect of drug solubility and lipid carrier on drug release from lipid nanoparticles for dermal delivery. *Eur J Pharm Biopharm* **110**, 39-46, doi:https://doi.org/10.1016/j.ejpb.2016.10.021 (2017).

238 Unbehauen, M. L. *et al.* Biodegradable core–multishell nanocarriers: Influence of inner shell structure on the encapsulation behavior of dexamethasone and tacrolimus. *Polymers* **9**, 316 (2017).

239 Du, F. *et al.* Development of biodegradable hyperbranched core-multishell nanocarriers for efficient topical drug delivery. *J Control Release* **242**, 42-49, doi:https://doi.org/10.1016/j.jconrel.2016.06.048 (2016).

240 Giulbudagian, M. *et al.* Enhanced topical delivery of dexamethasone by β-cyclodextrin decorated thermoresponsive nanogels. *Nanoscale* **10**, 469-479, doi:10.1039/C7NR04480A (2018).

241 Döge, N. *et al.* Ethyl cellulose nanocarriers and nanocrystals differentially deliver dexamethasone into intact, tape-stripped or sodium lauryl sulfate-exposed ex vivo human skin - assessment by intradermal microdialysis and extraction from the different skin layers. *J Control Release* **242**, 25-34, doi:https://doi.org/10.1016/j.jconrel.2016.07.009 (2016).

242 Bolzinger, M.-A., Briançon, S., Pelletier, J. & Chevalier, Y. Penetration of drugs through skin, a complex rate-controlling membrane. *Curr Opin Colloid Interface Sci* **17**, 156-165, doi:https://doi.org/10.1016/j.cocis.2012.02.001 (2012).

243 Dreher, F. *et al.* Comparison of cutaneous bioavailability of cosmetic preparations containing caffeine or α-tocopherol applied on human skin models or human skin ex vivo at finite doses. *Skin Pharmacol Phys* **15(suppl1)**, 40-58, doi:10.1159/000066680 (2002).

244 Shah, D. K., Khandavilli, S. & Panchagnula, R. Alteration of skin hydration and its barrier function by vehicle and permeation enhancers: a study using TGA, FTIR, TEWL

and drug permeation as markers. *Methods Find Exp Clin Pharmacol* **30**, 499-512, doi:10.1358/mf.2008.30.7.1159653 (2008).

245 Moghadam, S. H. *et al.* Effect of chemical permeation enhancers on stratum corneum barrier lipid organizational structure and interferon alpha permeability. *Mol Pharm* **10**, 2248-2260, doi:10.1021/mp300441c (2013).

246 Tregear, R. T. The Permeability of Mammalian Skin to Ions. *J Invest Dermatol* **46**, 16-23, doi:https://doi.org/10.1038/jid.1966.4 (1966).

247 Dąbrowska, A. K. *et al.* In vivo confirmation of hydration-induced changes in human-skin thickness, roughness and interaction with the environment. *Biointerphases* **11**, 031015, doi:10.1116/1.4962547 (2016).

248 Nakazawa, H., Ohta, N. & Hatta, I. A possible regulation mechanism of water content in human stratum corneum via intercellular lipid matrix. *Chem Phys Lipids* **165**, 238-243, doi:https://doi.org/10.1016/j.chemphyslip.2012.01.002 (2012).

249 Bendas, B., Schmalfuss, U. & Neubert, R. Influence of propylene-glycol as cosolvent on mechanisms of drug transport from hydrogels. *Int J Pharm* **116**, 19-30, doi:Doi 10.1016/0378-5173(94)00267-9 (1995).

250 Kandimalla, K. K., Kanikkannan, N. & Singh, M. Optimization of a vehicle mixture for the transdermal delivery of melatonin using artificial neural networks and response surface method. *J Control Release* **61**, 71-82, doi:https://doi.org/10.1016/S0168-3659(99)00107-8 (1999).

251 Panchagnula, R., Salve, P. S., Thomas, N. S., Jain, A. K. & Ramarao, P. Transdermal delivery of naloxone: effect of water, propylene glycol, ethanol and their binary combinations on permeation through rat skin. *Int J Pharm* **219**, 95-105, doi:https://doi.org/10.1016/S0378-5173(01)00634-2 (2001).

252 Yamamoto, K. *et al.* Selective Probing of the Penetration of Dexamethasone into Human Skin by Soft X-ray Spectromicroscopy. *Anal Chem* **87**, 6173-6179, doi:10.1021/acs.analchem.5b00800 (2015).

253 Ponec, M. & Kempenaar, J. A. Biphasic entry of glucocorticoids into cultured human skin keratinocytes and fibroblasts. *Arch Dermatol Res* **275**, 334-344, doi:10.1007/bf00417208 (1983).

254 Xiao Wen, L. *et al.* Penetration of Nanoparticles into Human Skin. *Curr Pharm Des* **19**, 6353-6366, doi:http://dx.doi.org/10.2174/1381612811319350011 (2013).

255 Lauterbach, A. & Müller-Goymann, C. C. Comparison of rheological properties, follicular penetration, drug release, and permeation behavior of a novel topical drug delivery system and a conventional cream. *Eur J Pharm Biopharm* **88**, 614-624, doi:https://doi.org/10.1016/j.ejpb.2014.10.001 (2014).

256 Kramer, A. *et al.* Quantity of ethanol absorption after excessive hand disinfection using three commercially available hand rubs is minimal and below toxic levels for humans. *BMC Infect Dis* **7**, 117, doi:10.1186/1471-2334-7-117 (2007).

257 Lee, A. J., King, J. R. & Barrett, D. A. Percutaneous absorption: a multiple pathway model. *J Control Release* **45**, 141-151, doi:https://doi.org/10.1016/S0168-3659(96)01567-2 (1997).

258 Chen, L., Lian, G. & Han, L. Modeling transdermal permeation. Part I. Predicting skin permeability of both hydrophobic and hydrophilic solutes. *AIChE Journal* **56**, 1136-1146, doi:10.1002/aic.12048 (2010).

259 Swartz, H. M., Sentjurc, M. & Morse, P. D. Cellular metabolism of water-soluble nitroxides: Effect on rate of reduction of cell/nitroxide ratio, oxygen concentrations and permeability of nitroxides. *Biochim Biophys Acta Mol Cell Res* **888**, 82-90, doi:https://doi.org/10.1016/0167-4889(86)90073-X (1986).

260 Bozkurt, A. *et al.* Unsupervised delineation of stratum corneum using reflectance confocal microscopy and spectral clustering. *Skin Res Technol* **23**, 176-185, doi:10.1111/srt.12316 (2017).

261 Cao, T. & Tey, H. L. High-definition optical coherence tomography – an aid to clinical practice and research in dermatology. *J Dtsch Dermatol Ges* **13**, 886-890, doi:10.1111/ddg.12768 (2015).

262 Ri, J. S. *et al.* In vivo Tracking of DNA for Precise Determination of the Stratum Corneum Thickness and Superficial Microbiome Using Confocal Raman Microscopy. *Skin Pharmacol Physiol*, 1-8, doi:10.1159/000503262 (2019).

263 Berdyshev, E. *et al.* Lipid abnormalities in atopic skin are driven by type 2 cytokines. *JCI Insight* **3**, e98006, doi:10.1172/jci.insight.98006 (2018).

264 Yamamoto, K. *et al.* Core-multishell nanocarriers: Transport and release of dexamethasone probed by soft X-ray spectromicroscopy. *J Control Release* **242**, 64-70, doi:10.1016/j.jconrel.2016.08.028 (2016).

265 Feiner-Gracia, N., Pujals, S., Delcanale, P. & Albertazzi, L. in *Smart Nanoparticles for Biomedicine* (ed Gianni Ciofani) 219-236 (Elsevier, 2018).

266 Greenspan, P. & Fowler, S. D. Spectrofluorometric studies of the lipid probe, nile red. *J Lipid Res* **26**, 781-789 (1985).

267 Küchler, S. *et al.* Influence of nanocarrier type and size on skin delivery of hydrophilic agents. *Int J Pharm* **377**, 169-172, doi:https://doi.org/10.1016/j.ijpharm.2009.04.046 (2009).

268 Yalkowsky, S. H. & Banerjee, S. *Aqueous solubility: Methods of estimation for organic compounds*. (Marcel Dekker, 1992).

269 Stefánsson, E. & Loftsson, T. in *Retinal Pharmacotherapy* (eds Quan Dong Nguyen, Eduardo Büchele Rodrigues, Michel Eid Farah, & William F. Mieler) 86-90 (W.B. Saunders, 2010).

270 Döge, N. *et al.* Identification of polystyrene nanoparticle penetration across intact skin barrier as rare event at sites of focal particle aggregations. *J Biophotonics* **11**, e201700169, doi:10.1002/jbio.201700169 (2018).